AD-A230 295

NAVAL POSTGRADUATE SCHOOL

Monterey, California

THESIS

CONSTRAINED VISCOELASTIC LAYER DAMPING
OF THICK ALUMINUM PLATES:
DESIGN, ANALYSIS, AND TESTING

by

MICHAEL J. BATEMAN

March 1990

Thesis Advisor:	Y. S. Shin
Co-Advisor:	K. S. Kim

91 1 2 0 1

REPORT DOCUMENTATION PAGE

1a REPORT SECURITY CLASSIFICATION UNCLASSIFIED	1b RESTRICTIVE MARKINGS
2a SECURITY CLASSIFICATION AUTHORITY	3 DISTRIBUTION / AVAILABILITY OF REPORT
2b DECLASSIFICATION / DOWNGRADING SCHEDULE	
4 PERFORMING ORGANIZATION REPORT NUMBER(S)	5 MONITORING ORGANIZATION REPORT NUMBER(S)

6a NAME OF PERFORMING ORGANIZATION Naval Postgraduate School	6b OFFICE SYMBOL (If applicable) 55	7a NAME OF MONITORING ORGANIZATION Naval Postgraduate School
6c ADDRESS (City, State, and ZIP Code) Monterey, CA 93943-5000		7b ADDRESS (City, State, and ZIP Code) Monterey, CA 93943-5000
8a NAME OF FUNDING / SPONSORING ORGANIZATION	8b OFFICE SYMBOL (If applicable)	9 PROCUREMENT INSTRUMENT IDENTIFICATION NUMBER

8c ADDRESS (City, State, and ZIP Code)	10 SOURCE OF FUNDING NUMBERS			
	PROGRAM ELEMENT NO	PROJECT NO	TASK NO	WORK UNIT ACCESSION NO

11 TITLE (Include Security Classification)
CONSTRAINED VISCOELASTIC LAYER DAMPING OF THICK ALUMINUM PLATES: DESIGN, ANALYSIS, AND TESTING

12 PERSONAL AUTHOR(S)
Bateman, Michael J. LT, USN

13a TYPE OF REPORT Master's Thesis	13b TIME COVERED FROM ___ TO ___	14 DATE OF REPORT (Year, Month, Day) March 1990	15 PAGE COUNT 118

16 SUPPLEMENTARY NOTATION The views expressed in this thesis are those of the author and do not reflect the official policy or position of the Department of Defense or the U.S. Government

17 COSATI CODES			18 SUBJECT TERMS (Continue on reverse if necessary and identify by block number)
FIELD	GROUP	SUB GROUP	vibration, vibration damping, viscoelastic damping, constrained layer damping

19 ABSTRACT (Continue on reverse if necessary and identify by block number)

Modern naval warfare has been increasingly dependent upon the acoustic silencing of the participants. Constrained viscoelastic layer damping of vibrating elements is one method which can be used to meet acoustic silencing goals. This paper considers constrained viscoelastic layer damping treatments applied to a thick aluminum plate, including single layer, double layer, a milled pocket plate, and a milled "floating element" configuration. High modal damping values were obtained for each configuration. The Modal Strain Energy method, using finite element analysis to estimate modal loss factors, was investigated for use as a tool in constrained viscoelastic layer damping design. A comparison of experimentally measured frequency response and modal loss factors with those predicted by the modal strain energy method is presented to confirm

20 DISTRIBUTION / AVAILABILITY OF ABSTRACT ☒ UNCLASSIFIED/UNLIMITED ☐ SAME AS RPT ☐ DTIC USERS	21 ABSTRACT SECURITY CLASSIFICATION Unclassified
22a NAME OF RESPONSIBLE INDIVIDUAL Professor Y.S. Shin	22b TELEPHONE (Include Area Code) (408)646-2568 — 22c OFFICE SYMBOL 69Sg

DD FORM 1473, 84 MAR   83 APR edition may be used until exhausted
All other editions are obsolete

[19]   the possible use of the modal strain energy method as a design
        tool.

CONSTRAINED VISCOELASTIC LAYER DAMPING OF THICK
ALUMINUM PLATES: DESIGN, ANALYSIS, AND TESTING

by

Michael John Bateman
Lieutenant, United States Navy
B.S.N.A., United States Naval Academy, 1982

Submitted in partial fulfillment of the
requirements for the degree of

MASTER OF SCIENCE IN MECHANICAL ENGINEERING

and

MECHANICAL ENGINEER

from the

NAVAL POSTGRADUATE SCHOOL
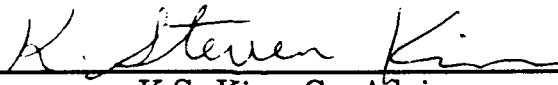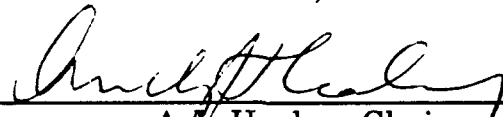March 1990

Author: _____
Michael John Bateman

Approved By: _____
Y.S. Shin, Thesis Advisor

_____
K.S. Kim, Co–Advisor

_____
A.J. Healey, Chairman,
Department of Mechanical Engineering

_____
DEAN OF FACULTY
AND GRADUATE STUDIES

iii

ABSTRACT

Modern naval warfare has been increasingly dependent upon the acoustic silencing of the participants. Constrained viscoelastic layer damping of vibrating elements is one method which can be used to meet acoustic silencing goals. This paper considers constrained viscoelastic layer damping treatments applied to a thick aluminum plate, including single layer, double layer, a milled pocket plate, and a milled "floating element" configuration. High modal damping values were obtained for each damping configuration. The Modal Strain Energy method, using finite element analysis to estimate modal loss factors, was investigated for use as a tool in constrained viscoelastic layer damping design. A comparison of experimentally measured frequency response and modal loss factors with those predicted by the modal strain energy method is presented to confirm the possible use of the modal strain energy method as a design tool.

iv

TABLE OF CONTENTS

ACKNOWLEDGMENTS

I. INTRODUCTION

A. BACKGROUND

Modern naval warfare, especially undersea warfare, depends heavily on the vessel being acoustically silent. A major source of radiated noise is the vibration of shipboard components. The reduction of these vibrations is of utmost importance if a ship is to accomplish its mission. One method of vibration damping that shows promise in damping over a broad spectrum of low frequency vibration is constrained viscoelastic layer damping. The constrained viscoelastic layer method uses shear deformation in viscoelastic material to absorb and dissipate the vibrational energy of the system in question. Unfortunately the design and analysis of such constrained viscoelastic layer systems is difficult, due in part to the following:

- The material properties of viscoelastic damping materials vary greatly with temperature and frequency.

- Closed form solutions to the equations of motion exist only for beams and plates with simple boundary conditions.

- The necessity for large amounts of computer storage and CPU time to conduct finite element analysis of constrained viscoelastic layer damping systems because of a large number of elements and the variation of material properties with frequency.

1

A finite element technique developed by Johnson and Kienholz known as the Modal Strain Energy (MSE) method uses structural strain energy to approximate the damping of a structure with an applied constrained viscoelastic damping system [Ref. 1]. Previous work by Maurer addressed the effectiveness of the MSE method for two damped plate configurations: 1) a simple sandwich configuration, and 2) a plate with a milled pocket with damping material inserted and a welded cover plate acting as a constraining layer [Ref.2]. Difficulties with the welded cover plate were reported because during welding, the cover plate warped and delaminated itself from the damping material, resulting in negligible damping [Ref. 2].

B.   PURPOSE

For certain naval applications the components to be damped will be thick in construction and may be exposed to an unfriendly environment. This paper addresses the experimental testing and analysis of four thick aluminum plates, each with a different constrained viscoelastic layer damping treatment.

This research further investigated the pocket plate configuration and also investigated a constrained viscoelastic layer damping system using two separate layers of damping material. In addition, a second milled plate using a "floating element" in conjunction with constrained layer damping was tested. The MSE method is used to analyze each of the structures, and

2

its accuracy and usefulness as a possible design tool are investigated. Although the intended use of the MSE method is the design of complex damping structures, simple plate geometries were used to facilitate the experimental and computational effort.

II. THEORY

A. VISCOELASTIC MATERIAL

Viscoelastic materials of interest for general naval applications are polymeric compounds made up of long molecular chains. These molecular chains can be strongly, or weakly, linked together, depending on their chemical composition and processing. The damping characteristics of viscoelastic arise from the deformation and recovery of the polymer network. Material properties of a viscoelastic material vary with temperature and frequency. As such, the damping characteristics of a system will vary as its operating environment changes. [Ref. 3]

Temperature will have the greatest effect on the material properties of damping materials [Ref. 3]. This effect is shown in Figure 2.1, where four distinct regions are observed. The lowest temperature region is the glassy region where the material's storage modulus is at its maximum value, and the loss factor is at a minimum. In the glassy region the modulus decreases slowly with temperature increase, whereas the loss factor increases rapidly with temperature. The second region is the transition region where the modulus decreases rapidly with increasing temperature and the loss factor reaches its peak value. The third region is the rubbery region where both the modulus and loss factor are at low values and show little variation with temperature. The fourth, and last, region is the flow region and characterizes the behavior of some materials, mostly

4

ceramics, at high temperatures. It should be noted that the transition region may vary in width from 20 °C up to a width of 200 °C. [Ref. 3]

The effect of frequency on viscoelastic materials is not as great as that of temperature. The modulus of the viscoelastic always increases with increasing frequency. The loss factor will initially increase with frequency, then peak, and subsequently decrease as frequency increases. A plot of storage modulus and loss factor versus frequency is shown in Figure 2.2. It should be noted that this plot is over a range of approximately ten decades, and hence it becomes obvious that a temperature change of a couple degrees will have a much greater effect on damping than a minor change in frequency. [Ref. 3]
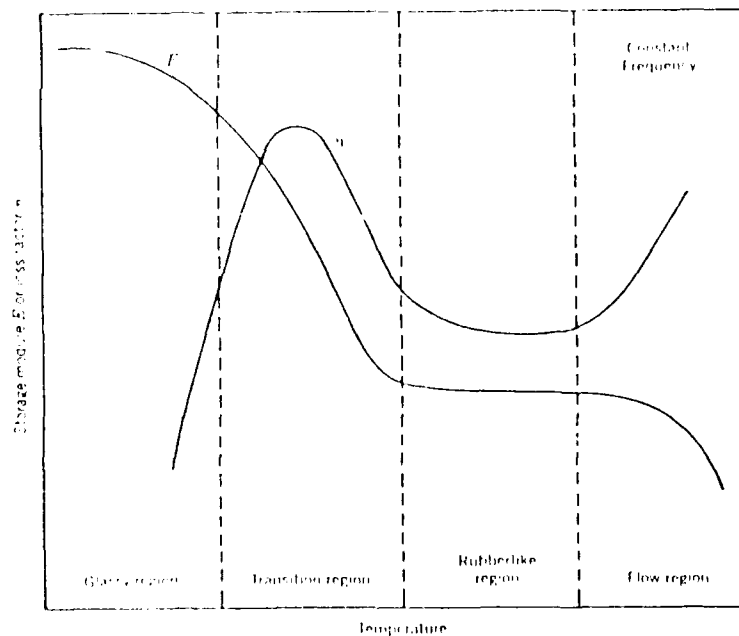
Figure 2.1. Variation of viscoelastic material
properties with temperature [Ref. 3].

5
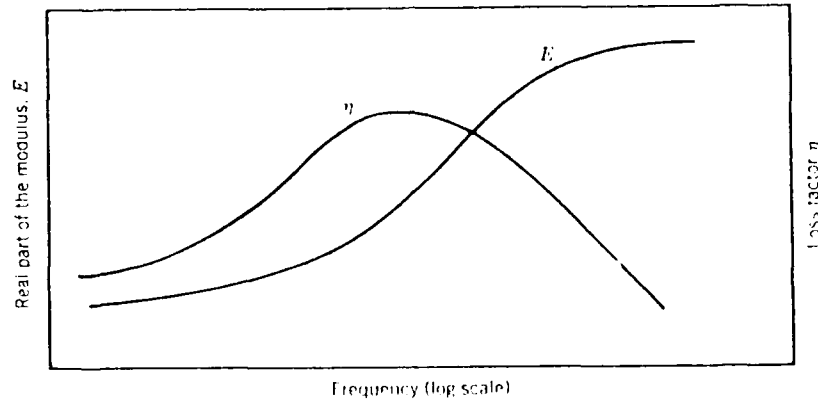
Figure 2.2. Variation of viscoelastic material properties
with frequency and constant temperature [Ref. 3].

Linear viscoelastic materials behave in a hysteretic manner under cyclic excitation. Therefore, the mechanical behavior of a viscoelastic material during steady state vibration is best described by using a complex stiffness, k* [Ref. 3].

$$k^* = k(1 + i\eta) \tag{2.1}$$

where,

η = material loss factor

The use of a complex stiffness then leads to the use of a complex Young's modulus and shear modulus [Ref. 3].

$$E^* = E(1 + i\eta) \qquad\qquad (2.2)$$

$$G^* = G(1 + i\eta) \qquad\qquad (2.3)$$

This concept of the complex modulus is used in subsequent analysis.

Viscoelastic material properties are commonly displayed using a "reduced frequency nomogram." The reduced frequency nomogram displays the variation of the viscoelastic material's loss factor and modulus with temperature and frequency. The "reduced frequency", $f_{\alpha t}$, is an empirically determined function that accounts for the viscoelastic's temperature and frequency dependence, and allows data for wide range of temperature and frequencies to be plotted on the same graph [Ref 4]. The reduced frequency nomogram for 3M ISD - 112 is shown in Figure 2.3. To find the loss factor and modulus using the nomogram, enter with the desired temperature and frequency. Follow the frequency line horizontally and the temperature line diagonally down the page until the two intersect. Then go vertically up or down to intersect the shear modulus or loss factor curves. Finally, read the value of the shear modulus or loss factor horizontally from the scale on the left [Ref. 4].
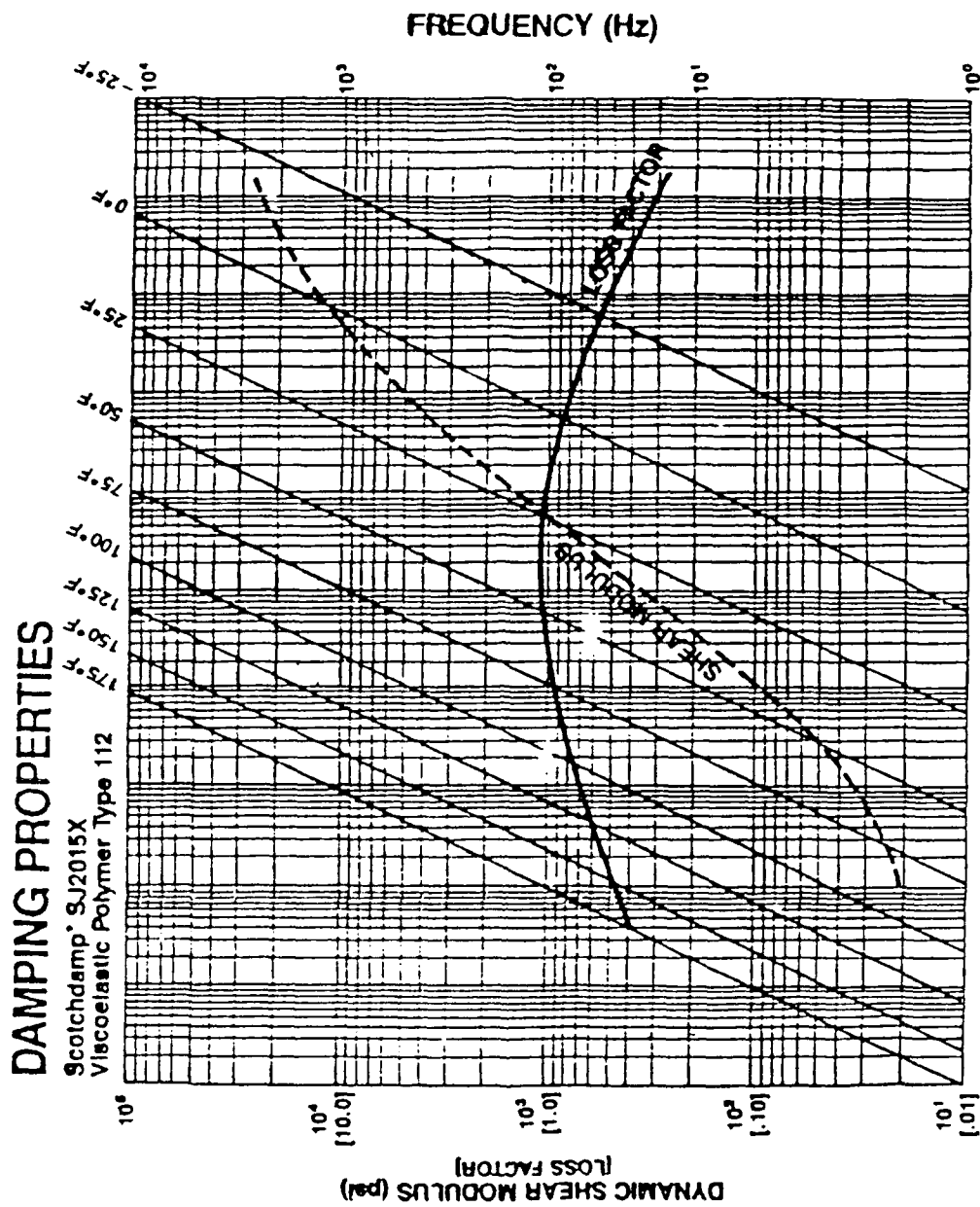
Figure 2.3. Reduced frequency nomogram for 3M ISD - 112.

B.   CONSTRAINED VISCOELASTIC LAYER DAMPING

A simple constrained layer damping treatment consists of a base layer (the structure to be damped), a damping layer, and the constraining layer. This configuration is shown in Figure 2.4 with the thicknesses of the damping and constraining layers exaggerated for clarity.

```
┌─────────────────────────────┐  ┬
│     CONSTRAINING LAYER       │  │ H3
├─────────────────────────────┤  ┴
│       DAMPING LAYER          │  ┬ H2
├─────────────────────────────┤  ┴
│                             │  ┬
│        BASE LAYER            │  │ H1
│                             │  ┴
└─────────────────────────────┘
```
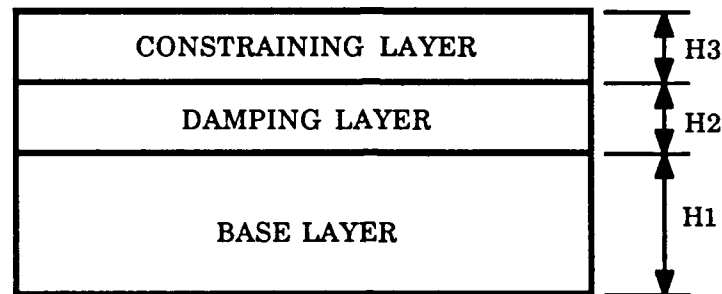
Figure 2.4. Simple constrained viscoelastic layer configuration.

The physical mechanism of damping can be explained by referring to Figure 2.4. When the base layer is deformed in a mode of vibration, the surface away from the neutral axis elongates, stretching the viscoelastic material. The top layer, being a stiff elastic material, tends not to elongate, and thereby "constrains" the viscoelastic material. Consequently, the cyclic motions of vibration induce a cyclic shearing strain in the viscoelastic. This cyclic shearing strain, together with its associated hysteresis loop cause the vibrational energy to be dissipated as heat. For the constraining layer to be effective, its stiffness should not exceed that of the base layer. [Ref. 4 & 5]

9

C.   SYSTEM EQUATIONS OF MOTION

Continuous systems, such as plates, possess distributed characteristics of mass, damping, and stiffness. Classical vibration analysis of such systems involves the formation of a mathematical model that discretizes the system into a finite number of components in order to approximate the total system. Such a formulation results in the following equation:

$$[M]\{\ddot{x}(t)\} + [C]\{\dot{x}(t)\} + [K]\{x(t)\} = \{F(t)\} \qquad (2.4)$$

where,

$[M]$ = system mass matrix

$[C]$ = system damping matrix

$[K]$ = system stiffness matrix

$\{F(t)\}$ = external excitation vector

$\{x(t)\}$ = displacement vector

For an undamped system without excitation, the above equation reduces to the eigenvalue problem.

$$[M]\{\ddot{x}(t)\} + [K]\{x(t)\} = 0 \qquad (2.5)$$

This equation is then transformed to modal space using the linear transformation:

$$\{x(t)\} = [\phi]\{q(t)\} \qquad (2.6)$$

where,

$[\phi]$ = modal matrix

$\{q(t)\}$ = modal response vector

Using this linear transformation the equation of motion can then be solved for the undamped modal frequencies and mode shapes.

To solve for the frequency response of a damped system, the linear transformation is applied to equation (2.4):

$$[M][\phi]\{\ddot{q}(t)\} + [C][\phi]\{\dot{q}(t)\} + [K][\phi]\{q(t)\} = \{F(t)\} \tag{2.7}$$

Assuming that the damping matrix [C] is proportional to a linear combination of the stiffness matrix [K] and mass matrix [M], the damping matrix can then be diagonalized using the same linear transformation used to diagonalize [K] and [M] in equation (2.5) above. The diagonal terms of the damping matrix then become $(\eta_i\omega_i)$, where η_i equals the modal loss factor and ω_i is the natural frequency of the ith mode [Ref. 1] . Using this approximate diagonal damping matrix results in a system of uncoupled modal equations of motion:

$$\ddot{q}_i(t) + \eta_i\omega_i\dot{q}_i(t) + \omega_i^2 q_i(t) = f_i(t) \tag{2.8}$$

where,

$\ddot{q}_i(t)$ = modal acceleration of ith mode

$\dot{q}_i(t)$ = modal velocity of ith mode

$q_i(t)$ = modal displacement of ith mode

η_i = modal loss factor of ith mode

11

$$\omega_i = i^{th} \text{ natural frequency}$$

$$f_i(t) = \text{modal force in } i^{th} \text{ mode}$$

$$j = \sqrt{-1}$$

Assuming that a sinusoidal excitation produces a sinusoidal response,

$$\{f(t)\} = \{\tilde{f}\}e^{j\omega t} \qquad \{q(t)\} = \{Q\}e^{j\omega t} \tag{2.9}$$

the response for the ith mode is then solved to be:

$$Q_i = \frac{\tilde{f}_i}{\omega_i^2 - \omega^2 + j\omega_i\eta_i\omega} \tag{2.10}$$

Subsequently, the response of the physical system can be found using:

$$\{x(t)\} = \left[\phi\right]\{Q\}e^{j\omega t} \tag{2.11}$$

D.   MODAL STRAIN ENERGY METHOD

The equations of motion used to define the response of a system with viscoelastic materials need a complex eigenvalue analysis. However, the actual solution of these equations may be quite difficult. This is especially true when the system to be analyzed is comprised of materials whose properties vary with both temperature and frequency. Finite element techniques are generally used to compute the response of complicated systems. However, for the case of varying material properties many time consuming and costly runs must be made with the material properties

12

changing at each frequency increment [Ref. 1]. In addition to the costly analysis of a single design configuration, changes in design options, design requirements, of the search for an optimum design can make the expense of finite element analysis too great. The development of the Modal Strain Energy (MSE) method by Johnson and Kienholz, however, makes the finite element analysis of complex viscoelastically damped structures a viable option [Ref. 1].

The MSE method assumes that a damped structure can be represented by the normal modes of the associated undamped system if appropriate damping terms are inserted into the uncoupled modal equations of motion (eqn 2.8) [Ref. 1]. The MSE method further assumes that the damping matrix of equation (2.4) can be diagonalized by the same real modal matrix that diagonalizes the system mass and stiffness matrices of equation (2.4).

The modal loss factors of equation (2.8) are calculated using the undamped mode shapes and material loss factors for each material. Since the material loss factors of the structure to be damped and the constraining layers are quite small compared to those of common viscoelastic cores, the modal loss factors can be estimated using the following equation [Ref. 1]:

$$\eta^{(r)} = \eta_v^{(r)} \frac{V_v^{(r)}}{V^{(r)}} \qquad (2.12)$$

where,

$\eta^{(r)}$ = system loss factor in the rth mode

1 3

$$\eta_v^{(r)} = \text{material loss factor of viscoelastic core at the } r^{th}$$

natural frequency

$$V_v^{(r)} = \text{strain energy in the viscoelastic core at } r^{th} \text{ mode}$$

$$V^{(r)} = \text{strain energy in the entire structure at } r^{th} \text{ mode}$$

The modal strain energies can be obtained for finite element analysis, and are a standard output option of the NASTRAN finite element code [Ref. 7].

The modal frequency response of the structure is then calculated using the modal loss factors found in equation (2.12). When computing the modal frequency response of a damped structure, the modal properties in the system matrices are assumed to be constant. However, viscoelastic materials have storage moduli which are frequency dependent. To account for this frequency dependence, Johnson and Kienholz devised the following correction factor to be applied to the modal loss factors calculated in equation (2.12) [Ref. 8].

$$\eta_c^{(r)} = \eta^{(r)} \sqrt{\frac{G_2(f_r)}{G_{2,ref}}} \tag{2.13}$$

where,

$$\eta_c^{(r)} = \text{corrected modal loss factor at the } r^{th} \text{ mode}$$

$$G_2(f_r) = \text{viscoelastic shear modulus at the } r^{th} \text{ modal}$$

frequency

$$G_{2,ref} = \text{reference viscoelastic shear modulus used in the}$$

frequency response calculation

III. DESIGN OF DAMPED PLATES

A. GENERAL SPECIMEN CONFIGURATIONS

For experimental testing and analysis purposes, four different, yet related, constrained layer damping treatments were selected in addition to an undamped "reference" plate. Two of the damping configurations were simple sandwich treatments consisting of one and two viscoelastic layers respectively. Another treatment was the "pocket plate" which was previously investigated by Maurer [Ref. 2]. The pocket plate was made from a solid plate which was then milled to accept damping material and a cover plate. The final damping treatment was a "floating element" configuration consisting of a solid plate milled to accept a double layer of damping material and a welded cover plate. Section views of these damping configurations are shown in Figure 3.1.

The purpose of the pocket plate is to protect the viscoelastic material from materials such as oil and salt water, which may harm the viscoelastic. Since previous attempts at using a welded cover plate were unsuccessful due to the heat of welding causing a delamination between the damping material and cover plate [Ref. 2], it was decided to move the viscoelastic material from the welding point by recessing it into a shallow pocket of its own as shown in Figure 3.1.

The "floating element" concept evolved because the welded cover plate of the pocket plate configuration does not produce the damping reaction that a true constraining layer would provide. If the cover plate is welded to the

1 5

surrounding structure it cannot deform in bending as much as an unwelded constraining layer, thereby causing a reduction in the damping capability of the system. By using a piece of metal in the milled pocket with dimensions slightly smaller than the surrounding pocket, along with two layers of viscoelastic and a welded cover plate, a true constraining layer effect should be obtained. This configuration is shown in Figure 3.1.

Single layer configuration

Double layer configuration

Milled "pocket plate"

Plate with "floating element"
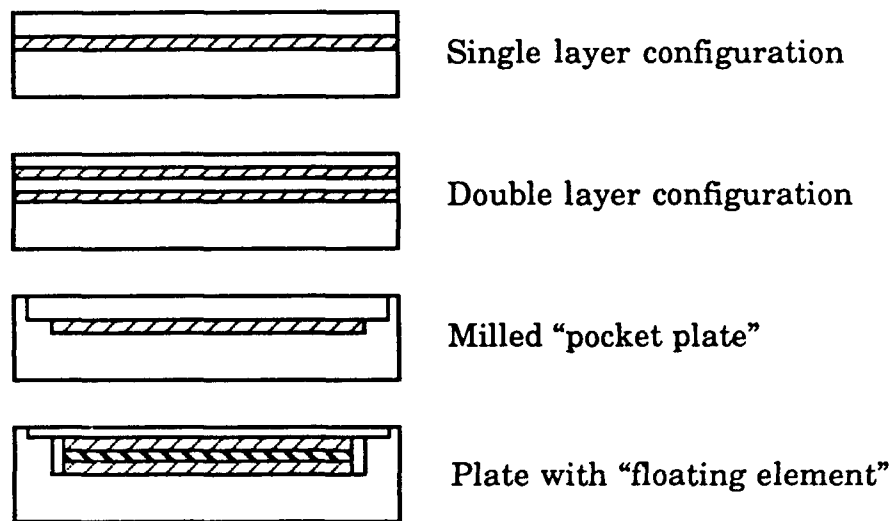
Figure 3.1. Generalized damping treatment configurations.

In order to approximate a possible system to be damped, a plate with large dimensions was selected. The dimensions of the plates used for the damping treatments are 114.3 cm (45 in) in length and 38.1 cm (15 in) in width. In addition, possible naval applications for this type of damping would probably consist of thick plate members. For this reason it was also decided that thick plates would be used for the damping treatments. All the

base plates and constraining layers were made of a standard 6061–T6 aluminum alloy. The design and selection of viscoelastic layer, base layer, and constraining layer thicknesses is discussed in the following sections.

B.   DESIGN OF THE SINGLE DAMPING LAYER CONFIGURATION

In an attempt to approximate system loss factors and hence determine viscoelastic and constraining layer thicknesses for maximum damping, a method developed by Nashif [Ref. 9] based on an analysis of simple sandwich damping systems by Ross, Kerwin, and Ungar [Ref. 10] was used. The Ross - Kerwin - Ungar (RKU) equations are base of the analysis of the simple sandwich system shown in Figure 3.2.
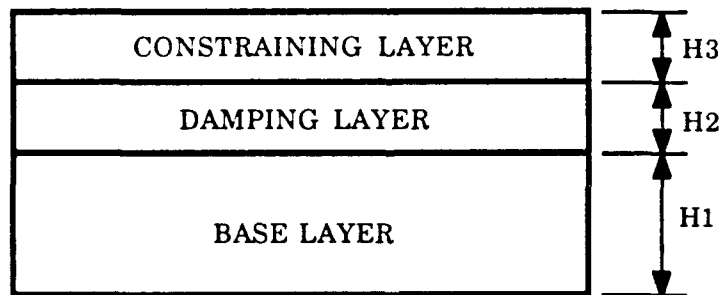
Figure 3.2. Elements of a simple sandwich damping system.

To find the loss factors of the damped system, the flexural rigidity of the system must first be determined. For the above system, the flexural rigidity, EI, is written as [Ref. 9]:

$$EI = \frac{E_1 H_1^3}{12} + \frac{E_2 H_2^3}{12} + \frac{E_3 H_3^3}{12} + E_1 H_1 D^2$$
$$+ E_2 H_2 (H_{21} - D)^2 + E_3 H_3 (H_{31} - D)^2$$
$$- \left[\frac{E_2 H_2^3}{12} + \frac{E_2 H_2}{2}(H_{21} - D) + E_3 H_3 (H_{31} - D) \right] \frac{H_{31} - D}{1 + g} \qquad (3.1)$$

where,

$$D = \frac{E_2 H_2 \left(H_{21} - \frac{H_{31}}{2} \right) + g(E_2 H_2 H_{21} + E_3 H_3 H_{31})}{E_1 H_1 + \frac{E_2 H_2}{2} + g(E_1 H_1 + E_2 H_2 + E_3 H_3)} \qquad (3.2)$$

$$H_{31} = \frac{H_1 + H_3}{2} + H_2 \qquad (3.3)$$

$$H_{21} = \frac{H_1 + H_2}{2} \qquad (3.4)$$

$$g = \frac{G_2}{E_3 H_3 H_2 K^2} \qquad (3.5)$$

E = Young's modulus

G = Shear modulus

I = second moment of area

H = thickness of member

K^2 = wave number

Subscripts refer to the layers labeled in Figure 3.1

No subscript refers to the composite system

For a simply supported plate the wave numbers and modal frequencies are found using [Ref.9]:

$$\omega_n = K_{nm}^2 \sqrt{\frac{EH^3 g_c}{12(1 - v^2)H\rho}} \qquad (3.6)$$

$$K_{nm}^2 = \left(\frac{n\pi}{a}\right)^2 + \left(\frac{m\pi}{b}\right)^2 \qquad (3.7)$$

where,

   a = semi–wave length of the plate

   b = semi–wave width of the plate

   v = Poisson's ratio of the composite plate

   ρ = density of the composite plate

   g_c = gravitational constant

To introduce damping into the equations it is necessary to use the complex modulus concept expressed in Section II. Substituting the appropriate expressions for the complex shear and Young's modulus into equations (3.1), and assuming that damping in the base layer, (η_1), is small, and that the extensional stiffness of the damping layer is small (since $E_2 \ll E_1$ and $E_2 \ll E_3$), the following expressions can be arrived at [Ref.9]:

$$EH^3 = E_1 H_1^3 + E_3 H_3^3 + \frac{12}{c^2 + d^2}(\alpha - \beta - \partial)_{RE} \qquad (3.8)$$

$$EH^3\eta = E_3H_3\eta_3 + \frac{12}{c^2 + d^2}(\alpha - \beta - \partial)_{IM} \qquad (3.9)$$

where,

$$\alpha = gE_1H_1E_3H_3H_{31}^2\{c(1 - \eta_2\eta_3) + d(\eta_2 + \eta_3) + j[c(\eta_2 + \eta_3)]\} \qquad (3.10)$$

$$\beta = E_1H_1E_2H_2H_{31}\left[c + d\eta_2 + j(c\eta_2 - d)\right] \qquad (3.11)$$

$$\partial = 2gE_2H_2E_3H_3H_{21}H_{31}\left\{ \begin{array}{l} c(1 - 2\eta_2\eta_3 - \eta_2^2) + d(2\eta_2 + \eta_3 - \eta_2^2\eta_3) \\ + j[c(2\eta_2 + \eta_3 - \eta_2^2\eta_3) - d(1 - 2\eta_2\eta_3 - \eta_2^2)] \end{array} \right\} \qquad (3.12)$$

$$c = E_1H_1(1 + g) + gE_3H_3(1 - \eta_2\eta_3) \qquad (3.13)$$

$$d = gE_1H_1\eta_2 + gE_3H_3(\eta_2 + \eta_3) \qquad (3.14)$$

$$j = \sqrt{-1} \qquad (3.15)$$

These equations were then applied to estimate the loss factors of the simple three–layer sandwich plate. The equations can be simplified by assuming that damping in the constraining layer (η_3) is negligible [Ref.9].

Since the boundary conditions for the plate used in this research (free-free-free-free) do not correspond to the simply supported conditions on which equation (3.7) is based, modal frequencies for the free-free case were estimated using results from finite element analysis of a free-free plate and equation (3.6). The natural frequencies of an undamped plate with the dimensions previously given, and a thickness of 1.91 cm (0.75 in) were found using a normal mode extraction in NASTRAN. By substituting these modal frequencies into equation (3.6) and estimate of the wave parameter for each mode, K_{nm}^2, was obtained. Then, by using an iterative procedure

20

outlined in Reference [9], modal loss factors were estimated for different layer thicknesses over a temperature range of 0.0 °C to 37.8 °C (30 °F to 100 °F).

The previous equations are easily programmed to compute loss factors for a wide variety of conditions. The variation of viscoelastic material properties with temperature and frequency was accounted for using a curve-fit to the reduced frequency nomogram developed by Drake [Ref. 11]. The material data for the following curve-fit equations is from the University of Dayton Research Institute [Ref. 12].

$$\log_{10}(M) = \log_{10}(ML) + \frac{\left[2 \log_{10}\left(\frac{MROM}{ML}\right)\right]}{\left[1 + \left(\frac{FROM}{FR}\right)^n\right]} \tag{3.16}$$

$$\log_{10}(ETA) = \log_{10}(ETAFROL) + \frac{1}{2}C\left[A(SL + SH) + (SL - SH)\left(1 - \sqrt{1 + A^2}\right)\right] \tag{3.17}$$

$$\log_{10}(FR) = \log_{10}(F) - \frac{12(T - T0)}{(525 + T - T0)} \tag{3.18}$$

$$A = \frac{\log_{10}(FR) - \log_{10}(FROL)}{C} \tag{3.19}$$

where,

   M = viscoelastic modulus

   ETA = viscoelastic material loss factor

   FR = reduced frequency (Hz)

   F = frequency (Hz)

   T = temperature (°F)

21

and,

$$T0 = 40\ ^\circ C\ (104\ ^\circ F)$$

$$FROM = 2.0 \times 10^4\ Hz$$

$$MROM = 4.75 \times 10^6\ Pa\ (688.94\ psi)$$

$$n = 0.275$$

$$ML = 6.0 \times 10^4\ Pa\ (8.7\ psi)$$

$$ETAFROL = 1.08$$

$$SL = 0.45$$

$$SH = -0.55$$

$$FROL = 5000\ Hz$$

$$C = 2.5$$

In addition to the above constants, a Poisson's ratio of 0.49 and a density of 0.909 gram per cubic centimeter (0.035 lbm/in^3) was used for ISD–112 [Ref.12]. The following material properties were used for 6061–T6 aluminum [Ref.13].

$$E = 70\ GPa\ (10 \times 10^6\ psi)$$

$$v = 0.33$$

$$\rho = 2.7\ gm/cm^3\ (0.0968\ lbm/in^3)$$

Using the previous equations and material properties, a computer program was written to compute estimated modal loss factors and frequencies for a variety of base layer, viscoelastic layer, and constraining layer thicknesses. A listing of this program appears in Appendix A. Modal loss factors were computed for base layer thicknesses of 9.53 mm

(0.375 in) to 19.05 mm (0.75 in) in 3.18 mm (0.125 in) increments. For each base layer thickness, the viscoelastic thickness was varied from 0.38 mm (0.015 in) to 1.52 mm (0.060 in) in 0.38 mm increments, and the constraining layer thickness was varied from 1.59 mm (0.0625 in) to 6.35 mm (0.25 in) in 1.59 mm increments. In addition, loss factors were also computed for a viscoelastic thickness of 0.127 mm (0.005 in). From the results of the analysis, a carpet plot [Ref. 3], was made for each of the base layer conditions. The carpet plot reflects, for the the first mode, the maximum loss factor and its corresponding temperature for each viscoelastic layer/constraining layer thickness configuration. The carpet plot for a base layer thickness of 12.7 mm (0.50 in) is shown in Figure 3.3. Based on the carpet plots and a desire for maximum damping, as well as a system which could be moved easily, a base layer thickness of 12.7 mm (0.50 in), a viscoelastic thickness of 0.38 mm (0.015 in), and a constraining layer thickness of 6.35 mm (0.25 in) was selected. The total system thickness was approximately 19.05 mm (0.75 in). This total system thickness would be maintained for all subsequent damping configurations.

To maintain continuity between damping systems, the milled "pocket plate" was given a viscoelastic thickness of 0.38 mm and a cover plate thickness of 6.35 mm for a total system thickness of 19.05 mm (0.75 in). In order to keep the heat of welding away from the viscoelastic material, the ISD–112 was recessed into a shallow pocket as indicated previously in Figure 3.1, and as shown in the pocket plate system arrangement in Figure 3.4. Detail drawings of the pocket plate are shown in Appendix C.
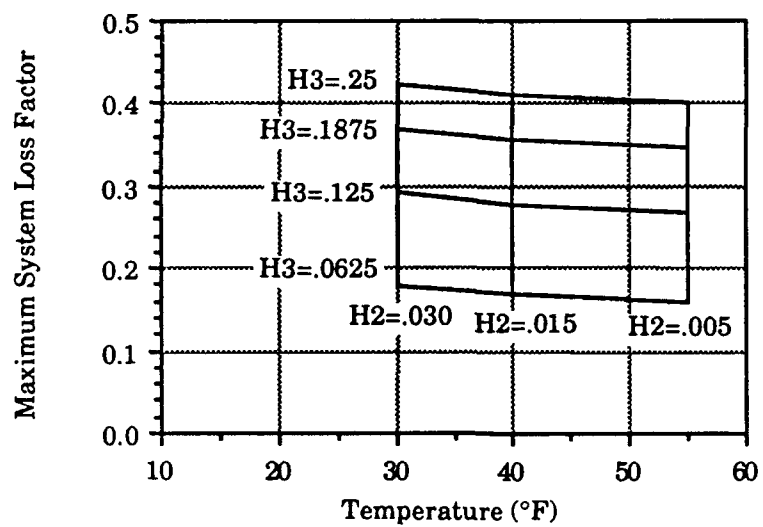
Figure 3.3. Carpet plot for a base layer thickness, H1 = 12.7 mm.

$44\frac{1}{2} \times 14\frac{1}{2} \times \frac{1}{4}$" ALUMINUM

ISD - 112

MILLED PLATE
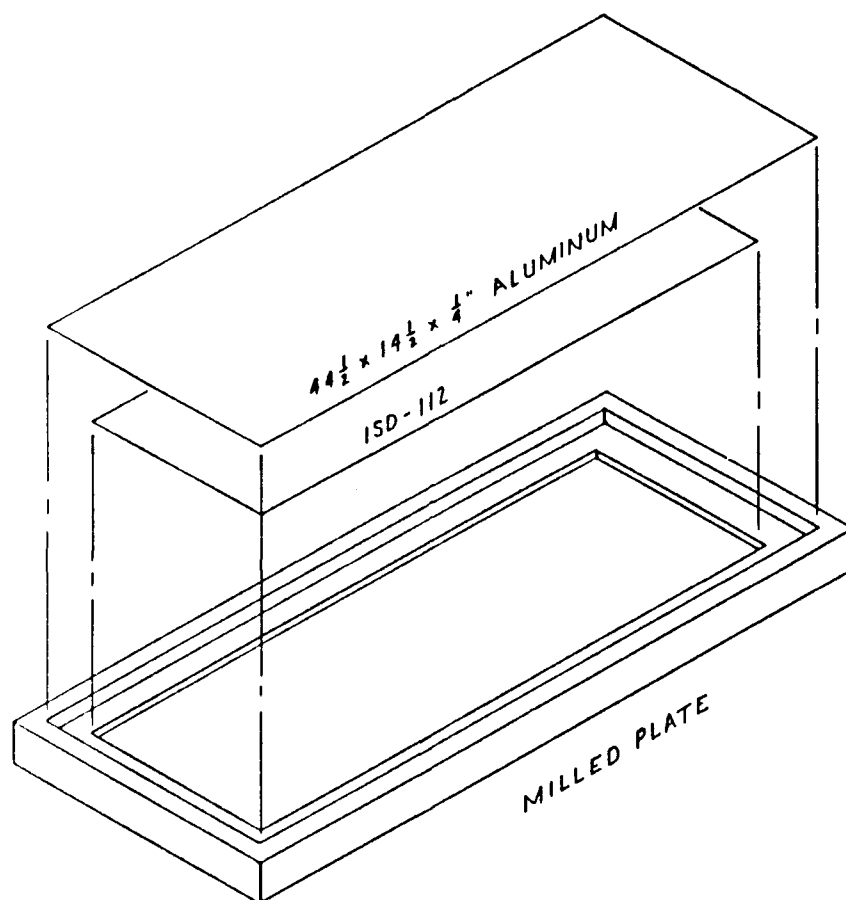
Figure 3.4. General arrangement of the pocket plate configuration.

C. DESIGN OF THE DOUBLE DAMPING LAYER

The design of the double layer damping system was accomplished using a modification of the RKU analysis used in the previous section. The RKU equations are used by working from the top layer of the damping system down towards the base layer. As shown in Figure 3.5, the H3' constraining layer along with the H2' viscoelastic layer are combined with the H1' layer to form a three-layer system. Using the RKU equations, the stiffness of this system is computed and considered to be the equivalent stiffness of the top three layers of the total constrained layer damping system. The top three layers were then considered as a single layer with the equivalent stiffness previously calculated, and the RKU equations were again applied to compute estimated modal loss factors for the entire double layer damping system. [Ref.3]

CONSTRAINING LAYER	H3'
VISCOELASTIC	H2'
CONSTRAINING LAYER	H1'
VISCOELASTIC	H2
BASE STRUCTURE	H1

Figure 3.5. General configuration of the double
constrained layer system.

To maintain continuity among all the damping configurations, a base layer thickness of 12.77 mm (0.50 in) was chosen, and a total system thickness of 19.05 mm (0.75 in) was maintained. A design for high damping was then selected by computing modal loss factors for the constraining and damping layer thickness combinations shown in Table 3.1. The estimated modal loss factors for the first mode of vibration in each configuration are plotted as shown in Figure 3.6. A listing of the program used to compute the loss factors is in Appendix B.

From the data presented in Figure 3.6, viscoelastic thickness of 0.38 mm (0.015 in) and constraining layer thicknesses of 3.18 mm (0.125 in) were selected for the double layer configuration. This particular configuration estimates high damping over a wider temperature range than the other thickness combinations.

TABLE 3.1. THICKNESSES USED IN CALCULATION OF DOUBLE LAYER MODAL LOSS FACTORS.

Configuration	1	2	3	4	5	6
H2 (mm)	0.38	0.38	0.38	0.76	0.38	1.14
H1' (mm)	3.18	2.38	3.18	2.38	2.38	2.38
H2' (mm)	0.38	0.38	0.38	0.76	1.14	0.38
H3' (mm)	3.18	3.18	2.38	2.38	2.38	2.38
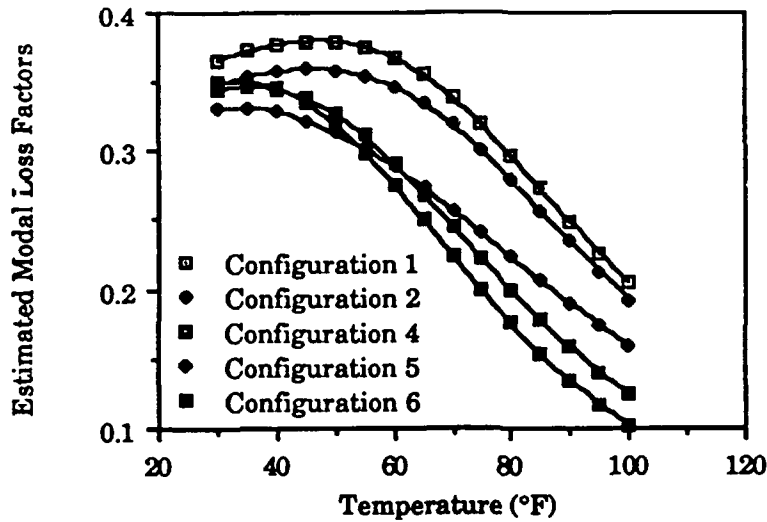
Figure 3.6. Modal loss factors for double constrained layer
damping configuration.

The milled "floating element" plate uses the same viscoelastic and
constraining layer thicknesses as the simple two–layer configuration. In a
design similar to that of the pocket plate, the floating element and both
layers of viscoelastic are recessed into a milled opening as shown
previously in Figure 3.1 and further described in the floating element
system configuration of Figure 3.7.

28
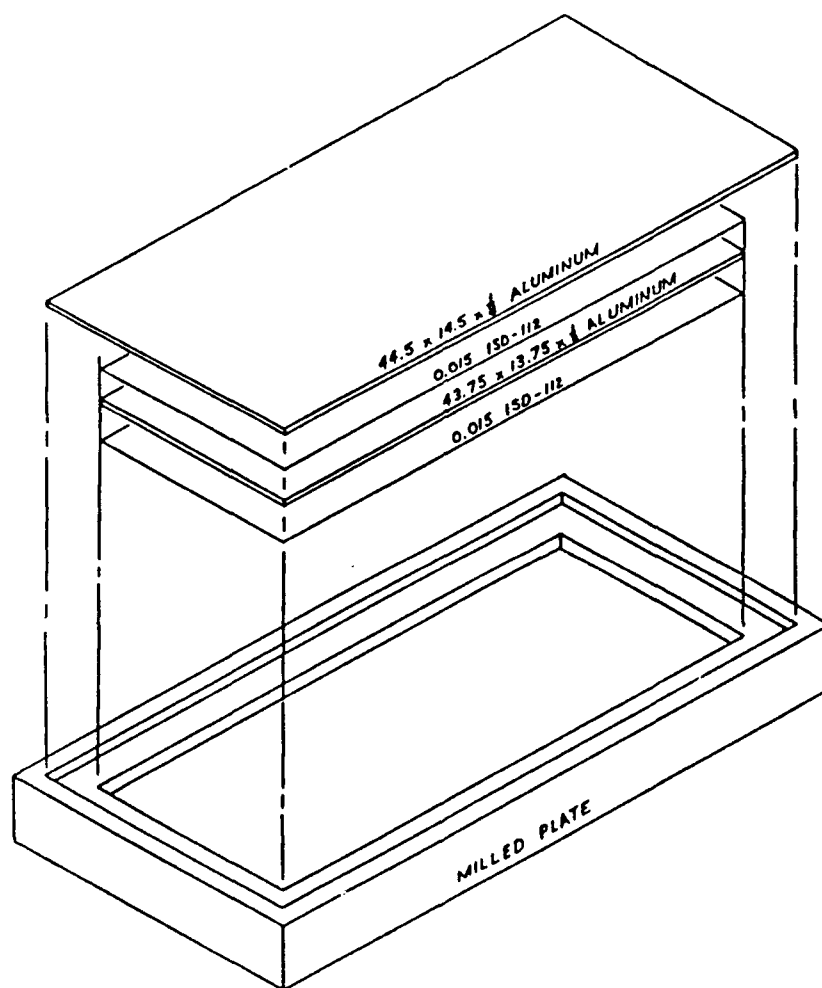
Figure 3.7. Floating element system configuration.

IV. EXPERIMENTAL RESULTS

A. TESTING ARRANGEMENT

Experimental testing was performed on each of the four damping configurations and the undamped reference plate. In order to approximate the free-free-free-free boundary condition, each plate was suspended from the roof of the testing chamber using elastic cords as shown in Figure 4.1. All of the tests were performed in a temperature controlled environmental chamber which enabled temperatures to be maintained within ±1 °C. The primary component and user interface was the Hewlett–Packard (HP) 3562A Dynamic Signal Analyzer (DSA). The HP-3562A was used to provide a swept sine signal to a vibration generator, and analyzed the returning data signals. The HP-3562A was used to compute the frequency response and coherence over a range of 50 Hz to 1050 Hz using the discrete Fourier Transform in the swept sine mode. Ten averages were performed at each data point using a frequency resolution of 625 mHz per step. The source level output to the vibration generator was set at 1.5 volts.

A schematic of the testing apparatus is shown in Figure 4.2. Swept sine source signals were fed from the output jack of the HP-3562A to a Wilcoxon F3 vibration generator via the piezoelectric output of a Wilcoxon PA7C power amplifier. The vibration generator was mounted 73.48 cm (28.93 in) from one end, and 12.7 cm (5.0 in) from the front edge of each specimen as shown in Figure 4.3. An integral force transducer was mounted in the base of the vibration generator to measure the force input to

the plate. This force signal was then fed to input channel one of the DSA via a PCB 462–A charge amplifier. Plate accelerations were recorded at various points using a PCB 303A–03 accelerometer as shown in Figure 4.3. Acceleration data was fed to input channel two of the DSA via a PCB 482A05 power supply. Frequency response and coherence data was then recorded on disk for further analysis.

Temperatures within the testing chamber were maintained using a NESLAB RTE–8 refrigerated circulating bath which pumped fluid through a small heat exchanger in the testing chamber as shown in Figure 4.2. In order to accurately monitor the temperature of the plates, a small thermocouple was inserted in the base of each plate.
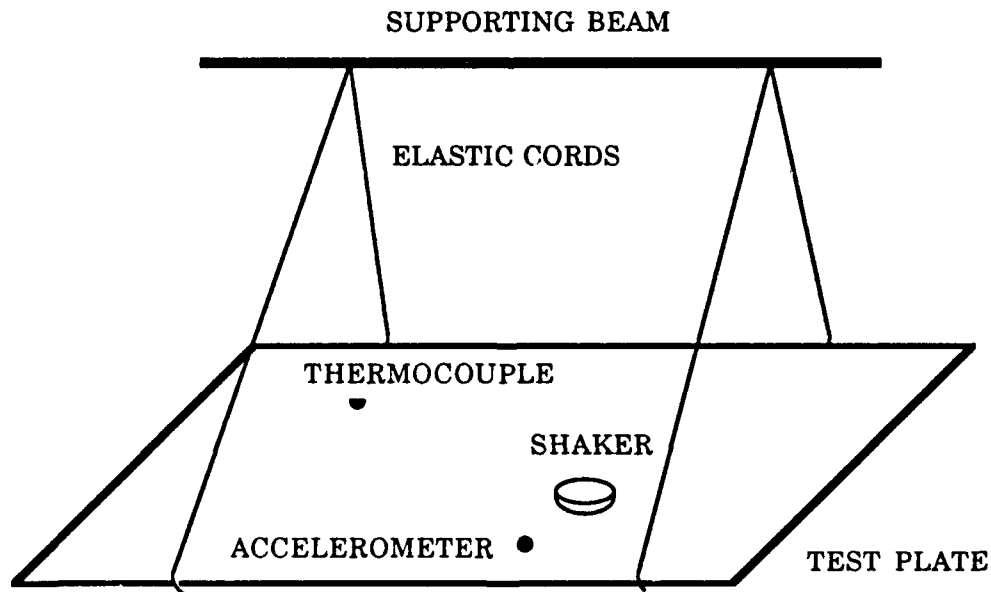
Figure 4.1. Configuration of plate in testing chamber.
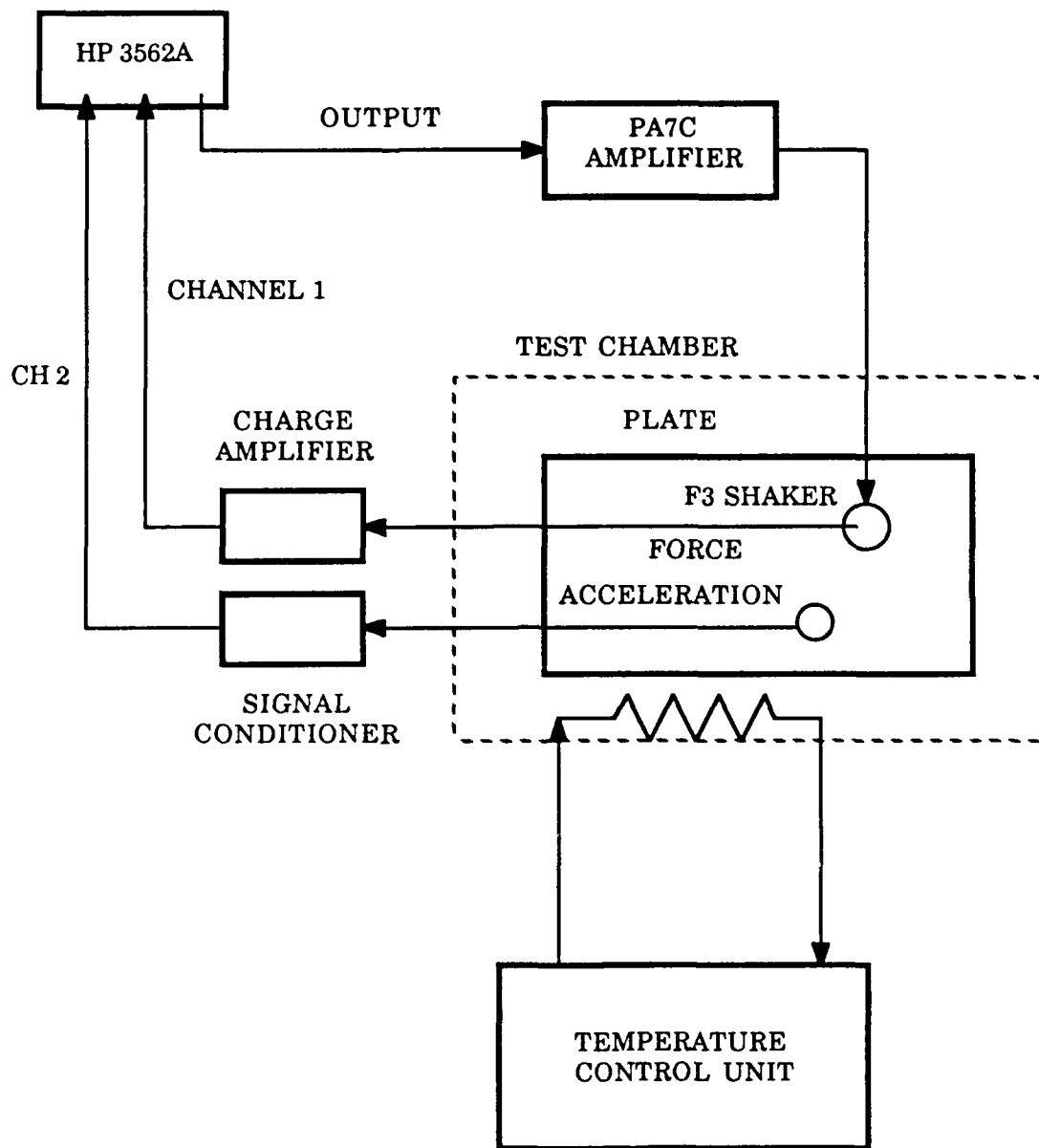
Figure 4.2. Experimental testing system schematic.

73.48 cm

SHAKER

12.7 cm

REPRESENTATIVE
MEASUREMENT POINTS
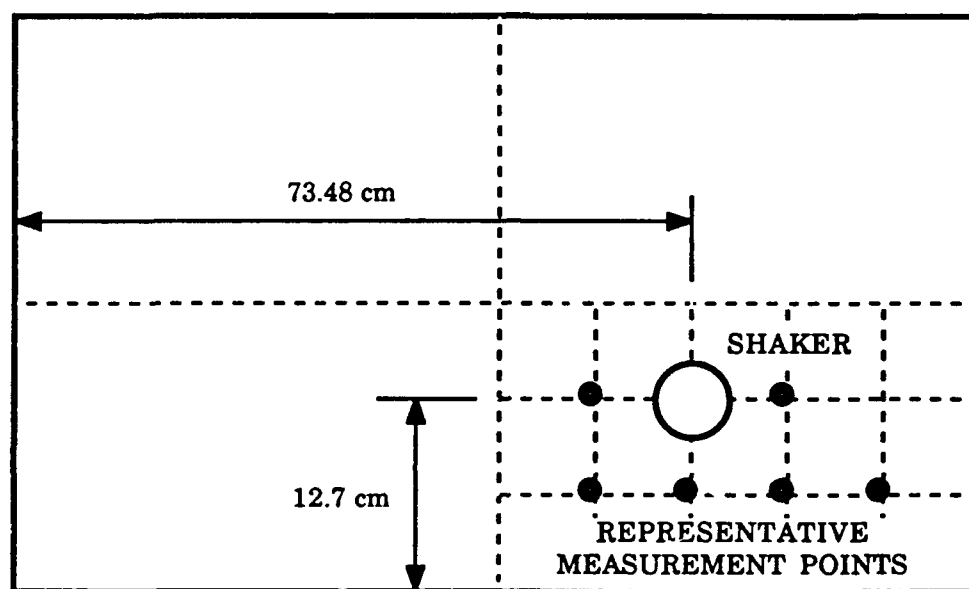
Figure 4.3. View of shaker and accelerometer locations.

B. TESTING PROCEDURE

1. Undamped reference plate

An undamped, reference, frequency response measurement was made at a temperature of 15.6 °C (60 °F) to set a standard response by which to measure the effectiveness of the damping treatments. The undamped frequency response was recorded over a frequency range of 50 – 1050 Hz using a resolution of 625 mHz per point in the DSA.

2. Damped plate measurements

Frequency response measurements of the damped plates were made at a temperature of 15.6 °C (60 °F) at several nodes on the plates in order to capture the damped response of as many modes as possible. A representation of these nodes is shown in Figure 4.3. Responses were recorded over a frequency range of 50 – 1050 Hz with a resolution of 625 mHz per point in the DSA. Zoom measurements were also made to capture better data for certain modes. Modal loss factors were then estimated from the frequency response and coherence measurements using a curve–fitting technique described in Reference [14].

C. SINGLE DAMPING LAYER RESULTS

The single damping layer treatment was tested at 4.44 °C (40 °F), 15.6 °C (60 °F), and 26.7 °C (80 °F) so that the effects of temperature on the damping treatment could be determined. A plot of the single damping layer frequency response at 15.6 °C is shown in Figure 4.4. The single layer damping treatment resulted in high damping with modal loss factors ranging from 0.223 at 53.4 Hz to 0.091 at 876.6 Hz. Due to the coupling of modes, loss factors for all modes were not measured. The frequency

34

response of the damped plate is characterized by a frequency shift to the left and a smoothing of the frequency response when compared to the undamped reference plate. The single layer treatment was especially effective at reducing the frequency response of a mode cluster between 650 and 950 Hz. The frequency band of this cluster was shifted approximately 200 Hz with the amplitudes of the responses of the modes being dramatically reduced. The single layer treatment was also effective at reducing the amplitude of the response peaks over the entire spectrum of measurement. On average, the highest peaks of the frequency response in the undamped condition were reduced by 25 decibels, a reduction of 17.8 times.

The effect of temperature on the damping was quite pronounced as shown in Figure 4.5. As the testing temperature was decreased, the viscoelastic layer became stiffer and damping levels were increased. A comparative listing of the loss factors at different temperature is in Table 4.1 and a plot of the modal loss factors is shown in Figure 4.6. Figure 4.5 shows the trend of increased damping with temperature decrease, and a corresponding shift of modal frequencies to the right as the viscoelastic becomes stiffer. These changes are especially discernible at the lower frequencies.
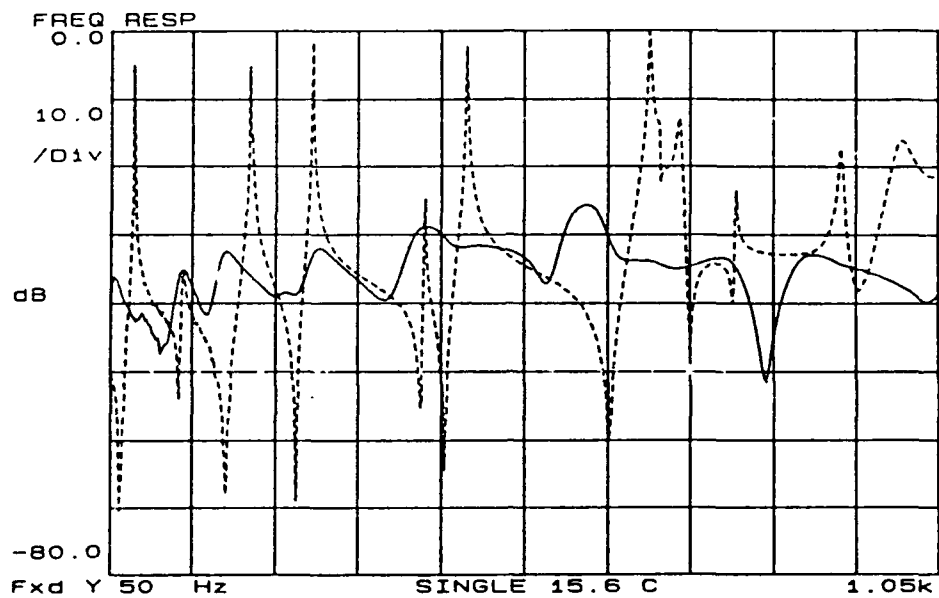
Figure 4.4. Frequency response of the single damping layer at 16.6 °C.

[– – – –: undamped response; ————: damped response]
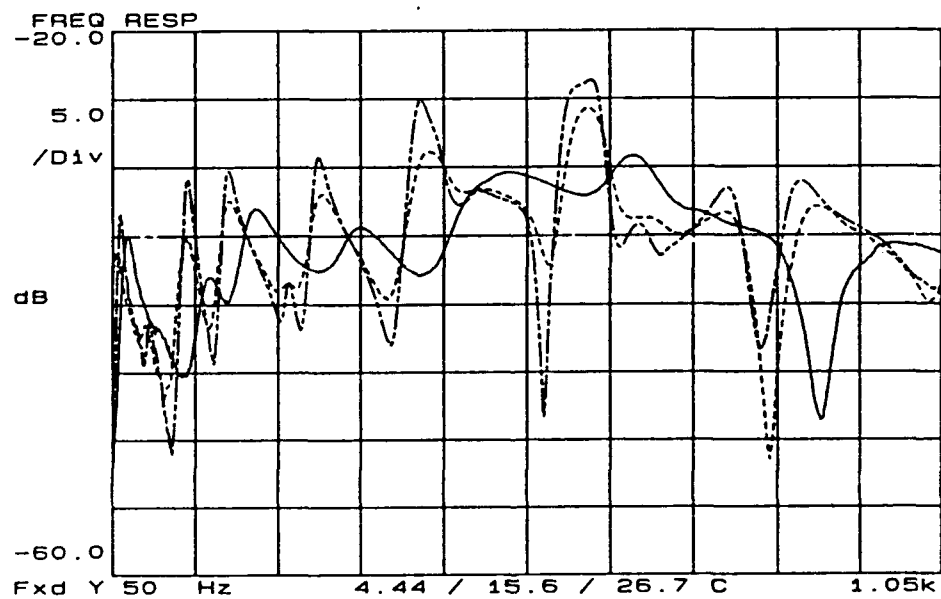
Figure 4.5. Frequency response of the single damping layer configuration

at different temperatures.

[————: 4.44 °C, – – – –: 15.6 °C, ———– – ——: 26.7 °C]

36

TABLE 4.1. MODAL LOSS FACTORS FOR THE SINGLE DAMPING LAYER AT DIFFERENT TEMPERATURE.

4.44 °C (40 °F)		15.6 °C (60 °F)		26.7 °C (80 °F)	
f (Hz)	η	f (Hz)	η	f (Hz)	η
64.3	0.217	53.7	0.223	49.0	0.117
102.8	0.223	89.1	0.145	83.5	0.089
157.4	0.203	138.9	0.172	129.6	0.082
208.4	0.183	188.1	0.184	177.9	0.072
327.5	0.158	301.6	0.120	243.9	0.062
440.1	0.144	424.8	0.109	409.4	0.053
474.9	0.205	476.8	0.111	450.3	0.066
653.1	0.079	608.1	0.067	552.9	0.068
768.0	0.135	644.2	0.069	586.7	0.052
852.0	0.093	722.5	0.130	629.3	0.042
919.0	0.104	817.6	0.081	681.4	0.096
953.5	0.073	876.6	0.091	790.1	0.049
				858.2	0.056
				978.1	0.069
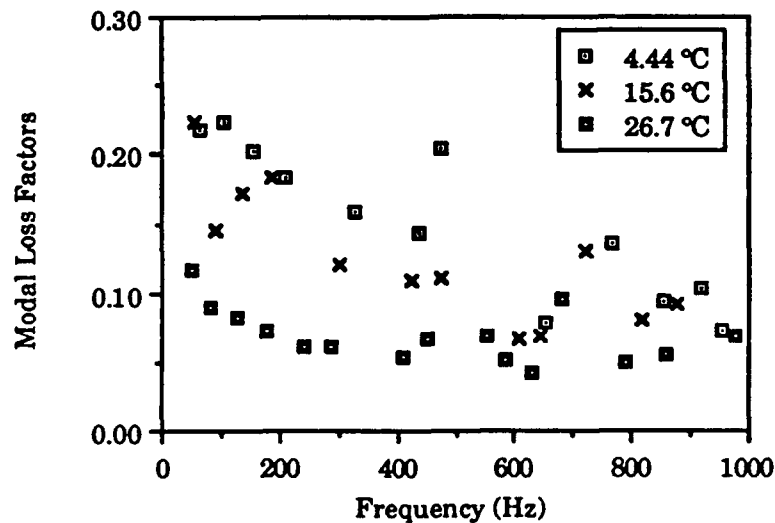
Figure 4.6. Comparison of modal loss factors for the single layer configuration at different temperatures.

D. DOUBLE DAMPING LAYER RESULTS

The double layer damping configuration was also tested at 4.44 °C, 15.6 °C, and 26.7 °C. The frequency response of this configuration at 15.6 °C as compared to the undamped reference plate is shown in Figure 4.7. Damping in the double layer configuration is also high, with modal loss factors ranging form 0.301 at 53.3 Hz to 0.107 at 832.4 Hz. Due to modal coupling loss factors for all modes were not measured. The frequency response of the two–layer configuration is also characterized by a dramatic reduction in response amplitude and a frequency shift to the left. The peak undamped responses were reduced by an average of 27 decibels, or a reduction of 22.4 times from the reference condition.

The effect of temperature on the double layer damping treatment is shown in Figure 4.8. As with the single layer case, damping in the double layer configuration increased with a decrease in temperature. This configuration also shows the shift of modal frequencies to the right as temperature decreases and the viscoelastic becomes stiffer. Modal loss factors for the double layer configuration are listed in Table 4.2, and are plotted for comparison in Figure 4.9.

To compare the effectiveness of the single layer and double layer configurations their frequency responses at 15.6 °C are plotted in Figure 4.10 with a plot comparing modal loss factors in Figure 4.11. The two responses are quite similar although the double layer configuration does show an increase of approximately 22 percent in modal loss factor.

38
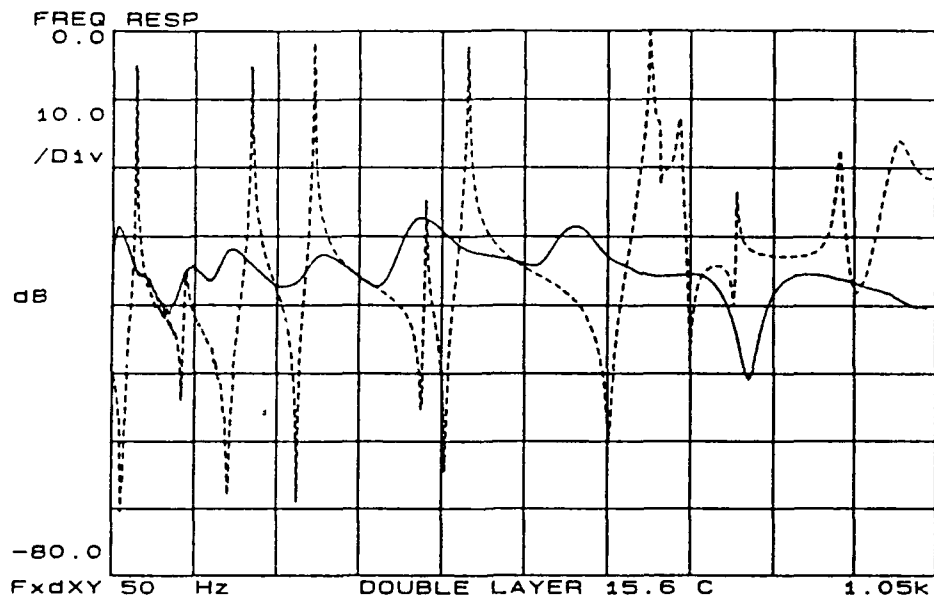
Figure 4.7. Frequency response of the double layer at 15.6 °C.

[– – – – : undamped response , ———— : damped response]
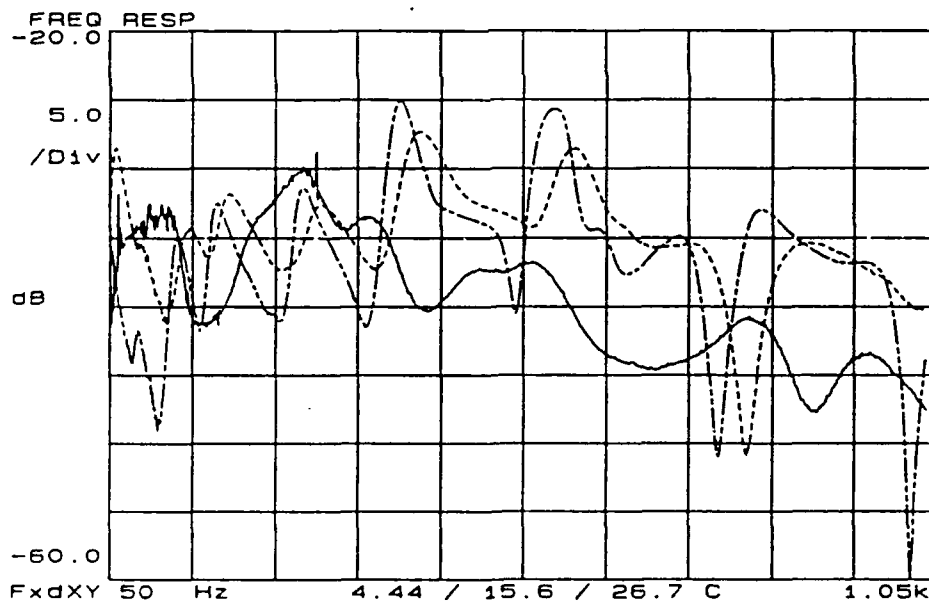
Figure 4.8. Frequency response comparison of the double layer

configuration at different temperatures.

[———— : 4.44 °C , – – – – : 15.6 °C , ——– · · ———— : 26.7 °C]

TABLE 4.2. MODAL LOSS FACTORS FOR THE DOUBLE LAYER
CONFIGURATION AT DIFFERENT TEMPERATURE

4.44 °C (40 °F)		15.6 °C (60 °F)		26.7 °C (80 °F)	
f (Hz)	η	f (Hz)	η	f (Hz)	η
51.9	0.273	55.3	0.301	49.7	0.202
122.5	0.224	87.1	0.215	81.9	0.188
212.7	0.187	142.1	0.217	127.6	0.156
290.5	0.197	190.5	0.212	172.4	0.117
382.7	0.174	297.8	0.139	278.2	0.097
494.2	0.144	366.8	0.154	317.7	0.077
558.2	0.169	419.3	0.125	396.1	0.070
602.2	0.198	441.2	0.100	428.5	0.077
642.4	0.157	618.7	0.098	602.0	0.067
752.8	0.168	680.9	0.096	638.4	0.072
815.4	0.159	715.5	0.060	738.0	0.071
896.3	0.156	832.4	0.107	802.6	0.077
968.3	0.130			846.1	0.050
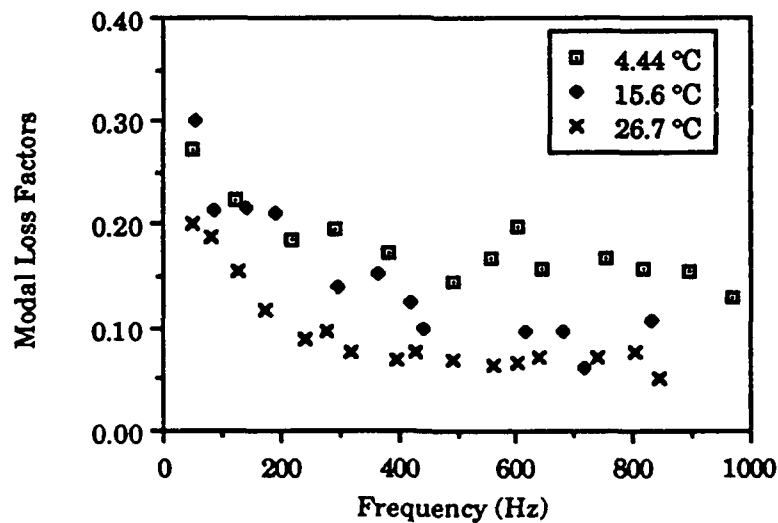
Figure 4.9. Comparison of modal loss factors for the double layer at different temperature.
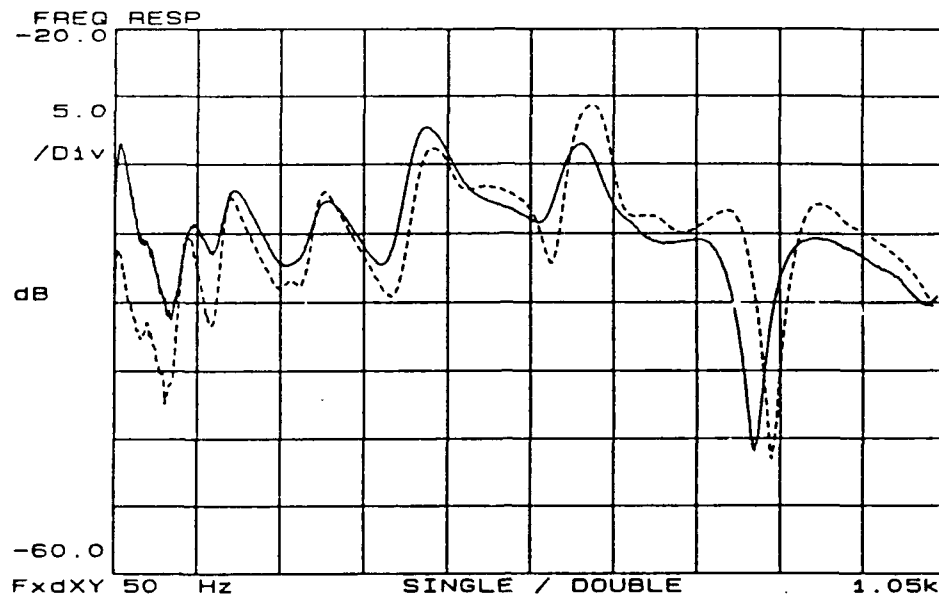
Figure 4.10. Frequency response of the double and
single layer at 15.6 °C (60 °F).
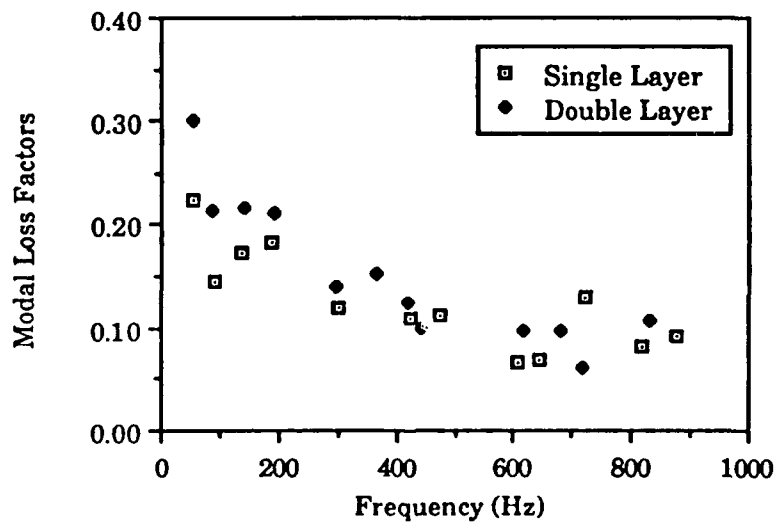
Figure 4.11. Single and double layer modal loss factor comparison.

E.   POCKET PLATE RESULTS

The milled pocket plate was constructed as previously shown in Figure 3.3. The constraining layer, or cover plate, was welded in place using tack welds in an attempt to keep the damping material away from the heat of welding, and the cover plate from warping, instead of using a continuous weld bead as was previously attempted [Ref. 2]. The cover plate was welded to the base at the corners, at the midpoint of the short side and at three equally spaced locations along the long dimension as shown in Figure 4.12. Following welding the plate was tested to ensure that the viscoelastic had not been damaged by the heat of welding.
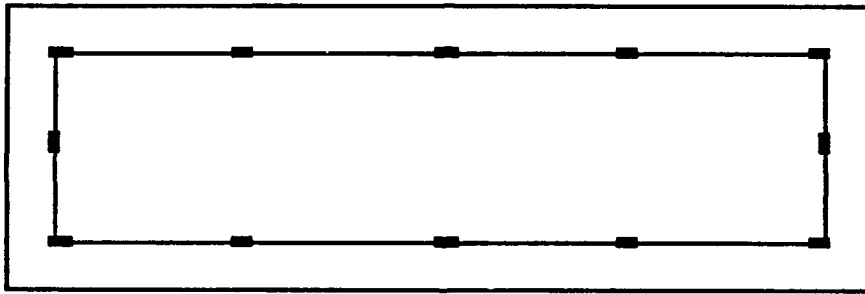
Figure 4.12. Location of tack welds on the cover plate
of the pocket plate configuration.

The pocket plate was tested at 15.6 °C (60 °F) and the frequency response is shown in Figure 4.13. The response indicates that the viscoelastic layer was not damaged by welding and that good damping was attained. Modal loss factors ranged from 0.067 at 62.1 Hz to 0.090 at 923 Hz. Although damping is good, it is approximately half that of the single layer configuration. One reason for this is that the viscoelastic material does not

42

completely cover the base structure. Another reason is the presence of the welded cover plate. Due to the welded conditions the cover plate cannot induce shear deformation in the viscoelastic layer as well as a true constraining layer, and therefore produces less damping than the single layer configuration. The effects of the welded cover plate are especially felt in modes below 300 Hz where the frequency response is quite peaked. The response curve becomes more rounded and the effects of the damping layer are seen as frequency increases.

The modal loss factors for the pocket plate are listed in Table 4.3 and are plotted in Figure 4.14. Even though the damping is less than the single layer, the plate is still adequately damped as shown in the frequency response plot in Figure 4.13. In this configuration the modal loss factors remained relatively constant throughout the testing spectrum. The increase in modal loss factor values above 800 Hz is due primarily to modal coupling, and the measured modal loss factors in this range are not reliable.
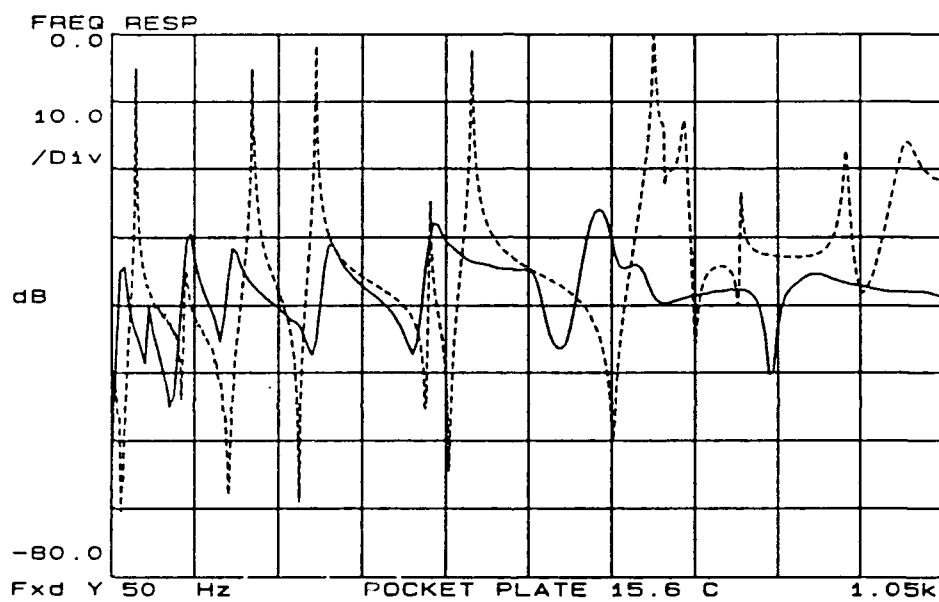
Figure 4.13. Frequency response of the pocket plate at 15.6 °C (60 °F).

[— — — — : reference plate , ———— : pocket plate]

44

TABLE 4.3 MODAL LOSS FACTORS FOR THE
POCKET PLATE CONFIGURATION.

f (Hz)	η	f (Hz)	η
62.1	0.067	565.3	0.043
93.4	0.042	625.7	0.047
142.0	0.056	643.2	0.049
194.9	0.060	687.0	0.044
308.9	0.051	841.9	0.056
437.5	0.041	891.5	0.077
495.6	0.036	923.0	0.090
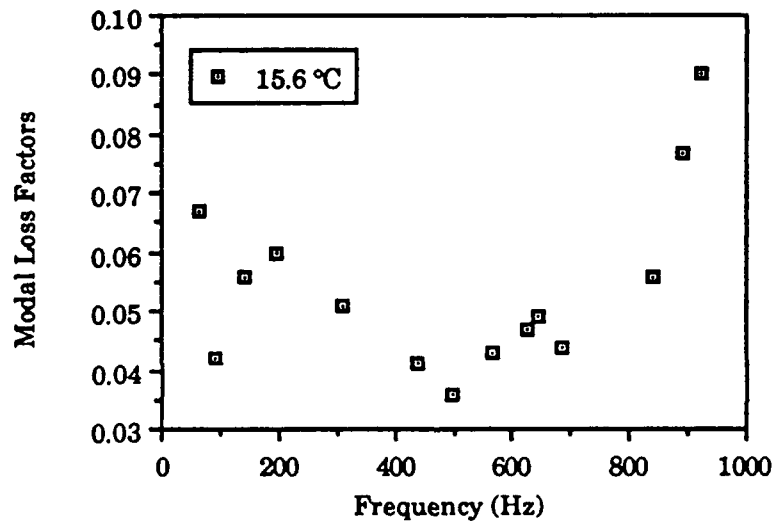
Figure 4.14. Modal loss factors versus frequency for
the pocket plate configuration.

F.   FLOATING ELEMENT RESULTS

The milled "floating element" configuration was constructed as previously shown in Figure 3.7. The cover plate was welded in a fashion similar to the pocket plate as shown in Figure 4.12. The center constraining layer, or floating element, was made slightly smaller than the surrounding structure thus allowing the floating element to act as a "true" constraining layer.

The frequency response of the floating element configuration at 15.6 °C (60 °F) is shown in Figure 4.15. The floating element is quite effective as the response shows a good reduction in peak modal response. Measured modal loss factors range from 0.089 at 66 Hz to 0.064 at 935 Hz. A listing of measured modal loss factors is in Table 4.4 and are plotted in Figure 4.16. As with the previous cases, the frequency response of the floating element configuration is characterized by a frequency shift to the left and a smoothing of the response as frequency increases.

In a comparison of the pocket plate and floating element configurations, the frequency responses are plotted in Figure 4.17. A comparison of modal loss factors for the two configurations is shown in Figure 4.18. The two frequency response plots are similar, however, the frequency response of the floating element configuration is more rounded than that of the pocket plate. The major difference between the two configurations is seen in Figure 4.18. Modal loss factors for the floating element show an average increase of 25 percent over those of the pocket plate. Reasons for this increase are the added constraining effect of the floating element and additional layer of damping material present
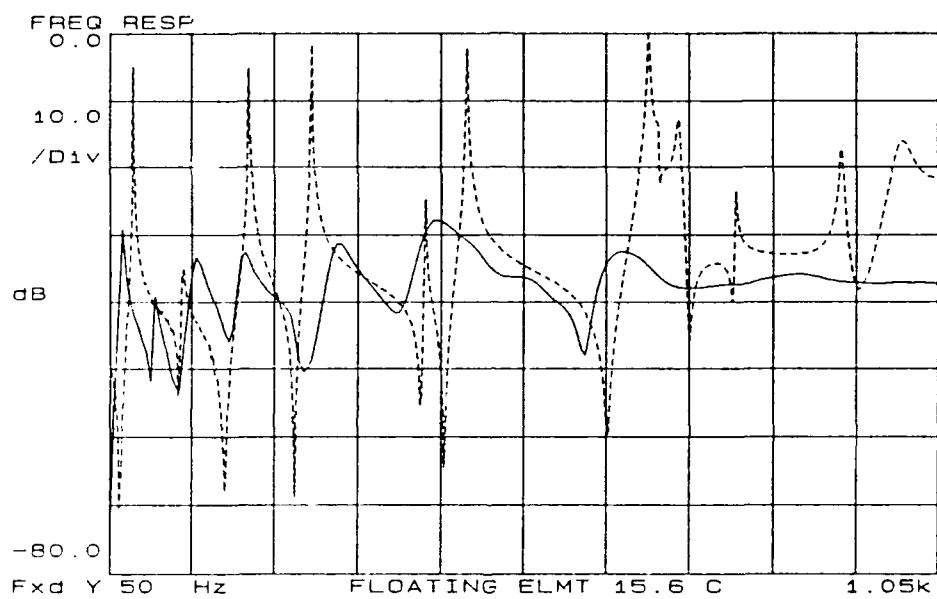
Figure 4.15. Frequency response of the floating element at 15.6 °C (60 °F).

[– – – – : undamped plate , ——— : floating element]

47

TABLE 4.4 MEASURED MODAL LOSS FACTORS FOR THE FLOATING ELEMENT CONFIGURATION.

f (Hz)	η	f (Hz)	η
66.0	0.089	508.1	0.089
104.9	0.040	540.6	0.115
154.0	0.094	618.7	0.121
211.4	0.058	656.7	0.100
272.8	0.063	708.6	0.088
323.5	0.075	857.6	0.089
435.8	0.090	935.4	0.064
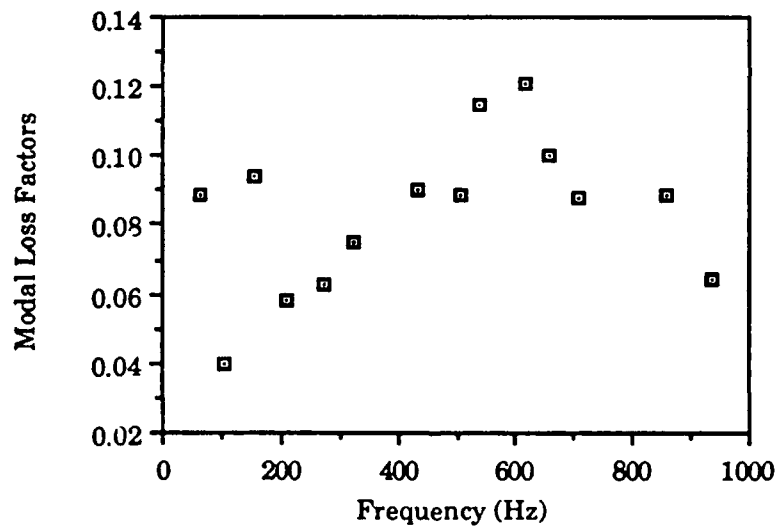
Figure 4.16. Modal loss factors for the floating element configuration.

48
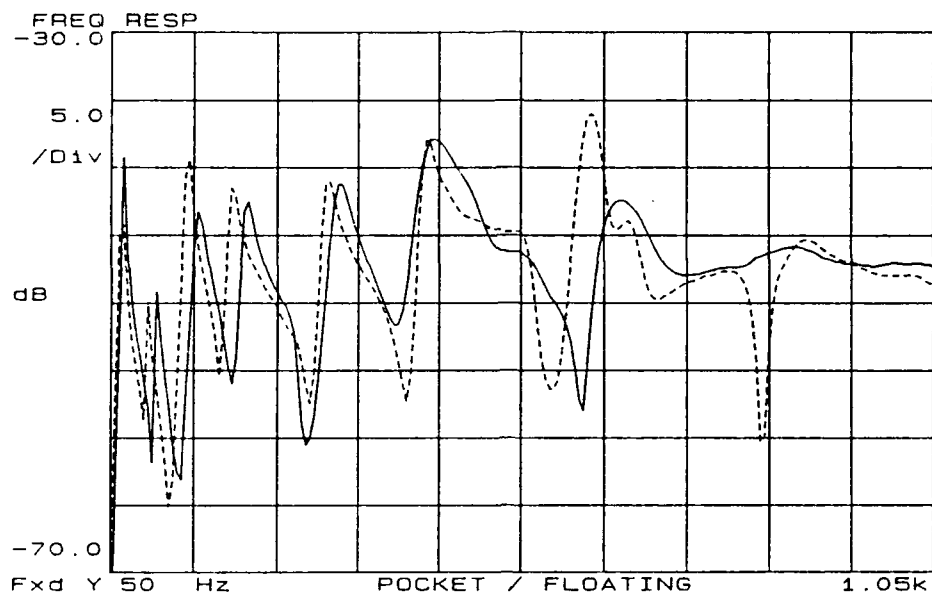
Figure 4.17. Frequency response comparison for the pocket plate and
floating element configurations.

[− − − − : pocket plate , ——— : floating element]
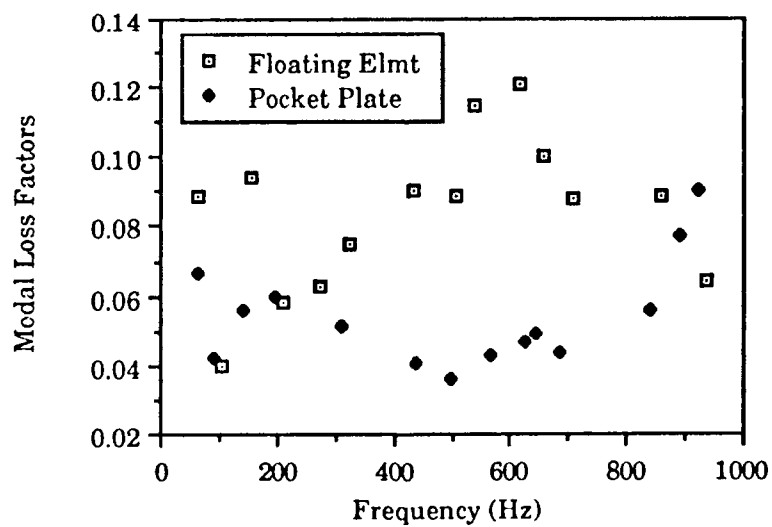
Figure 4.18. Modal loss factor comparison for the pocket plate and floating
element configurations.

49

V. FINITE ELEMENT RESULTS

A. UNDAMPED REFERENCE PLATE

The first step in the finite element analysis procedure was to model and analyze the undamped reference plate for its modal frequencies and frequency response. The finite element model was generated using PATRAN, a computer aided interactive graphics program developed by PDA Engineering. PATRAN is widely used for conceptual, preliminary, and detailed design and analysis of complex systems. One of PATRAN's major advantages is in the interactive construction of finite element models for use by MSC/NASTRAN, and its ability to display MSC/NASTRAN results in an easily understood graphic format [Ref. 15].

The reference plate was modeled using 84 plate (QUAD4) elements as shown in Figure 5.1. The QUAD4 element is an isoparametric element with four nodes, one at each corner of the element [Ref. 7]. A normal mode extraction was then performed in order to compare numerical results with experimentally determined modal frequencies. Once satisfactory agreement between the modal frequencies calculated in NASTRAN and those obtained experimentally was attained, a direct frequency response calculation was performed in NASTRAN. This frequency response was then used as the reference response for further finite element models incorporating viscoelastic damping treatments. The excitation for the frequency response calculation was a sinusoidal force with an amplitude of 1.0 applied at node 66. The response point was node 58 as shown in Figure

50

5.1. These two nodes correspond to the points on the plates used in the experimental portion of the research where the vibration generator and accelerometer were attached.
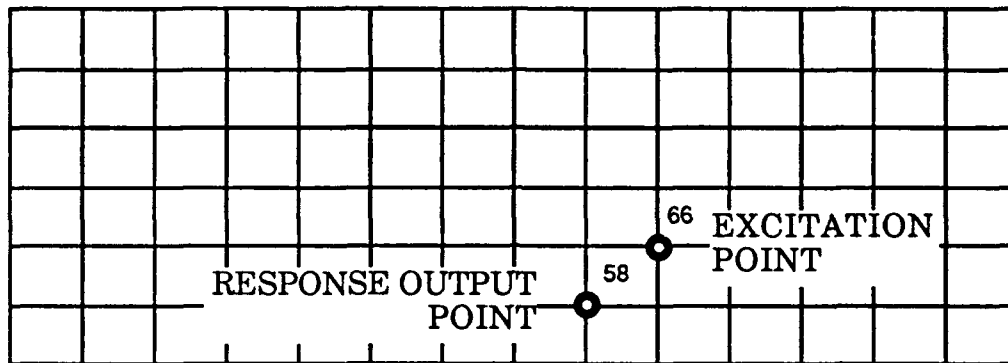
Figure 5.1. Finite element model of the undamped reference plate.

B.   SINGLE DAMPING LAYER

The modeling of the single constrained layer damping system was done using techniques described by Joh son and Kienholz [Ref. 1]. As shown in Figure 5.2, the viscoelastic layer is modeled using solid (HEXA) elements, while the base layer and constraining layer were modeled using QUAD4 elements. The HEXA element is a solid, isoparametric element having eight nodes, one at each corner of the element with three translational degrees of freedom at each node [Ref. 7]. The use of solid elements for the viscoelastic layer allows the strain energy due to shearing to be adequately represented. Plate elements are used in the base layer and constraining layer because of their ability to account for stretching and

bending deformations. The plate element allows its nodes to be offset from the plate's center to the surface of the plate, coincident with the corner nodes of the solid viscoelastic elements [Ref. 1]. Thus, the single constrained layer system was modeled using only two layers of nodes, a simple process in PATRAN. For the single layer configuration, a model having 84 elements per layer, and an element meshing scheme shown in Figure 5.2 was used.
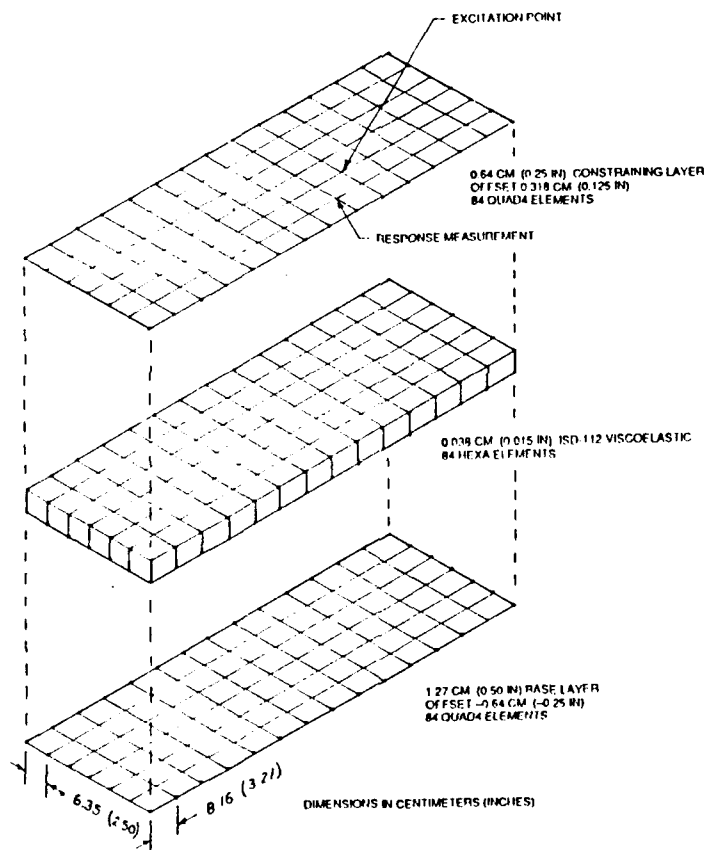
Figure 5.2. Finite element representation of the single constrained layer.

Once the damped plate had been modeled, normal mode extractions were made using MSC/NASTRAN. Five separate runs were conducted using the material properties of ISD–112 at 50, 200, 500, 800, and 1000 Hz and at a temperature of 15.6 °C (60 °F). In addition to the modal frequencies, the strain energy in the viscoelastic elements and the entire model were output from NASTRAN.

Since the shear modulus of a viscoelastic material changes with frequency, it was necessary to estimate the actual modal frequencies of the damped plate using an interpolation procedure outlined by Johnson and Kienholz [Ref. 16]. The first step of the interpolation process was to plot the shear modulus of ISD–112 versus frequency from 5 to 1000 Hz. Then, for the first mode, using NASTRAN results based on ISD–112 material properties a 50 Hz, the first modal frequency predicted by NASTRAN and the corresponding shear modulus were plotted. The same was then done using the first natural frequency predicted by normal mode extraction based on ISD–112 material properties at frequencies of 500 and 1000 Hz. A curve was then passed through these three points. The point where the NASTRAN modal frequencies for the first mode intersected the ISD–112 shear modulus curve was taken to be the interpolated modal frequency of the single damping layer configuration. A plot of the intersection of these two curves for the first and second modes is shown in Figure 5.3. This interpolation process was then repeated for each mode through 1000 Hz.

53
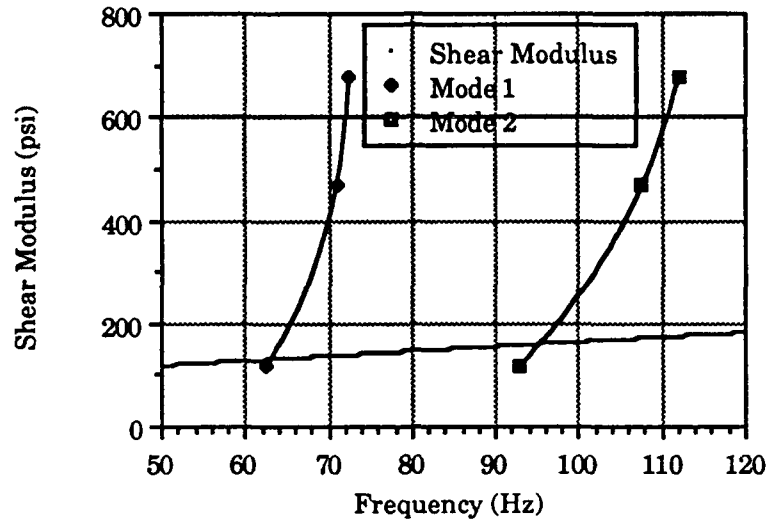
Figure 5.3. Interpolation of the first and second modal frequencies
for the single constraining layer configuration.

Once the interpolated modal frequencies were found, the modal
strain energy equations (2.14) and (2.15) were used to compute modal loss
factors for the single layer configuration. A set of modal loss factors was
computed based on the modal strain energies computed using viscoelastic
properties at reference frequencies of 50 ,200, 500, and 800 Hz. A set of
composite modal loss factors for the modal frequencies near these reference
frequencies was then selected. The resulting modal loss factors are shown
in Table 5.1 and are plotted versus frequency in Figure 5.4. As seen in
Figure 5.4, the modal strain energy method is predicting high damping for
this configuration with an average modal loss factor of 0.195.

TABLE 5.1. MODAL LOSS FACTORS FOR THE SINGLE

LAYER CONFIGURATION AS COMPUTED USING

THE MODAL STRAIN ENERGY METHOD

f (Hz)	η	f (Hz)	η
63	0.249	517	0.237
95	0.181	586	0.217
153	0.234	632	0.164
202	0.212	663	0.155
285	0.229	712	0.180
322	0.214	827	0.134
447	0.200	869	0.152
463	0.108	883	0.115
483	0.258		
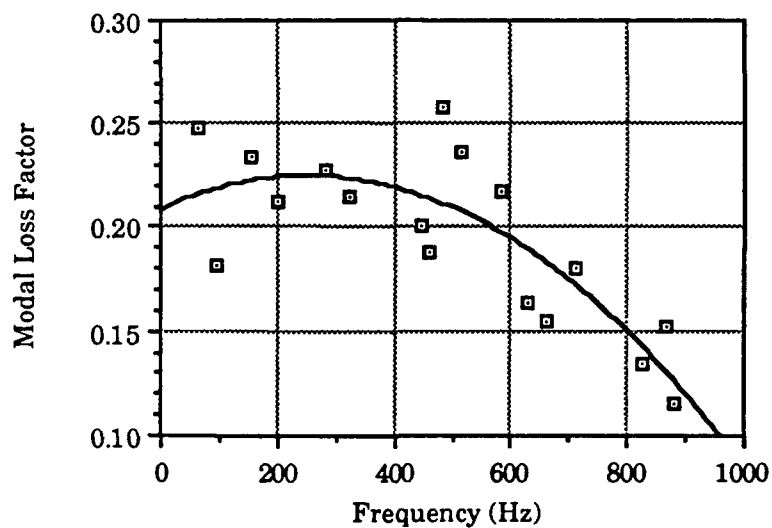
Figure 5.4. Estimated modal loss factors for the single layer configuration with the curve fit used for the MSC/NASTRAN damping table.

Using the set of composite modal loss factors, the modal frequency response of the damped plate was computed using MSC/NASTRAN. Modal damping was introduced to the model using the SDAMP option in the Case Control Deck and the TABDMP1 damping table in the Bulk Data Deck as described in the MSC/NASTRAN Handbook for Dynamic Analysis [Ref. 17]. Since NASTRAN uses a linear interpolation between points in the damping table to describe the modal damping in the model [Ref. 7], a simple curve fit was applied to the set of composite modal loss factors as shown in Figure 5.4. Points from this curve fit were then used in the NASTRAN damping table. To compute the modal frequency response, a unit excitation force was applied at the same node as the undamped plate, and the node used for the response was also the same as the undamped plate.

The results of the modal frequency response calculations are shown in Figure 5.5. The dashed line represents the undamped reference plate, and the solid line represents the modal frequency response of the single layer configuration. Material properties at 200 Hz were used for the ISD–112 damping material. The first thirty modes were used in the modal summation for the response. A listing of the MSC/NASTRAN data deck used to compute the modal frequency response is in Appendix D.
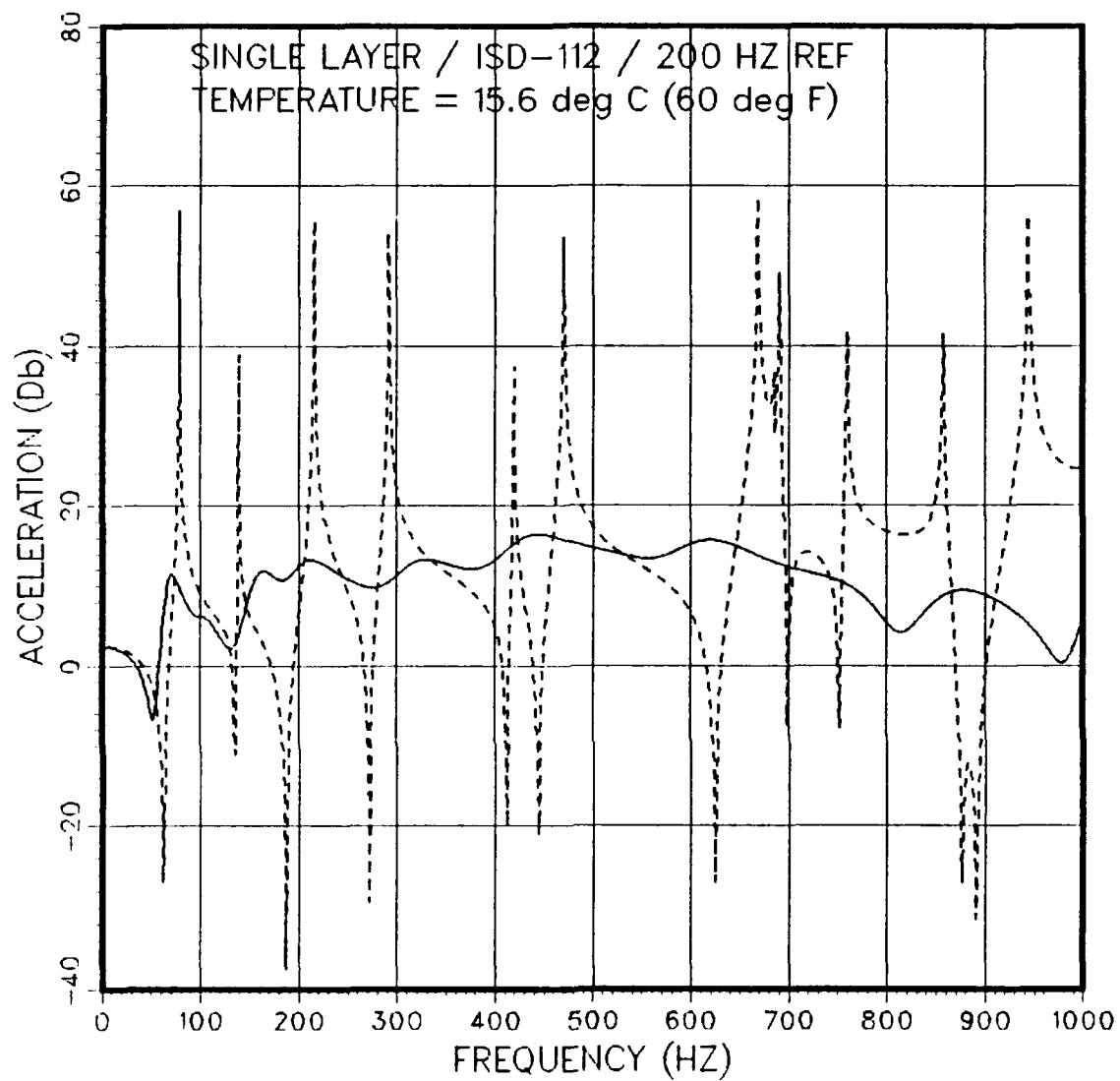
Figure 5.5. Modal frequency response of the single layer

configuration as computed in NASTRAN.

[− − − − : reference plate , ——— : single layer]

57

The modal loss factors estimated using the modal strain energy method are compared to those measured experimentally for the single layer configuration in Figure 5.6. The estimated loss factors are greater than the experimentally determined loss factors throughout the spectrum of interest, and especially in the middle frequencies.

The modal frequency response of the single layer configuration is compared to the experimentally measured frequency response in Figure 5.7. The comparison was accomplished by normalizing both the experimentally determined frequency response and the frequency response computed in NASTRAN. Both responses were normalized using a value of $1.0 \frac{\text{in/sec}^2}{\text{lb}}$. The effects of the greater loss factors estimated by the modal strain energy method are obvious as the level of the predicted response is lower than the measured response. The shift in frequency between the two curves is due to the finite element model being inherently stiffer than the actual system. The correlation between the two curves is especially good below 250 Hz as this is where the differences between estimated and measured modal loss factors are the least.
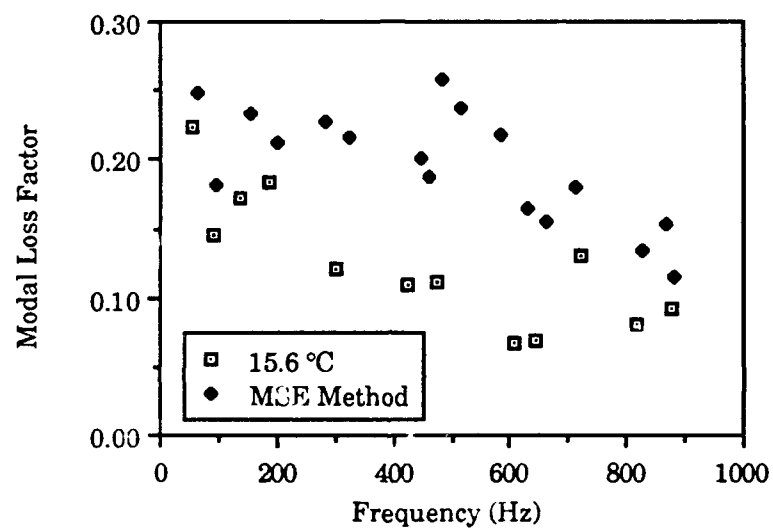
Figure 5.6. Comparison of estimate 1 and measured modal loss factors for the single layer configuration.
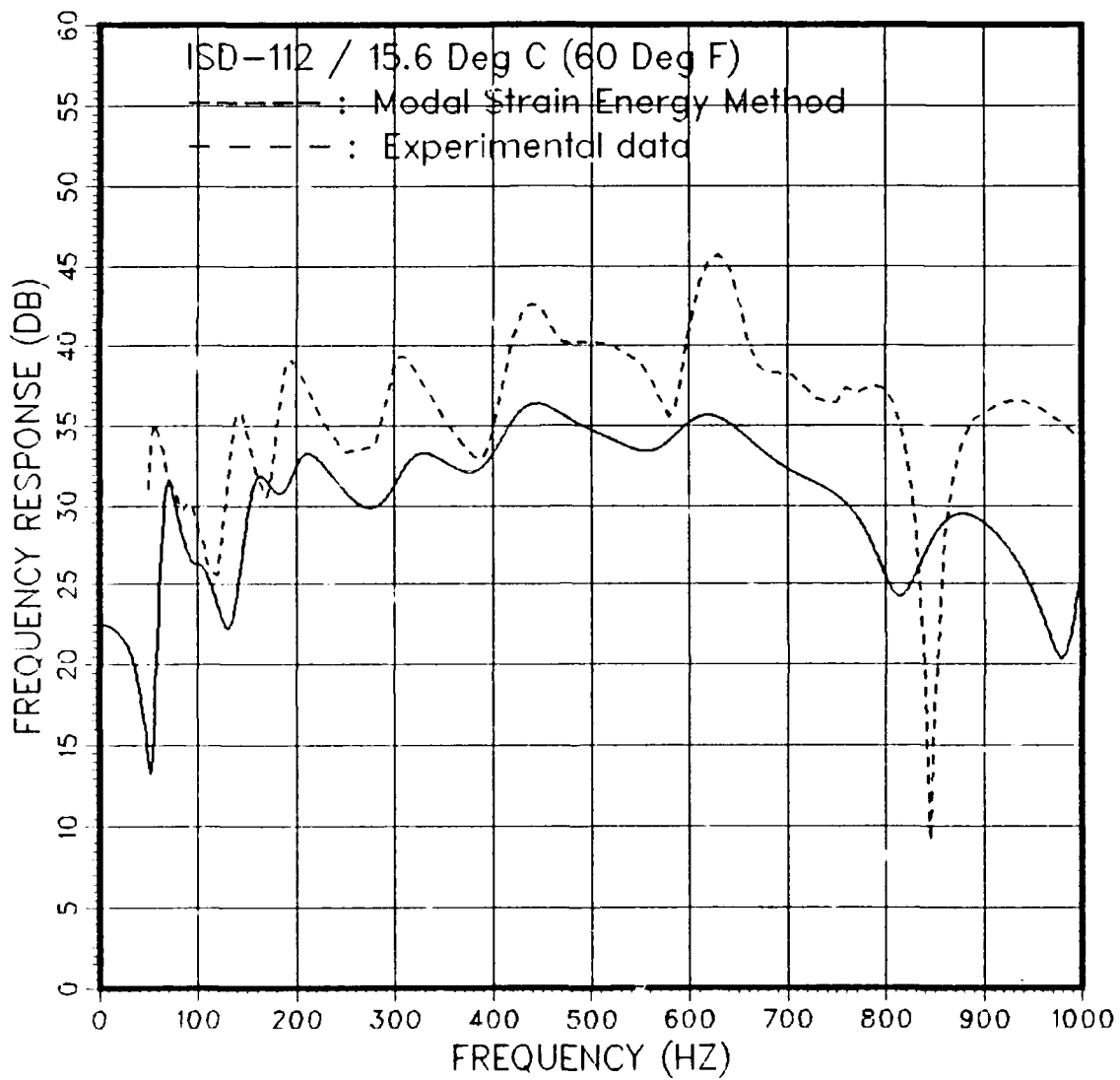
Figure 5.7. Frequency response comparison for
the single layer configuration.

60

C.   DOUBLE DAMPING LAYER

The modeling of the double constrained layer damping system was accomplished as shown in Figure 5.8. The double layer configuration consists of a base layer modeled with offset QUAD4 elements, two viscoelastic layers consisting of HEXA elements, and the top constraining layer modeled with offset QUAD4 elements. The middle constraining layer was modeled using three layers of HEXA elements in order to give this layer the stiffness necessary to act as a constraining layer. The model was meshed using 60 elements in each layer as shown in Figure 5.8.

Using this model, the modal strain energy method was applied to determine approximate modal frequencies and loss factors for the double layer configuration. To determine the loss factors, normal mode extractions were performed using reference frequencies of 50, 200, 500, 800, and 1000 Hz. A composite set of modal loss factors for the double layer system was then compiled based on the estimated modal frequency's relation to the reference frequency used to calculate modal strain energies. This composite set of modal loss factors is listed in Table 5.2, and is plotted in Figure 5.19 as a comparison to the experimentally determined modal loss factors for the double layer configuration. The estimated modal loss factors for the double layer show high damping, but they compare favorably with those measured experimentally.

6 1

RESPONSE MEASUREMENT

EXCITATION POINT

0.318 CM (0.125 IN) CONSTRAINING LAYER
OFFSET 0.159 CM (0.063 IN)
60 QUAD4 ELEMENTS

0.038 CM (0.015 IN) ISD-112 VISCOELASTIC
60 HEXA ELEMENTS

0.318 CM (0.125 IN) CONSTRAINING LAYER
3 LAYERS HEXA ELEMENTS
60 ELEMENT PER LAYER

0.038 CM (0.015 IN) ISD-112 VISCOELASTIC
60 HEXA ELEMENTS

1.27 CM (0.50 IN) BASE LAYER
OFFSET −0.64 CM (−0.25 IN)
60 QUAD4 ELEMENTS

6.35 (2.50)

11.43 (4.50)

DIMENSIONS IN CENTIMETERS (INCHES)

Figure 5.8. Finite element representation of the double layer configuration.

62

TABLE 5.2. ESTIMATED MODAL LOSS FACTORS FOR THE DOUBLE LAYER CONFIGURATION.

f (Hz)	η	f (Hz)	η
59	0.278	544	0.209
89.5	0.219	578	0.141
140	0.239	593	0.131
189	0.213	659	0.177
258	0.214	754	0.102
300	0.205	783	0.076
402	0.179	802	0.144
427	0.176	956	0.077
456	0.264	969	0.111
486	0.242	994	0.048
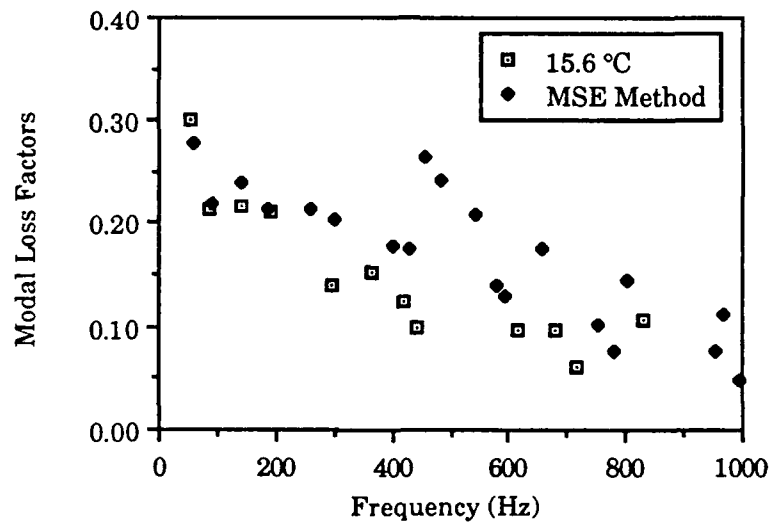
Figure 5.9. Modal loss factors for the double layer configuration as determined from the modal strain energy method and determined experimentally.

The modal frequency response of the double layer configuration was computed in a manner similar to the single layer in that smoothed loss factor data was used in the MSC/NASTRAN damping table. Likewise, a unit excitation force was applied, and the first thirty modes were used in the modal summation. The results of the modal frequency response calculation are shown in Figure 5.10. The dashed line represents the undamped response, and the solid line represents the frequency response of the double layer configuration.

The frequency response calculated using NASTRAN was compared to the experimentally determined frequency response of the double layer configuration as shown in Figure 5.11. Comparison of the two frequency response curves shows similarity in form, but a much lower response level for the numerically determined response. Once again this could be due to the higher damping predicted by the modal strain energy method and the inherently higher stiffness of the finite element model.
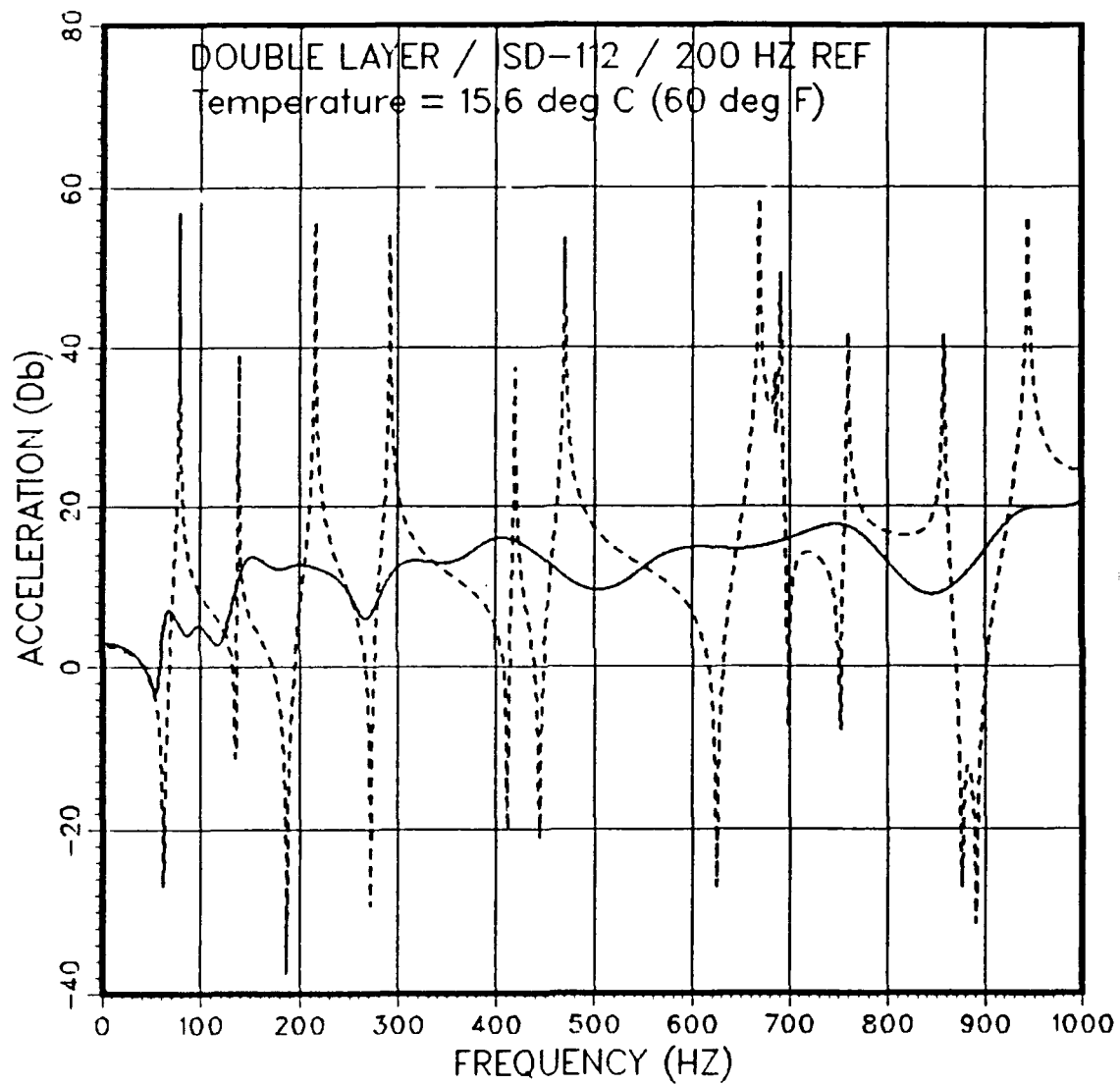
Figure 5.10. Modal frequency response for the double layer

configuration as computed in NASTRAN.

[— — — — : reference plate , ———— : double layer]
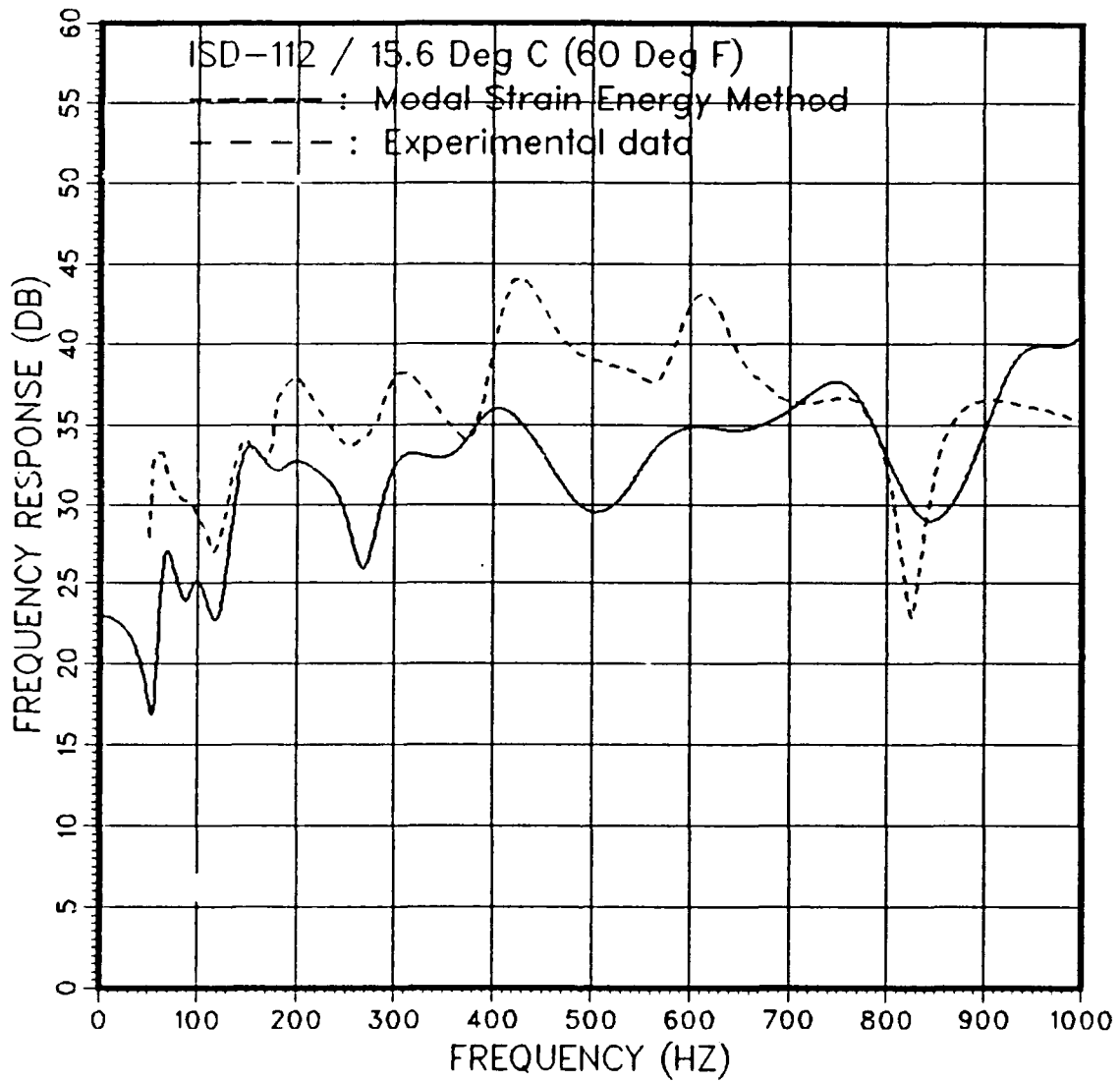
Figure 5.11. Comparison of the experimentally determined
and numerically predicted frequency responses
for the double layer configuration.

D. POCKET PLATE RESULTS

The pocket plate configuration was modeled with the same offset plate elements and solid viscoelastic elements as the single layer configuration. However, the pocket plate required the modeling of the milled structure around the viscoelastic material and the welds between the cover plate and milled plate. A representation of the model is shown in Figure 5.12. The base structure, cover plate, and the structure immediately around the cover plate was modeled using offset plate elements. The viscoelastic material and the portion of the structure immediately adjacent to it were modeled using the solid HEXA elements. Since the viscoelastic material and cover plate are physically separated from the surrounding plate, except where the viscoelastic is adhered to the base structure, care was necessary in creating the finite element mesh.

The model was created in PATRAN using PATRAN's node editing and equivalencing capabilities [Ref. 18]. This allowed the generation of a finite element mesh with two nodes at the same geometric point in space. Using this node editing technique, a mesh was created which allowed the viscoelastic and cover plate to vibrate separately from the surrounding structure, yet at the same time, keep the number of elements and nodes in the model to a minimum. The welded points on the cover plate were also modeled using node editing techniques. At weld points the finite element node on the cover plate was equivalenced with its corresponding node on the base structure, resulting in a single node and a connection between an otherwise separate base structure and cover plate. At non–welded points on the cover plate there were two nodes at the same geometric point; one to

represent the cover plate, and the other to represent the base structure. The model was meshed using a 5x11 mesh resulting in 40 elements in the cover plate, viscoelastic and base layer as shown in Figure 5.12.

Using this modeling scheme, the modal strain energy method was employed to estimate the modal frequencies and loss factors. Normal mode extractions were made using viscoelastic material properties at 50, 200, 500, 800, and 1000 Hz. Using these reference frequencies a composite set of modal loss factors was obtained. These loss factors are listed in Table 5.3 and are plotted versus frequency in Figure 5.13. The estimated loss factors give good damping over the spectrum of interest with an average modal loss factor of 0.075. As with the previous cases, damping values used for the modal frequency response calculation came from a curve–fit to the set of composite modal loss factors.

The modal frequency response of the pocket plate was computed using the first 30 modes and viscoelastic material properties at 200 Hz. The resulting estimated frequency response is shown in Figure 5.14. The response shows a definite frequency shift to the left along with good damping of the frequency response when compared to the undamped response.
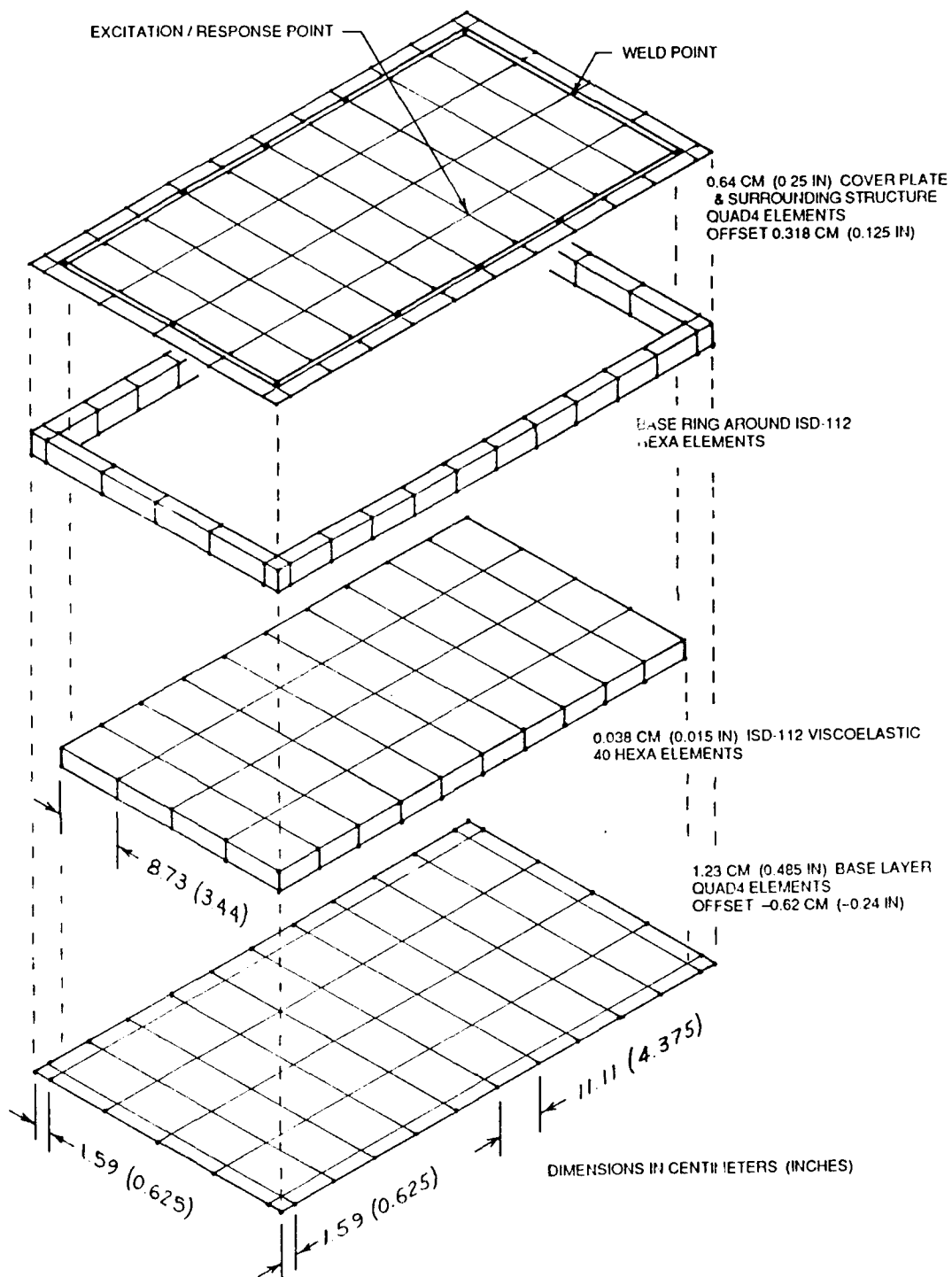
Figure 5.12. Finite element representation of the pocket plate configuration.

TABLE 5.3. ESTIMATED MODAL LOSS FACTORS FOR THE POCKET PLATE CONFIGURATION.

f (Hz)	η	f (Hz)	η
67	0.046	511	0.113
109	0.034	588	0.104
162	0.091	625	0.086
217.5	0.063	668	0.089
295	0.091	713	0.077
333	0.047	831	0.077
453	0.07	834	0.065
477	0.093	868	0.051
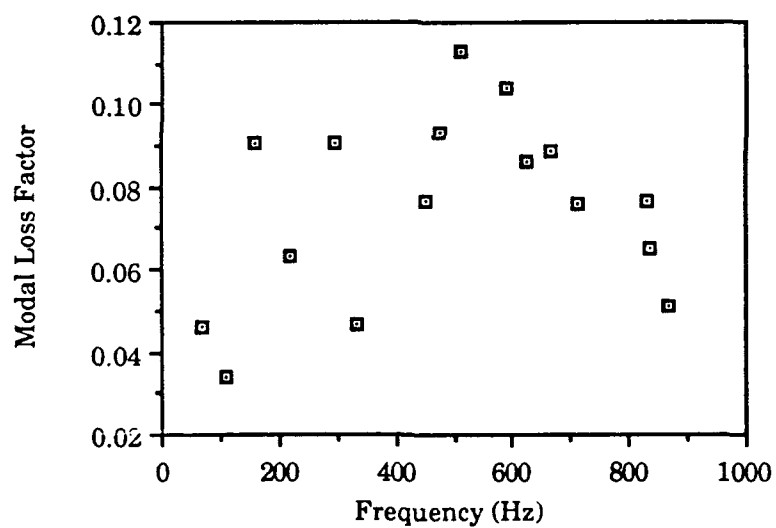
Figure 5.13. Estimated modal loss factors versus frequency for the pocket plate.
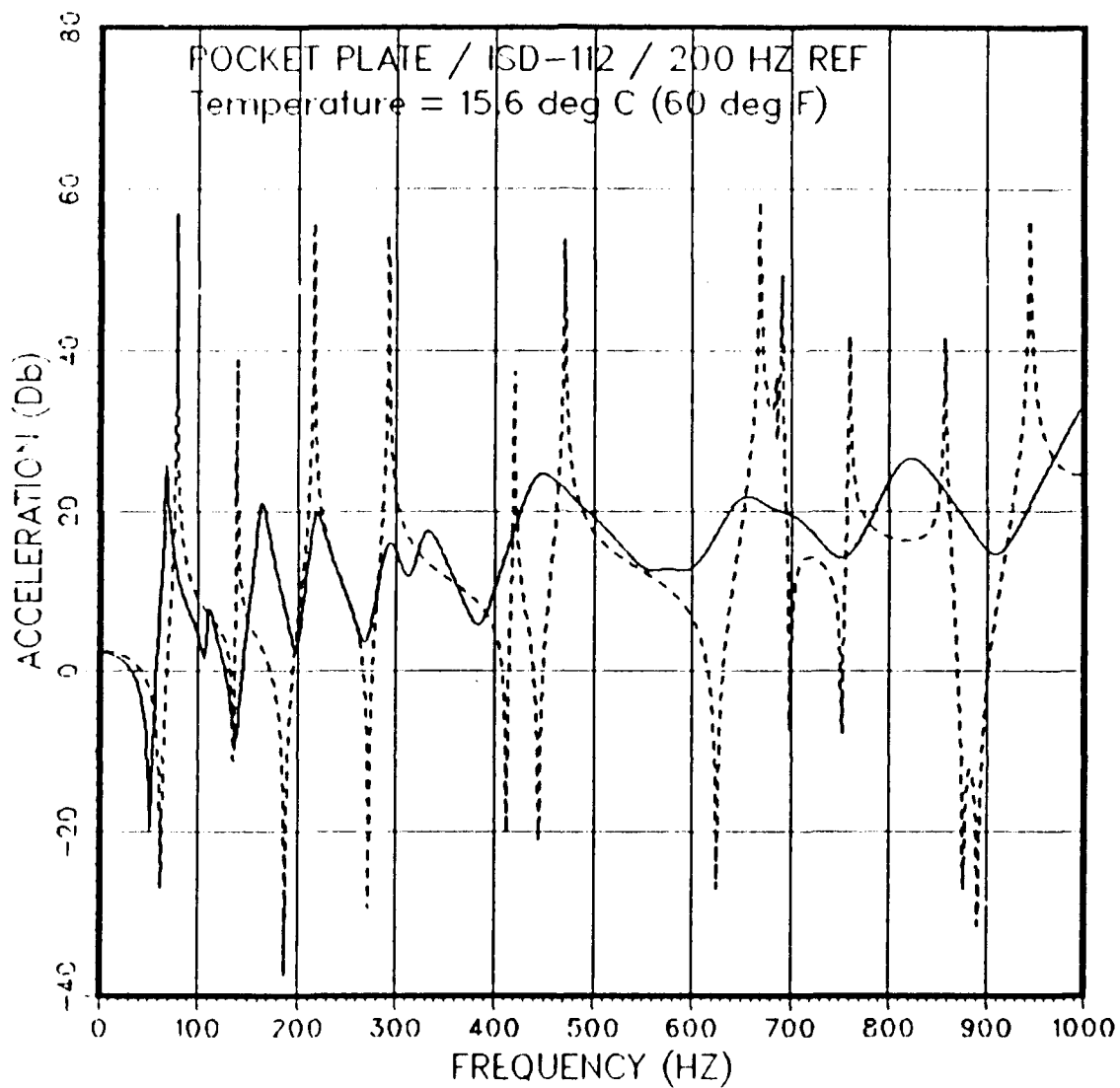
Figure 5.14. Estimated modal frequency response

for the pocket plate configuration.

[————: reference plate , ———— : pocket plate]

The estimated modal loss factors and modal frequency response for the pocket plate were compared to those measured experimentally. The loss factor comparison is shown is Figure 5.15 and the frequency response comparison is shown in Figure 5.16. The estimated modal loss factors are higher than those measured experimentally, however, the frequency responses compare quite favorably with each other. The frequency response curve calculated through finite element analysis has a lower response level and a frequency shift to the right of the measured frequency response. This is expected due to the increase in damping predicted by the modal strain energy method and by the fact that the finite element model is inherently stiffer than the physical system.
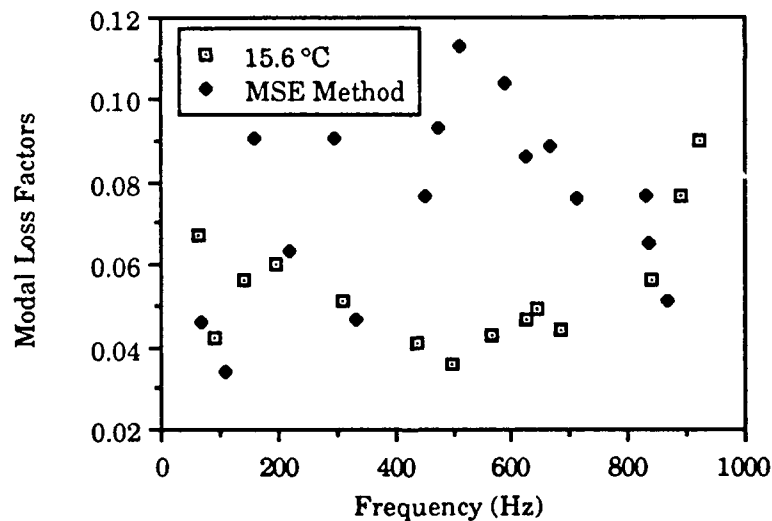
Figure 5.15 Comparison of experimentally measured and numerically estimated modal loss factors for the pocket plate configuration.
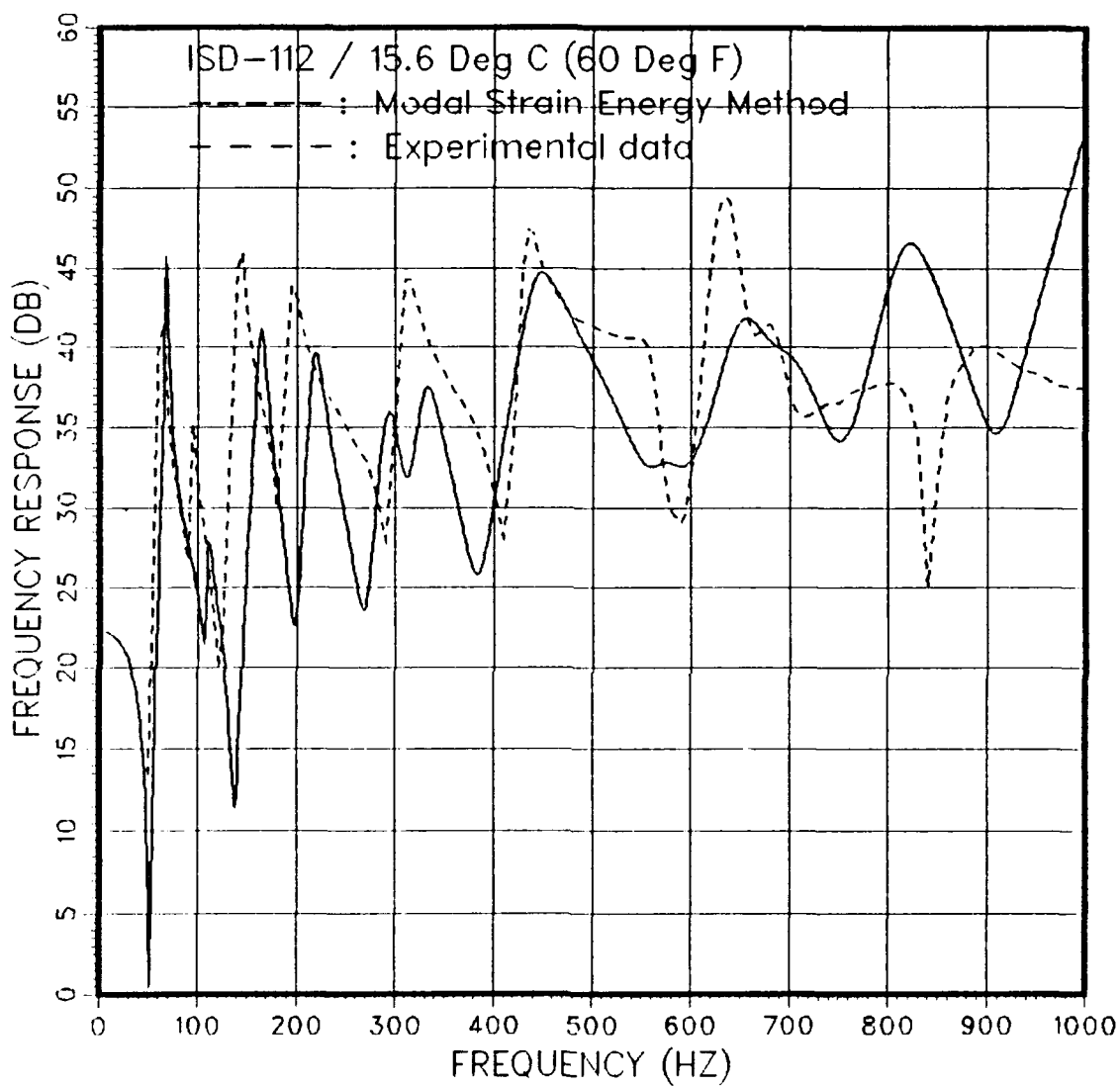
Figure 5.16. Comparison of experimental and predicted frequency
responses for the pocket plate configuration.

73

VI. CONCLUSIONS

Constrained viscoelastic layer damping is an extremely effective method for reducing broadband vibration. In each of the experimental cases the peak amplitudes of frequency response were reduced by approximately 25 decibels, a reduction of 18 times below the undamped reference plate.

Of particular note are the performance of the pocket plate and floating element configurations. Although they are not ideal configurations in terms of "true" constrained viscoelastic layer damping, the damping levels achieved are quite satisfactory. In a final comparison of experimentally determined modal loss factors for the four treatments, the double layer configuration yields the greatest damping and the pocket plate the least. This comparison is shown in Figure 6.1. As was previously reported in Section IV, tl floating element configuration yielded an average increase of 25 percent over the modal loss factors of the pocket plate. It is also noted that the average modal loss factor for the pocket plate is approximately 50 percent of the average modal loss factor of the single layer configuration. Similarly, the average modal loss factor for the floating element configuration is approximately 50 percent that of the double layer treatment.
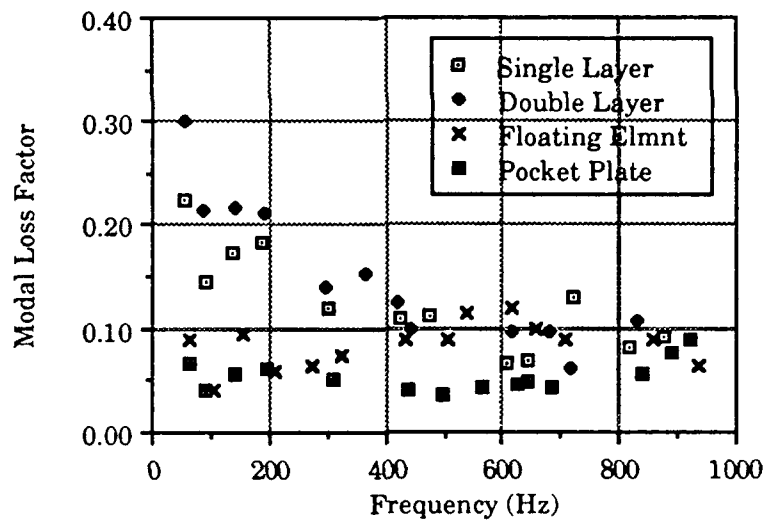
Figure 6.1. Experimental modal loss factor comparison
for the four damping configurations.

The modal strain energy method tends to overpredict the modal loss factors for these highly damped, thick plates. Although the modal strain energy method predicted modal loss factors greater than those measured, the same relative differences in modal loss factor between damping configurations are maintained as shown in Figure 6.2. The estimated modal loss factors for the pocket plate are approximately 60 percent less than those of the single layer configuration This indicates that there is a consistency between the damping values predicted by the modal strain energy method and those of the actual physical system.
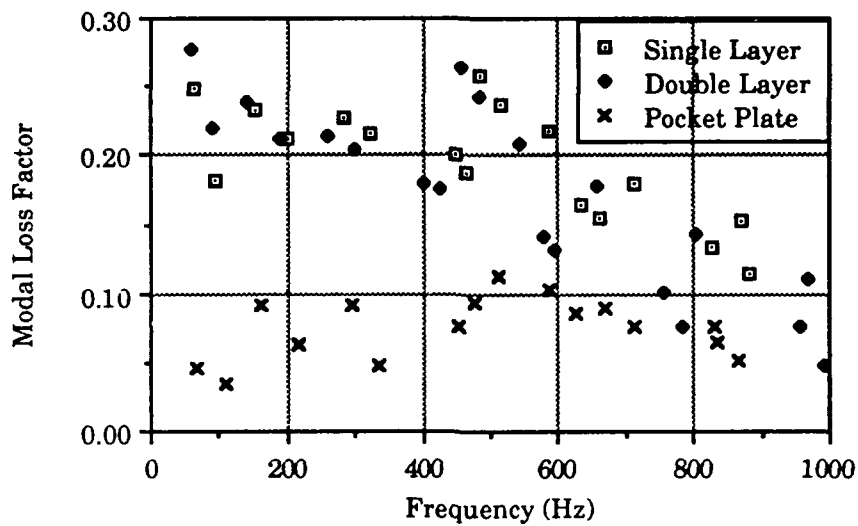
Figure 6.2. Comparison of numerically estimated modal loss factors for the single layer, double layer, and pocket plate configurations.

There are several possible reasons for the differences between the experimentally determined modal loss factors and those estimated by the modal strain energy method. The first is that the material properties of ISD-112 as reported by the 3M Corporation on the reduced frequency nomogram may not be consistent with the material properties actually present in the material used. Since the numerical analysis was based on the reported material properties this is a possible source of uncertainty in the results.

The second source of uncertainty is in the adhesion of the ISD-112 to the aluminum plates. Although the plates were clean when the ISD-112 was applied, it was noted that the adhesive qualities of the ISD-112 were not uniform throughout the material. A lack of adhesion may cause a reduction in the damping capability of the system.

Another source for the difference between the experimental results and numerical results lies within the finite element model. The number of elements used in the model greatly affects its "stiffness." As the number of elements is increased the model should become less stiff and results are expected to approach those that are measured. Also, the type of element used to model the base layer and constraining layer may have an effect. In this research plate elements were used to model both the base and constraining layers. It is possible that one or more layers of solid elements may produce results that agree better with experimental results.

The modal strain energy method is a useful tool for vibration damping design, however, the method appears to overestimate modal loss factors for thick, highly damped plates by as much as 50 percent. In each configuration that was modeled, the modal loss factors estimated below 300 Hz were fairly close to the actual values, and above 300 Hz the difference between estimated as measured loss factors increased.

One drawback to the modal strain energy method in design is the CPU time required for normal mode extraction and modal frequency response; especially in complex structures with a large number of elements. Although the modal strain energy method is good for finalizing a design, it should not be used for design optimization due to the amount of CPU time required for normal mode extraction and modal frequency response calculations.

VII. RECOMMENDATIONS

The thick plate used in this research is a generic model of many physical systems that may see use in naval application. There are several areas which deserve more research and clarification, including the following:

- Model the floating element configuration in finite elements and check the effectiveness of the modal strain energy method in predicting modal loss factors for this configuration.

- Investigate the capability of the modal strain energy method to predict loss factors for thick, lightly damped plate configurations. It is possible that the modal strain energy method works better for lightly damped configurations.

- Investigate methods for improving the adhesion of ISD–112 to the base structure and constraining layer.

- Investigate the possible use of the floating element as an additional vibration absorber by changing its mass in order to damp a specific frequency. In this same idea, the use of tuned dampers along with the constrained layer treatments could be looked at.

APPENDIX A

FORTRAN PROGRAM USED TO COMPUTE MODAL LOSS FACTORS
FOR THE SINGLE DAMPING LAYER DESIGN

This program used the Ross–Kerwin–Ungar equations of Section III to compute estimated modal frequencies and loss factors for the single layer configuration. Modal frequencies for an undamped plate are read from a data file and estimated modal frequencies and loss factors for various layer thicknesses are output to another file. Material properties of ISD–112 are computed using University of Dayton data and curve-fitting equations to the reduced frequency nomogram [Ref. 9,12]. The units used in this program are pounds, inches, and seconds.

```
      PROGRAM CARPET
C ***********************************************************************
C  THIS PROGRAM IS TO CALCULATE SYSTEM LOSS FACTORS FOR VARIOUS
C  TEMPERATURES AND MODES OF A CONSTRAINED LAYER VISCOELASTIC
C  DAMPING SYSTEM USING THE ROSS-KERWIN-UNGAR EQUATIONS.  SYSTEM LOSS
C  FACTORS ARE COMPUTED FOR A TEMPERATURE RANGE OF 30-100 DEGREES
C  FARENHEIT.  BASE PLATE THICKNESSES VARY FROM 0.375 TO 0.75 INCHES
C  IN 0.125 INCREMENTS.  FOR EACH BASE PLATE THICKNESS, THE VISCOELASTIC
C  THICKNESS IS VARIED FROM 0.015 TO 0.060 INCHES IN 0.015 INCH
C  INCREMENTS.  FOR EACH VISCOELASTIC THICKNESS THE CONSTRAINING
C  LAYER THICKNESS IS VARIED FROM 0.0625 TO 0.25 INCHES IN
C  0.0625 INCH INCREMENTS.
C  THIS PROGRAM APLIES TO A FREE-FREE-FREE-FREE PLATE.
C
C  THE VISCOELASTIC MATERIAL IS 3M ISD-112.
C
C  THE FOLLOWING COEFFICIENTS ARE DEFINED:
C       E1 = YOUNG'S MODULUS OF BASE PLATE (PSI)
C       E2 = YOUNG'S MODULUS OF VISCOELASTIC LAYER (PSI)
C       E3 = YOUNG'S MODULUS OF CONSTRAINING LAYER (PSI)
C       G2 = SHEAR MODULUS OF VISCOELASTIC MATERIAL (PSI)
C       NU1 = POISSON'S RATIO OF BASE PLATE
C       NU2 = POISSON'S RATIO OF VISCOELASTIC MATERIAL
C       H1 = THICKNESS OF BASE PLATE (IN)
C       H2 = THICKNESS OF VISCOELASTIC LAYER (IN)
C       H3 = THICKNESS OF CONSTRAINING LAYER (IN)
C       HTOT = TOTAL PLATE THICKNESS (IN)
C       RHO1 = DENSITY OF BASE PLATE (LBF-SEC**2/IN**4)
C       RHO2 = DENSITY OF VISCOELASTIC MATERIAL
C       RHO3 = DENSITY OF CONSTRAINING LAYER
C       TO,FROM,MROM.N,ML,ETFROL,SL,SH,FROL, & C ARE COEFFICIENTS
C         FOR THE REDUCED FREQUENCY NOMOGRAM EQUATIONS
C       FP = MODAL FREQUENCY OF THE UNDAMPED BASE PLATE (HZ)
C       FCP = MODAL FREQUENCY OF THE COMPOSITE PLATE (HZ)
C       ETA2 = LOSS FACTOR OF VISCOELASTIC MATERIAL
C       ETAS = SYSTEM LOSS FACTOR
C       KQR = WAVE NUMBER OF PLATE
C       GC = GRAVITATIONAL CONSTANT (IN/SEC**2)
C       T = TEMPERATURE OF VISCOELASTIC MATERIAL (DEG F)
C       WP = MODAL FREQUENCY OF UNDAMPED PLATE (RAD/SEC)
C       FP = MODAL FREQUENCY OF UNDAMPED PLATE (HZ)
C       WCP = MODAL FREQUENCY OF DAMPED PLATE (RAD/SEC)
C       FCP = MODAL FREQUENCY OF DAMPED PLATE (HZ)
C
C  THE UNITS USED IN THIS PROGRAM ARE LB, INCH, SEC, DEGREES F
C
C  UNDAMPED MODAL FREQUENCIES ARE FROM A FINITE ELEMENT ANALYSIS
C  OF THE FREE-FREE-FREE-FREE PLATE.
C
C  RESULTS ARE OUTPUT TO DATA FILE "LOSFCTR DATA"
C  PRIOR TO RUNNING THE PROGRAM TYPE THE COMMAND
C       "FILEDEF LOSFCTR DISK LOSFCTR DATA"
C
C  FINITE ELEMENT MODAL FREQUENCIES ARE INPUT FROM FILE:
C       "PLTFRQ DATA"
C
C ***********************************************************************
C
      REAL E1,E2,E3,NU1,NU2,H1,H2,H3,RHO1,RHO2,RHO3,HTOT
      REAL TO,FROM,MROM,N,ML,ETFROL,SL,SH,FROL,C
      REAL FP,FCP,ETA2,ETAS,KQR,PI,GC,T
      REAL FR10,ETA210,SUB1,SUB2,SUB3,M10
      REAL H21,H31,G,C1,ALPHRE,ALPHIM,BRE,BIM,DELRE
      REAL DELIM,EHCUBE,SUB4,SUB5,WP,WCP,DENS,SUB6,SUB7,SUB8
      INTEGER V
      DIMENSION WP(8)
      PI=4.*ATAN(1.)
C
      OPEN(UNIT=10,FILE='LOSFCTR',STATUS='OLD')
      OPEN(UNIT=11,FILE='PLTFRQ',STATUS='OLD')
C
C  ASSIGN MATERIAL CONSTANTS FOR BASE PLATE,CONSTRAINING LAYER
```

80

```
C   AND VISCOELASTIC
C
        E1=1.0E7
        H1=0.750
        RHO1=.0968
        NU1=.33
        RHO2=.035
        E3=1.0E7
        RHO3=.0968
        GC=386.
        NU2=.5
C
C   DEFINE CONSTANTS FOR NOMOGRAM EQUATIONS
C
        TO=104.0
        FROM=2.0E4
        MROM=688.94
        N=.275
        ML=8.7
        ETFROL=1.08
        SL=0.45
        SH=-.55
        FROL=5000.0
        C=2.5
C
C   BASE PLATE THICKNESS LOOP
C
        H1=0.375
        DO 100 J=1,4
        WRITE(10,703) 'BASE PLATE THICKNESS, H1=',H1
703     FORMAT(A27,F4.3)
        WRITE(10,*)
C
C   VISCOELASTIC THICKNESS LOOP
C
        H2=0.015
        DO 150 V=1,4
C
C   CONSTRAINING LAYER THICKNESS LOOP
C
        H3=0.0625
        DO 200 L=1,4
        WRITE(10,702) 'VISCOELASTIC LAYER THICKNESS, H2=',H2
        WRITE(10,*)
        WRITE(10,702) 'CONSTRAINING LAYER THICKNESS, H3=',H3
702     FORMAT(A35,F6.4)
        WRITE(10,*)
        WRITE(10,700) 'TEMP','MODE','FCP','ETA2','ETAS','G2'
700     FORMAT(A8,3X,A5,4A15)
C
C   PLATE MODE LOOP, READ MODAL FREQUENCY AND COMPUTE WAVE NUMBER
C
        HTOT=H1+H2+H3
        DO 300 I=1,8
        READ(11,*) WP(I)
C
C   CALCULATE MODAL FREQUENCY AND WAVE NUMBER OF BASE PLATE
C
        SUB7 = SQRT((E1*(HTOT**3)*GC)/(12.*(1.-NU1**2)*RHO1*H1))
        KQR=WP(I)/SUB7
        FP=WP(I)/(2.*PI)
C
C   TEMPERATURE LOOP
C
        T=30.0
        DO 400 K=1,15
C
C   CALCULATE PROPERTIES OF VISCOELASTIC FOR GIVEN TEMPERATURE AND
C   MODE
C
501     FR10=LOG10(FP)-(12.*(T-TO))/(525.+T-TO)
        FR=10.**(FR10)
```

```fortran
        A=(FR10-LOG10(FROL))/C
        SUB1=C*((SL+SH)*A+(SL-SH)*(1.-SQRT(1.+A**2.)))/2.
        ETA210=LOG10(ETFROL)+SUB1
C
C   VISCOELASTIC LOSS FACTOR
C
        ETA2=10.**(ETA210)
        SUB2=2.*LOG10(MROM/ML)
        SUB3=1.+(FROM/FR)**N
        M10=LOG10(ML)+SUB2/SUB3
C
C   VISCOELASTIC SHEAR MODULUS
C
        G2=10.**(M10)
C
C   VISCOELASTIC YOUNG'S MODULUS
C
        E2=G2*2.*(1.+NU2)
C
C   CALCULATIONS FOR DAMPED PLATE AT TEMPERATURE T USING ROSS-
C   KERWIN-UNGAR EQUATIONS
C
        G=G2/(E3*H3*H2*KQR)
        H21=(H1+H2)/2.
        H31=H2+(H1+H3)/2.
        C1=E1*H1*(1.+G)+G*E3*H3
        D=G*ETA2*(E1*H1+E3*H3)
        ALPHRE=G*E1*H1*E3*H3*(H31**2.)*(C1+D*ETA2)
        ALPHIM=G*E1*H1*E3*H3*(H31**2.)*C1*ETA2
        BRE=E1*H1*E2*H2*H31*(C1+D*ETA2)
        BIM=E1*H1*E2*H2*H31*(C1*ETA2-D)
        SUB8=2.*G*E2*H2*E3*H3*H21*H31*C
        DELRE=SUB8*((1.-(ETA2**2.))+(D*(2.*ETA2)))
        DELIM=SUB8*(C1*(2.*ETA2)-(D*(1.-(ETA2**2.))))
        SUB4=(12./(C1**2.+D**2.))*(ALPHRE-BRE-DELRE)
        ENCUBE=(E1*(H1**3.))+E3*(H3**3.)+SUB4
C
C   MODAL FREQUENCY OF DAMPED PLATE
C
        DENS=RHO1*H1+RHO2*H2+H3*RHO3
        SUB5=(ENCUBE*GC)/(12.*(1.-NU1**2.)*DENS)
        WCP=KQR*SQRT(SUB5)
        FCP=WCP/(2.*PI)
C
C   COMPARISON OF FP AND FCP
C
        IF (ABS(1.-FP/FCP).LE. 0.1) THEN
            GOTO 500
        ELSE
            FP=FCP
            GOTO 501
        ENDIF
C
C   COMPUTE SYSTEM LOSS FACTOR
C
500     SUB6=(12./(C1**2.+D**2.))*(ALPHIM-BIM-DELIM)
        ETAS=(1./ENCUBE)*SUB6
C
C   PRINT RESULTS
C
        WRITE(10,701) T,I,FCP,ETA2,ETAS,G2
701     FORMAT(5X,F7.3,2X,I2,3X,4E15.4)
C
C   NEXT TEMPERATURE
C
        T=T+5.0
400     CONTINUE
C
C   NEXT MODE
C
        WRITE(10,*)
300     CONTINUE
```

82

```
        REWIND(UNIT=11)
C
C   NEXT CONSTRAINING LAYER THICKNESS
C
        H3=H3+0.0625
200     CONTINUE
C
C   NEXT VISCOELASTIC LAYER THICKNESS
C
        H2=H2+0.015
150     CONTINUE
C
C   NEXT BASE PLATE THICKNESS
C
        H1=H1+0.125
100     CONTINUE
        CLOSE(UNIT=10)
        CLOSE(UNIT=11)
        END
```

APPENDIX B

FORTRAN PROGRAM USED TO COMPUTE MODAL LOSS FACTORS
FOR THE DOUBLE DAMPING LAYER CONFIGURATION DESIGN

This program uses the Ross–Kerwin–Ungar equations of Chapter 3 to compute estimated modal frequencies and loss factors for the double layer configuration. Modal frequencies for an undamped plate are read from a data file and estimated modal frequencies and loss factors for various layer thickness combinations in the double layer configuration are output to another data file. Material properties of ISD–112 are computed using University of Dayton data and curve-fitting equations to the reduced frequency nomogram [Ref. 9,12]. The units used in this program are pounds, inches, and seconds.

```
      PROGRAM THOLYR
C
C  ***********************************************************************
C
C     THIS PROGRAM COMPUTES THE SYSTEM LOSS FACTOR AND MODAL FREQUENCY OF
C     A DOUBLE CONSTRAINED LAYER VISCOELASTICALLY DAMPED PLATE.  THE LOSS
C     FACTORS ARE COMPUTED FOR A SPECIFIC PLATE/DAMPING LAYER
C     CONFIGURATION AND OVER A TEMPERATURE RANGE OF 30-100 DEGREES
C     FARENHEIT.
C
C     THIS PROGRAM APPLIES TO A FREE-FREE-FREE-FREE PLATE AND THE UNDAMPED
C     MODAL FREQUENCIES ARE DETERMINED FROM FINITE ELEMENT ANALYSIS AND
C     ARE READ INTO THIS PROGRAM FROM FILE 'PLTFRQ'.
C
C     THE VISCOELASTIC MATERIAL IS 3M ISD-112.  VISCOELASTIC MATERIAL
C     DATA IS FROM UNIVERSITY OF DAYTON RESEARCH INSTITUTE
C
C     THE UNITS USED IN THIS PROGRAM ARE LB, INCH, SEC, AND DEGREES F.
C
C     LOSS FACTORS, DAMPED PLATE MODAL FREQUENCIES, AND ISD-112 PROPERTIES
C     ARE COMPUTED IN SUBROUTINE 'RKU' FOR EACH N-TH CONSTRAINED LAYER
C     SYSTEM.  UPON COMPLETION OF EACH TEMPERATURE COMPUTATION THE SYSTEM
C     LOSS FACTOR AND CORRESPONDING DAMPED PLATE FREQUENCY ARE WRITTEN TO
C     FILE 'THOLYR DATA'.
C
C     THE FOLLOWING COEFFICIENTS ARE DEFINED:
C         E1 = YOUNG'S MODULUS OF BASE PLATE (PSI)
C         E3 = EQUIVALENT YOUNG'S MODULUS OF N-TH CONSTRAINED LAYER SYSTEM
C         E3PRM = YOUNG'S MODULUS OF THE CONSTRAINING LAYER IN N-TH LAYER
C         EHCUBE = EQUIVALENT STIFFNESS OF CONSTRAINED LAYER SYSTEM
C         ETAS = SYSTEM LOSS FACTOR
C         ETA3 = LOSS FACTOR OF N-TH CONSTRAINED LAYER SYSTEM
C         ETA3PM = LOSS FACTOR OF CONSTRAINING LAYER IN THE N-TH LAYER (=0
C         FCP = FREQUENCY OF THE DAMPED PLATE  (HZ)
C         FP = FREQUENCY OF UNDAMPED PLATE  (HZ)
C         GC = GRAVITATIONAL CONSTANT
C         H1 = THICKNESS OF BASE PLATE
C         H2 = THICKNESS OF 1ST VISCOELASTIC LAYER
C         H3 = THICKNESS OF N-TH CONSTRAINED LAYER SYSTEM
C         H4 = TOTAL DAMPED PLATE THICKNESS
C         H1PRM = THICKNESS OF BASE LAYER IN N-TH LAYER
C         H2PRM = THICKNESS OF VEM IN N-TH LAYER
C         H3PRM = THICKNESS OF CONSTRAINING LAYER IN N-TH LAYER
C         KQR = WAVE NUMBER OF UNDAMPED PLATE
C         NU1 = POISSON'S RATIO OF BASE PLATE AND CONSTRAINING LAYERS
C         NU2 = POISSON'S RATIO OF VISCOELASTIC MATERIAL
C         NU2PRM = POISSON'S RATIO OF VEM IN N-TH LAYER
C         RHO1 = DENSITY OF BASE PLATE AND CONSTRAINING LAYERS
C         RHO2 = DENSITY OF VISCOELASTIC MATERIAL
C         RHO2PM = DENSITY OF VEM IN N-TH LAYER
C         RHO3 = DENSITY OF N-TH LAYER (= RHO1)
C         RHO3PM = DENSITY OF N-TH LAYER CONSTRAINING LAYER
C         T = TEMPERATURE VARIABLE
C         WP = FREQUENCY OF UNDAMPED PLATE  (RAD/SEC)
C
C         C,EIFROL,FROL,FROM,ML,MROM,N,SH,SL,TO = COEFFICIENTS FOR THE
C              REDUCED FREQUENCY NOMOGRAM EQUATIONS
C
C  ***********************************************************************
C
      REAL C,E1,E3,E3PRM,EHCUBE,ETAS,ETA3,ETA3PM,EIFROL,FCP,FP,FROL
      REAL FROM,GC,H1,H2,H3,H4,H1PRM,H2PRM,H3PRM,KQR,ML,MROM,N,NU1
      REAL NU2,NU2PM,PI,RHO1,RHO2,RHO2PM,SH,SL,SUB1,T,TO,WP
      REAL RHO3,RHO3PM
C
      DIMENSION WP(17)
      PI=4.0*ATAN(1.0)
C
      OPEN(UNIT=10,FILE='PLTFRQ',STATUS='OLD')
      OPEN(UNIT=11,FILE='THOLYR',STATUS='OLD')
C
C  ASSIGN LAYER THICKNESSES
```

```
C
      H1=0.5
      H2=0.045
      H1PRM=0.09375
      H2PRM=0.015
      H3PRM=0.09375
      H3=H1PRM+H2PRM+H3PRM
      H4=H1+H2+H3
C
C  ASSIGN MATERIAL CONSTANTS
C
      E1=1.0E7
      RHO1=0.0968
      NU1=0.33
      RHO2=0.035
      NU2=0.49
      RHO2PM=0.035
      NU2PM=0.5
      RHO3=0.0968
      E3PRM=1.0E7
      RHO3PM=0.0968
      ETA3PM=0.0
      ETA3 = 0.0
C
      GC=386.0
C
C  DEFINE VISCOELASTIC CONSTANTS FOR NOMOGRAM EQUATIONS
C
      TO= 104.0
      FROM=2.0E4
      MROM=638.94
      N=0.275
      NL=8.7
      ETAROL=1.08
      SL=0.45
      SH=0.55
      FROL=5000.0
      C=2.5
C
C  WRITE PLATE CHARACTERISTICS
C
      WRITE(11,700) 'H1 =',H1
      WRITE(11,700) 'H2 =',H2
      WRITE(11,700) 'H1PRIME =',H1PRM
      WRITE(11,700) 'H2PRIME =',H2PRM
      WRITE(11,700) 'H3PRIME =',H3PRM
      WRITE(11,*)
      WRITE(11,*)
700   FORMAT(A12,F6.5)
      WRITE(11,701) 'TEMP','MODE','FCP','ETAS'
701   FORMAT(A8,3X,A5,2A15)
      WRITE(11,*)
C
C  PLATE MODE LOOP
C
      DO 100 I=1,17
      READ(10,*) HP(I)
C
C  CALCULATE MODAL FREQUENCY AND WAVE NUMBER OF UNDAMPED PLATE
C
      SUB1=SQRT((E1*(H4**3)*GC)/(12.*(1.-NU1**2)*RHO1*H4))
      KQB=HP(I)/SUB1
      FP=HP(I)/(2.*PI)
C
C  TEMPERATURE LOOP
C
      T=30.0
      DO 200 K=1,15
C
C  COMPUTE SYSTEM LOSS FACTOR AND STIFFNESS FOR N-TH LAYER
C
      CALL RKU(H1PRM,H2PRM,H3PRM,E1,RHO1,NU1,NU2PM,RHO2PM,E3PRM,RHO3PM,
```

86

```
              CETA3FM,T,FP,KQR,ETAS,ENCUBE,FCP,TO,FROM,MROM,N,ML,ETFROL,SL,SH,
              CFROL,C)
C
C     CONVERT RESULTS FROM N-TH LAYER CALCULATION TO TOTAL PLATE
C
              ETA3= 0.0
              FP = WP(I)/(2.*PI)
C             FP=FCP
              E3=ENCUBE/(H3**3)
C
C     COMPUTE SYSTEM LOSS FACTOR AND FREQUENCY FOR TOTAL PLATE
C
              CALL RKU(H1,H2,H3,E1,RHO1,NU1,NU2,RHO2,E3,RHO3,ETA3,T,FP,KQR,ETAS,
              CENCUBE,FCP,TO,FROM,MROM,N,ML,ETFROL,SL,SH,FROL,C)
C
C     PRINT RESULTS
C
              WRITE(11,702) T,I,FCP,ETAS
702           FORMAT(5X,F7.3,2X,I2,3X,2E15.4)
C
C     NEXT TEMPERATURE
C
              T=T+5.0
200           CONTINUE
C
C     NEXT MODE
C
              WRITE(11,*)
100           CONTINUE
C
              CLOSE(UNIT=11)
              CLOSE(UNIT=10)
              END
C
C     *************************************************************************
C     *************************************************************************
C
              SUBROUTINE RKU(H1,H2,H3,E1,RHO1,NU1,NU2,RHO2,E3,RHO3,ETA3,T,FP,
              CKQR,ETAS,ENCUBE,FCP,TO,FROM,MROM,N,ML,ETFROL,SL,SH,FROL,C)
C
C     *************************************************************************
C
C     THIS SUBROUTINE CALCULATES VISCOELASTIC PROPERTIES BASED ON THE
C     UNIVERSITY OF DAYTON REDUCED FREQUENCY NOMOGRAM EQUATIONS, AND THEN
C     CALCULATES PLATE STIFFNESSES AND LOSS FACTORS BASED ON THE ROSS-
C     KERWIN-UNGAR EQUATIONS.
C
C     THE FOLLOWING ADDITIONAL VARIABLES ARE DEFINED FOR USE IN THIS
C     SUBROUTINE:
C
C         A = COEFFICIENT FOR NOMOGRAM EQUATIONS
C         ALPHIM,ALPHRE = IMAGINARY AND REAL COMPONENTS OF COEFFICIENT
C             ALPHA IN THE RKU EQUATIONS
C         BIM,BRE = IMAGINARY AND REAL COMPONENTS OF COEFFICIENT 'B' IN
C             THE RKU EQUATIONS
C         C1,D = COEFFICIENTS FOR RKU EQUATIONS
C         DELIM,DELRE = IMAGINARY AND REAL COMPONENTS OF COEFFICIENT
C             DELTA IN THE RKU EQUATIONS
C         DENS = COMBINATION OF MATERIAL DENSITIES USED TO COMPUTE THE
C             FREQUENCY OF THE DAMPED PLATE AND DAMPING LAYERS
C         ENCUBE = EQUIVALENT STIFFNESS OF DAMPED PLATE AS COMPUTED
C             USING RKU EQUATIONS
C         ETA2 = LOSS FACTOR OF VEM COMPUTED IN NOMOGRAM EQUATIONS
C         ETA210 = LOG10(ETA2)
C         ETAS = SYSTEM LOSS FACTOR COMPUTED BY RKU EQUATIONS
C         FCP = MODAL FREQUENCY OF DAMPED PLATE (HZ)
C         FP = MODAL FREQUENCY OF UNDAMPED PLATE (HZ)
C         FR = REDUCED FREQUENCY OF VEM
C         FR10 = LOG10(FR)
C         G2 = SHEAR MODULUS OF VEM
C         H21,H31 = RKU EQUATION COEFFICIENTS
C         M10 = LOG10(G2) AS COMPUTED BY NOMOGRAM EQUATIONS
```

```
C        HCP = FREQUENCY OF DAMPED PLATE (RAD/SEC)
C
C   ***********************************************************************
C
        REAL A,ALPHIM,ALPHRE,BIM,BRE,C,C1,D,DELIM,DELRE,DENS,E1,E2,E3
        REAL ENCUBE,ETA2,ETA3,ETA210,ETAS,ETFROL,FCP,FP,FR,FR10,FROL,FROM
        REAL G,G2,GC,H1,H2,H3,H21,H31,KQR,M10,ML,MROM,N,NU1,NU2,PI,RHO1
        REAL RHO2,RHO3,SH,SL,SUB1,SUB2,SUB3,SUB4,SUB5,SUB6,SUB7,SUB8
        REAL SUB9,SUB10,SUB11,T,T0,HCP
C
        PI=4.0*ATAN(1.0)
        GC=386.0
C
C  CALCULATE PROPERTIES OF VEM FOR GIVEN TEMPERATURE AND MODE
C
501     FR10=LOG10(FP)-(12.*(T-T0))/(525.+T-T0)
        FR=10.**(FR10)
        A=(FR10-LOG10(FROL))/C
        SUB1=C*((SL+SH)*A+(SL-SH)*(1.-SQRT(1.+A**2)))/2.
        ETA210=LOG10(ETFROL)+SUB1
C
C  VISCOELASTIC LOSS FACTOR
C
        ETA2=10.**(ETA210)
C
C  VISCOELASTIC SHEAR MODULUS
C
        SUB2=2.*LOG10(MROM/ML)
        SUB3=1.+(FROM/FR)**N
        M10=LOG10(ML)+SUB2/SUB3
        G2=10.**(M10)
C
C  VISCOELASTIC YOUNG'S MODULUS
C
        E2=G2*2.*(1.+NU2)
C
C  CALCULATIONS FOR DAMPED PLATE USING RKU EQUATIONS
C
        G=G2/(E3*H3*H2*KQR)
        H21=(H1+H2)/2.
        H31=H2+(H1+H3)/2.
        C1=E1*H1*(1.+G)+G*E3*H3*(1.-ETA2*ETA3)
        D=G*E1*H1*ETA2+G*E3*H3*(ETA2+ETA3)
        SUB4=G*E1*H1*E3*H3*(H31**2)
        ALPHRE=SUB4*(C1*(1.-ETA2*ETA3)+D*(ETA2+ETA3))
        ALPHIM=SUB4*(C1*(ETA2+ETA3))
        SUB5=E1*H1*E2*H2*H31
        BRE=SUB5*(C1+D*ETA2)
        BIM=SUB5*(C1*ETA2-D)
        SUB6=2.*G*E2*H2*E3*H3*H21*H31
        SUB7=1.-2.*ETA2*ETA3-(ETA2**2)
        SUB8=2.*ETA2+ETA3-(ETA2**2)*ETA3
        DELRE=SUB6*(C1*SUB7+D*SUB8)
        DELIM=SUB6*(C1*SUB8-D*SUB7)
C
        SUB9=(12./(C1**2+D**2))*(ALPHRE-BRE-DELRE)
        ENCUBE=E1*(H1**3)+E3*(H3**3)+SUB9
C
C  MODAL FREQUENCY OF DAMPED PLATE
C
        DENS=RHO1*H1+RHO2*H2+RHO3*H3
        SUB10=(ENCUBE*GC)/(12.*(NU1**2)*DENS)
        HCP=KQR*SQRT(SUB10)
        FCP=HCP/(2.*PI)
C
C  COMPARISON OF FP AND FCP
C
        IF(ABS(1.-FP/FCP) .LE. 0.10) THEN
            GOTO 500
        ELSE
            FP=FCP
            GOTO 501
```

```
      ENDIF
C
C   COMPUTE SYSTEM LOSS FACTOR
C
500   SUB11=(12./(C1**2+D**2))*(ALPHIM-BIM-DELIM)
      ETAS=(1./EHCUBE)*((E3*H3*ETA3)+SUB11)
C
      END
```

APPENDIX C

DESIGN DRAWINGS FOR THE MACHINING
OF THE FLOATING ELEMENT AND
POCKET PLATE CONFIGURATIONS

The drawings shown in Figures C.1 and C.2 were used to machine the pocket plate and floating element plate used in the experiments. These drawings are included to show the relation of the pocket for the ISD–112 to the cover plate and how the viscoelastic was protected from the heat of welding.

SECTION A – A

DIMENSIONS IN CENTIMETERS

A = 0.635   C = 0.038

B = 0.953   D = 0.635

38.10

34.93

1.91

111.13

114.30
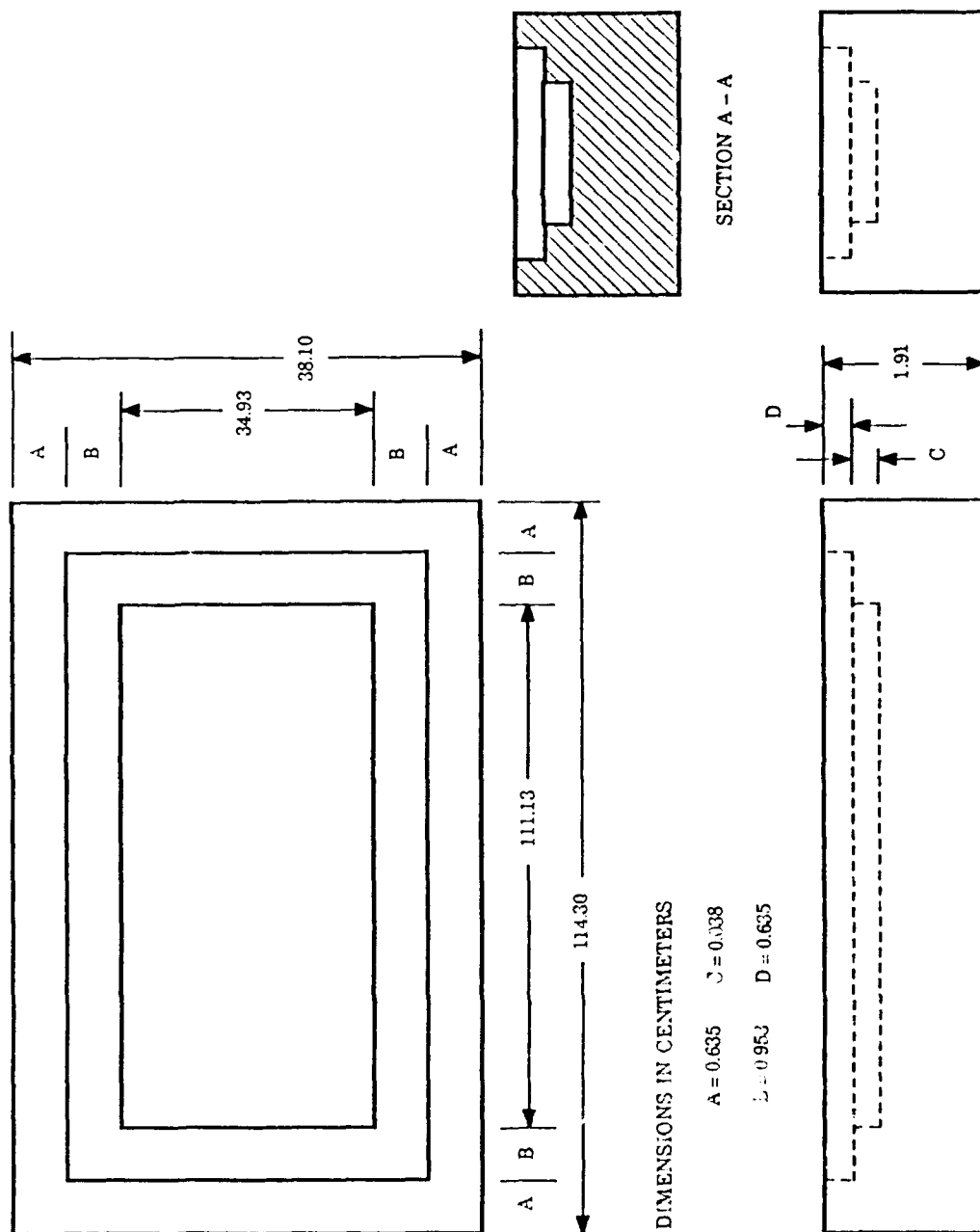
Figure C.1. Design drawing of the pocket plate configuration.
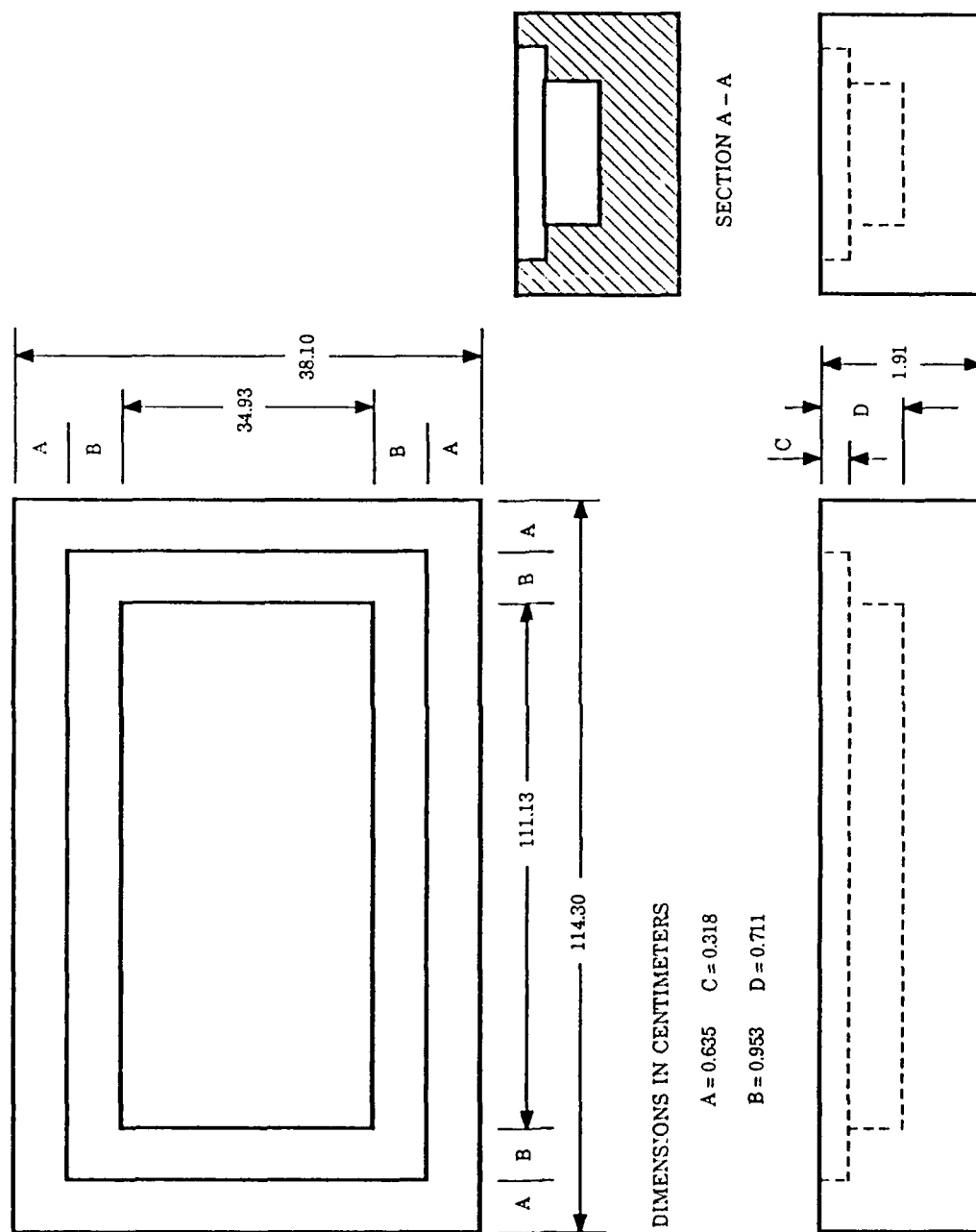
Figure C.2. Design drawing of the floating element configuration.

DIMENSIONS IN CENTIMETERS

A = 0.635   C = 0.318

B = 0.953   D = 0.711

SECTION A – A

APPENDIX D

REPRESENTATIVE MSC/NASTRAN DATA DECK FOR
THE DAMPING CONFIGURATIONS

This data deck was used to compute the modal frequency response of the single layer damping configuration and is a representative sample of the NASTRAN decks used for the other finite element models. The values in the damping table are from a curve fit to the modal loss factors estimated from the modal strain energy method. Since the data deck for the normal mode and modal strain energy extraction is virtually identical to this deck, the Case Control deck commands for the normal mode analysis are included, but are commented out.

The OUTPUT request provides data for an x–y plot of the modal frequency response.

The units used in this deck are pounds, inches, and seconds.

```
id single,mfr
sol 30
$
$ **************************************************************************
$         THIS DECK IS TO COMPUTE THE MODAL FREQUENCY RESPONSE OF A 15x45
$ INCH ALUMINUM PLATE WITH A CONSTRAINED VISCOELASTIC DAMPING LAYER.
$ THE MODEL HAS 252 ELEMENTS WITH 84 ELEMENTS IN EACH LAYER.  THE QUAD
$ ELEMENTS ARE OFFSET FROM THE HEX ELEMENTS AS SUGGESTED BY THE
$ LITERATURE.
$
$         THE MATERIAL PROPERTIES OF ISD-112 ARE FROM THE 3M CORPORATION.
$
$         THE MODAL LOSS FACTORS IN THE DAMPING TABLE ARE FROM A CURVE-FIT
$ TO THE SET OF MODAL LOSS FACTORS COMPUTED FROM THE MODAL STRAIN ENERGY
$ METHOD.
$
$         THE UNITS USED IN THIS DECK ARE POUNDS,INCHES, AND SECONDS
$ **************************************************************************
time 3000
cend
title = MODAL FREQUENCY RESPONSE / 200 HZ / 3M
method = 1
spc = 1
dload = 10
frequency = 10
sdamping = 101
set 111 = 95 .
svector = all
acceleration(plot,phase) = 111
output(xyplot)
xyprint acce / 95(t3)
$
$ *****************
$         THE FOLLOWING LINES ARE THE CASE CONTROL DECK CARDS FOR THE
$ NORMAL MODE EXTRACTION AND STRAIN ENERGY REQUEST
$ method = 1
$ spc = 1
$ set 10 = all
$ set 11 = 169,thru,252
$ ese = 11
$
$ *****************
BEGIN BULK
$ TITLE = SINGLE LAYER WITH QUAD OFFSET
$ DATA DECK PRODUCED BY PATMAS VERSION 2.0: 24-NOV-89 08:31:48
GRID          1         45.0000 15.0000 0.51500
GRID          2         45.0000 15.0000 0.50000
GRID          3         45.0000 12.5000 0.51500
GRID          4         45.0000 12.5000 0.50000
GRID          5         45.0000 10.0000 0.51500
GRID          6         45.0000 10.0000 0.50000
```

94

```
GRID        7           45.0000 7.50000 0.51500
GRID        8           45.0000 7.50000 0.50000
GRID        9           45.0000 5.00000 0.51500
GRID        10          45.0000 5.00000 0.50000
GRID        11          45.0000 2.50000 0.51500
GRID        12          45.0000 2.50000 0.50000
GRID        13          45.0000 0.      0.51500
GRID        14          45.0000 0.      0.50000
GRID        15          41.7857 15.0000 0.51500
GRID        16          41.7857 15.0000 0.50000
GRID        17          41.7857 12.5000 0.51500
GRID        18          41.7857 12.5000 0.50000
GRID        19          41.7857 10.0000 0.51500
GRID        20          41.7857 10.0000 0.50000
GRID        21          41.7857 7.50000 0.51500
GRID        22          41.7857 7.50000 0.50000
GRID        23          41.7857 5.00000 0.51500
GRID        24          41.7857 5.00000 0.50000
GRID        25          41.7857 2.50000 0.51500
GRID        26          41.7857 2.50000 0.50000
GRID        27          41.7857 0.      0.51500
GRID        28          41.7857 0.      0.50000
GRID        29          38.5714 15.0000 0.51500
GRID        30          38.5714 15.0000 0.50000
GRID        31          38.5714 12.5000 0.51500
GRID        32          38.5714 12.5000 0.50000
GRID        33        ' 38.5714 10.0000 0.51500
GRID        34          38.5714 10.0000 0.50000
GRID        35          38.5714 7.50000 0.51500
GRID        36          38.5714 7.50000 0.50000
GRID        37          38.5714 5.00000 0.51500
GRID        38          38.5714 5.00000 0.50000
GRID        39          38.5714 2.50000 0.51500
GRID        40          38.5714 2.50000 0.50000
GRID        41          38.5714 0.      0.51500
GRID        42          38.5714 0.      0.50000
GRID        43          35.3571 15.0000 0.51500
GRID        44          35.3571 15.0000 0.50000
GRID        45          35.3571 12.5000 0.51500
GRID        46          35.3571 12.5000 0.50000
GRID        47          35.3571 10.0000 0.51500
GRID        48          35.3571 10.0000 0.50000
GRID        49          35.3571 7.50000 0.51500
GRID        50          35.3571 7.50000 0.50000
GRID        51          35.3571 5.00000 0.51500
GRID        52          35.3571 5.00000 0.50000
GRID        53          35.3571 2.50000 0.51500
GRID        54          35.3571 2.50000 0.50000
GRID        55          35.3571 0.      0.51500
GRID        56          35.3571 0.      0.50000
GRID        57          32.1429 15.0000 0.51500
```

```
GRID        58           32.1429 15.0000 0.50000
GRID        59           32.1429 12.5000 0.51500
GRID        60           32.1429 12.5000 0.50000
GRID        61           32.1429 10.0000 0.51500
GRID        62           32.1429 10.0000 0.50000
GRID        63           32.1429 7.50000 0.51500
GRID        64           32.1429 7.50000 0.50000
GRID        65           32.1429 5.00000 0.51500
GRID        66           32.1429 5.00000 0.50000
GRID        67           32.1429 2.50000 0.51500
GRID        68           32.1429 2.50000 0.50000
GRID        69           32.1429 0.      0.51500
GRID        70           32.1429 0.      0.50000
GRID        71           28.9286 15.0000 0.51500
GRID        72           28.9286 15.0000 0.50000
GRID        73           28.9286 12.5000 0.51500
GRID        74           28.9286 12.5000 0.50000
GRID        75           28.9286 10.0000 0.51500
GRID        76           28.9286 10.0000 0.50000
GRID        77           28.9286 7.50000 0.51500
GRID        78           28.9286 7.50000 0.50000
GRID        79           28.9286 5.00000 0.51500
GRID        80           28.9286 5.00000 0.50000
GRID        81           28.9286 2.50000 0.51500
GRID        82           28.9286 2.50000 0.50000
GRID        83           28.9286 0.      0.51500
GRID        84           28.9286 0.      0.50000
GRID        85           25.7143 15.0000 0.51500
GRID        86           25.7143 15.0000 0.50000
GRID        87           25.7143 12.5000 0.51500
GRID        88           25.7143 12.5000 0.50000
GRID        89           25.7143 10.0000 0.51500
GRID        90           25.7143 10.0000 0.50000
GRID        91           25.7143 7.50000 0.51500
GRID        92           25.7143 7.50000 0.50000
GRID        93           25.7143 5.00000 0.51500
GRID        94           25.7143 5.00000 0.50000
GRID        95           25.7143 2.50000 0.51500
GRID        96           25.7143 2.50000 0.50000
GRID        97           25.7143 0.      0.51500
GRID        98           25.7143 0.      0.50000
GRID        99           22.5000 15.0000 0.51500
GRID        100          22.5000 15.0000 0.50000
GRID        101          22.5000 12.5000 0.51500
GRID        102          22.5000 12.5000 0.50000
GRID        103          22.5000 10.0000 0.51500
GRID        104          22.5000 10.0000 0.50000
GRID        105          22.5000 7.50000 0.51500
GRID        106          22.5000 7.50000 0.50000
GRID        107          22.5000 5.00000 0.51500
GRID        108          22.5000 5.00000 0.50000
```

```
GRID    109         22.5000 2.50000 0.51500
GRID    110         22.5000 2.50000 0.50000
GRID    111         22.5000 0.       0.51500
GRID    112         22.5000 0.       0.50000
GRID    113         19.2857 15.0000 0.51500
GRID    114         19.2857 15.0000 0.50000
GRID    115         19.2857 12.5000 0.51500
GRID    116         19.2857 12.5000 0.50000
GRID    117         19.2857 10.0000 0.51500
GRID    118         19.2857 10.0000 0.50000
GRID    119         19.2857 7.50000 0.51500
GRID    120         19.2857 7.50000 0.50000
GRID    121         19.2857 5.00000 0.51500
GRID    122         19.2857 5.00000 0.50000
GRID    123         19.2857 2.50000 0.51500
GRID    124         19.2857 2.50000 0.50000
GRID    125         19.2857 0.       0.51500
GRID    126         19.2857 0.       0.50000
GRID    127         16.0714 15.0000 0.51500
GRID    128         16.0714 15.0000 0.50000
GRID    129         16.0714 12.5000 0.51500
GRID    130         16.0714 12.5000 0.50000
GRID    131         16.0714 10.0000 0.51500
GRID    132         16.0714 10.0000 0.50000
GRID    133         16.0714 7.50000 0.51500
GRID    134         16.0714 7.50000 0.50000
GRID    135         16.0714 5.00000 0.51500
GRID    136         16.0714 5.00000 0.50000
GRID    137         16.0714 2.50000 0.51500
GRID    138         16.0714 2.50000 0.50000
GRID    139         16.0714 0.       0.51500
GRID    140         16.0714 0.       0.50000
GRID    141         12.8571 15.0000 0.51500
GRID    142         12.8571 15.0000 0.50000
GRID    143         12.8571 12.5000 0.51500
GRID    144         12.8571 12.5000 0.50000
GRID    145         12.8571 10.0000 0.51500
GRID    146         12.8571 10.0000 0.50000
GRID    147         12.8571 7.50000 0.51500
GRID    148         12.8571 7.50000 0.50000
GRID    149         12.8571 5.00000 0.51500
GRID    150         12.8571 5.00000 0.50000
GRID    151         12.8571 2.50000 0.51500
GRID    152         12.8571 2.50000 0.50000
GRID    153         12.8571 0.       0.51500
GRID    154         12.8571 0.       0.50000
GRID    155         9.64286 15.0000 0.51500
GRID    156         9.64286 15.0000 0.50000
GRID    157         6.42857 15.0000 0.51500
GRID    158         6.42857 15.0000 0.50000
GRID    159         3.21429 15.0000 0.51500
```

GRID	160	3.21429	15.0000	0.50000
GRID	161	0.	15.0000	0.51500
GRID	162	0.	15.0000	0.50000
GRID	163	9.64286	12.5000	0.51500
GRID	164	9.64286	12.5000	0.50000
GRID	165	9.64286	10.0000	0.51500
GRID	166	9.64286	10.0000	0.50000
GRID	167	9.64286	7.50000	0.51500
GRID	168	9.64286	7.50000	0.50000
GRID	169	9.64286	5.00000	0.51500
GRID	170	9.64286	5.00000	0.50000
GRID	171	9.64286	2.50000	0.51500
GRID	172	9.64286	2.50000	0.50000
GRID	173	9.64286	0.	0.51500
GRID	174	9.64286	0.	0.50000
GRID	175	6.42857	12.5000	0.51500
GRID	176	6.42857	12.5000	0.50000
GRID	177	3.21429	12.5000	0.51500
GRID	178	3.21429	12.5000	0.50000
GRID	179	0.	12.5000	0.51500
GRID	180	0.	12.5000	0.50000
GRID	181	6.42857	10.0000	0.51500
GRID	182	6.42857	10.0000	0.50000
GRID	183	6.42857	7.50000	0.51500
GRID	184	6.42857	7.50000	0.50000
GRID	185	6.42857	5.00000	0.51500
GRID	186	6.42857	2.50000	0.51500
GRID	187	6.42857	5.00000	0.50000
GRID	188	6.42857	2.50000	0.50000
GRID	189	6.42857	0.	0.51500
GRID	190	6.42857	0.	0.50000
GRID	191	3.21429	10.0000	0.51500
GRID	192	3.21429	10.0000	0.50000
GRID	193	0.	10.0000	0.51500
GRID	194	0.	10.0000	0.50000
GRID	195	3.21429	0.	0.51500
GRID	196	3.21429	0.	0.50000
GRID	197	0.	0.	0.51500
GRID	198	0.	0.	0.50000
GRID	199	3.21429	7.50000	0.51500
GRID	200	3.21429	5.00000	0.51500
GRID	201	3.21429	2.50000	0.51500
GRID	202	3.21429	7.50000	0.50000
GRID	203	3.21429	5.00000	0.50000
GRID	204	3.21429	2.50000	0.50000
GRID	205	0.	7.50000	0.51500
GRID	206	0.	5.00000	0.51500
GRID	207	0.	2.50000	0.51500
GRID	208	0.	7.50000	0.50000
GRID	209	0.	2.50000	0.50000
GRID	210	0.	5.00000	0.50000

98

CQUAD4	1	1	198	196	204	209	-.25
CQUAD4	2	1	196	199	188	204	-.25
CQUAD4	3	1	190	174	172	188	-.25
CQUAD4	4	1	174	154	152	172	-.25
CQUAD4	5	1	154	140	138	152	-.25
CQUAD4	6	1	140	126	124	138	-.25
CQUAD4	7	1	126	112	110	124	-.25
CQUAD4	8	1	112	98	96	110	-.25
CQUAD4	9	1	98	84	82	96	-.25
CQUAD4	10	1	84	70	68	82	-.25
CQUAD4	11	1	70	56	54	68	-.25
CQUAD4	12	1	56	42	40	54	-.25
CQUAD4	13	1	42	28	26	40	-.25
CQUAD4	14	1	28	14	12	26	-.25
CQUAD4	15	1	209	204	203	210	-.25
CQUAD4	16	1	204	188	187	203	-.25
CQUAD4	17	1	188	172	170	187	-.25
CQUAD4	18	1	172	152	150	170	-.25
CQUAD4	19	1	152	138	136	150	-.25
CQUAD4	20	1	138	124	122	136	-.25
CQUAD4	21	1	124	110	108	122	-.25
CQUAD4	22	1	110	96	94	108	-.25
CQUAD4	23	1	96	82	80	94	-.25
CQUAD4	24	1	82	68	66	80	-.25
CQUAD4	25	1	68	54	52	66	-.25
CQUAD4	26	1	54	40	38	52	-.25
CQUAD4	27	1	40	26	24	38	-.25
CQUAD4	28	1	26	12	10	24	-.25
CQUAD4	29	1	210	203	202	208	-.25
CQUAD4	30	1	203	187	184	202	-.25
CQUAD4	31	1	187	170	168	184	-.25
CQUAD4	32	1	170	150	148	168	-.25
CQUAD4	33	1	150	136	134	148	-.25
CQUAD4	34	1	136	122	120	134	-.25
CQUAD4	35	1	122	108	106	120	-.25
CQUAD4	36	1	108	94	92	106	-.25
CQUAD4	37	1	94	80	78	92	-.25
CQUAD4	38	1	80	66	64	78	-.25
CQUAD4	39	1	66	52	50	64	-.25
CQUAD4	40	1	52	38	36	50	-.25
CQUAD4	41	1	38	24	22	36	-.25
CQUAD4	42	1	24	10	8	22	-.25
CQUAD4	43	1	208	202	192	194	-.25
CQUAD4	44	1	202	184	182	192	-.25
CQUAD4	45	1	184	168	166	182	-.25
CQUAD4	46	1	168	148	146	166	-.25
CQUAD4	47	1	148	134	132	146	-.25
CQUAD4	48	1	134	120	118	132	.25
CQUAD4	49	1	120	106	104	118	-.25
CQUAD4	50	1	106	92	90	104	-.25
CQUAD4	51	1	92	78	76	90	-.25

CQUAD4	52	1	78	64	62	76	-.25
CQUAD4	53	1	64	50	48	62	-.25
CQUAD4	54	1	50	36	34	48	-.25
CQUAD4	55	1	36	22	20	34	-.25
CQUAD4	56	1	22	8	6	20	-.25
CQUAD4	57	1	194	192	178	180	-.25
CQUAD4	58	1	192	182	176	178	-.25
CQUAD4	59	1	182	166	164	176	-.25
CQUAD4	60	1	166	146	144	164	-.25
CQUAD4	61	1	146	132	130	144	-.25
CQUAD4	62	1	132	118	116	130	-.25
CQUAD4	63	1	118	104	102	116	-.25
CQUAD4	64	1	104	90	88	102	-.25
CQUAD4	65	1	90	76	74	88	-.25
CQUAD4	66	1	76	62	60	74	-.25
CQUAD4	67	1	62	48	46	60	-.25
CQUAD4	68	1	48	34	32	46	-.25
CQUAD4	69	1	34	20	18	32	-.25
CQUAD4	70	1	20	6	4	18	-.25
CQUAD4	71	1	180	178	160	162	-.25
CQUAD4	72	1	178	176	158	160	-.25
CQUAD4	73	1	176	164	156	158	-.25
CQUAD4	74	1	164	144	142	156	-.25
CQUAD4	75	1	144	130	128	142	-.25
CQUAD4	76	1	130	116	114	128	-.25
CQUAD4	77	1	116	102	100	114	-.25
CQUAD4	78	1	102	88	86	100	.25
CQUAD4	79	1	88	74	72	86	-.25
CQUAD4	80	1	74	60	58	72	-.25
CQUAD4	81	1	60	46	44	58	-.25
CQUAD4	82	1	46	32	30	44	-.25
CQUAD4	83	1	32	18	16	30	-.25
CQUAD4	84	1	18	4	2	16	-.25
CQUAD4	85	85	197	195	201	207	.125
CQUAD4	86	85	195	189	186	201	.125
CQUAD4	87	85	189	173	171	186	.125
CQUAD4	88	85	173	153	151	171	.125
CQUAD4	89	85	153	139	137	151	.125
CQUAD4	90	85	139	125	123	137	.125
CQUAD4	91	85	125	111	109	123	.125
CQUAD4	92	85	111	97	95	109	.125
CQUAD4	93	85	97	83	81	95	.125
CQUAD4	94	85	83	69	67	81	.125
CQUAD4	95	85	69	55	53	67	.125
CQUAD4	96	85	55	41	39	53	.125
CQUAD4	97	85	41	27	25	39	.125
CQUAD4	98	85	27	13	11	25	.125
CQUAD4	99	85	207	201	200	206	.125
CQUAD4	100	85	201	186	185	200	.125
CQUAD4	101	85	196	171	169	185	.125
CQUAD4	102	85	171	151	149	169	.125

CQUAD4	103	85	151	137	135	149	.125
CQUAD4	104	85	137	123	121	135	.125
CQUAD4	105	85	123	109	107	121	.125
CQUAD4	106	85	109	95	93	107	.125
CQUAD4	107	85	95	81	79	93	.125
CQUAD4	108	85	81	67	65	79	.125
CQUAD4	109	85	67	53	51	65	.125
CQUAD4	110	85	53	39	37	51	.125
CQUAD4	111	85	39	25	23	37	.125
CQUAD4	112	85	25	11	9	23	.125
CQUAD4	113	85	206	200	199	205	.125
CQUAD4	114	85	200	185	183	199	.125
CQUAD4	11	85	185	169	167	183	.125
CQUAD4	116	85	169	149	147	167	.125
CQUAD4	117	85	149	135	133	147	.125
CQUAD4	118	85	135	121	119	133	.125
CQUAD4	119	85	121	107	105	119	.125
CQUAD4	120	85	107	93	91	105	.125
CQUAD4	121	85	93	79	77	91	.125
CQUAD4	122	85	79	65	63	77	.125
CQUAD4	123	85	65	51	49	63	.125
CQUAD4	124	85	51	37	35	49	.125
CQUAD4	125	85	37	23	21	35	.125
CQUAD4	126	85	23	9	7	21	.125
CQUAD4	127	85	205	199	191	193	.125
CQUAD4	128	85	199	183	181	191	.125
CQUAD4	129	85	183	167	165	181	.125
CQUAD4	130	85	167	147	145	165	.125
CQUAD4	131	85	147	133	131	145	.125
CQUAD4	132	85	133	119	117	131	.125
CQUAD4	133	85	119	105	103	117	.125
CQUAD4	134	85	105	91	89	103	.125
CQUAD4	135	85	91	77	75	89	.125
CQUAD4	136	85	77	63	61	75	.125
CQUAD4	137	85	63	49	47	61	.125
CQUAD4	138	85	49	35	33	47	.125
CQUAD4	139	85	35	21	19	33	.125
CQUAD4	140	85	21	7	5	19	.125
CQUAD4	141	85	193	191	177	179	.125
CQUAD4	142	85	191	181	175	177	.125
CQUAD4	143	85	181	165	163	175	.125
CQUAD4	144	85	165	145	143	163	.125
CQUAD4	145	85	145	131	129	143	.125
CQUAD4	146	85	131	117	115	129	.125
CQUAD4	147	85	117	103	101	115	.125
CQUAD4	148	8	103	89	87	101	.125
CQUAD4	149	85	89	75	73	87	.125
CQUAD4	150	85	75	61	59	73	.125
CQUAD4	151	85	61	47	45	59	.125
CQUAD4	152	85	47	33	31	45	.125
CQUAD4	153	85	33	19	17	31	.125

101

CQUAD4	154	85	19	5	3	17		.125		
CQUAD4	155	85	179	177	159	161		.125		
CQUAD4	156	85	177	175	157	159		.125		
CQUAD4	157	85	175	163	155	157		.125		
CQUAD4	158	85	163	143	141	155		.125		
CQUAD4	159	85	143	129	127	141		.125		
CQUAD4	160	85	129	115	113	127		.125		
CQUAD4	161	85	115	101	99	113		.125		
CQUAD4	162	85	101	87	85	99		.125		
CQUAD4	163	85	87	73	71	85		.125		
CQUAD4	164	85	73	59	57	71		.125		
CQUAD4	165	85	59	45	43	57		.125		
CQUAD4	166	85	45	31	29	43		.125		
CQUAD4	167	85	31	17	15	29		.125		
CQUAD4	168	85	17	3	1	15		.125		
CHEXA	169	2	198	196	204	209	197	195	E	169
+E 169	201	207								
CHEXA	170	2	196	190	188	204	195	189	E	170
+E 170	186	201								
CHEXA	171	2	190	174	172	188	189	173	E	171
+E 171	171	186								
CHEXA	172	2	174	154	152	172	173	153	E	172
+E 172	151	171								
CHEXA	173	2	154	140	138	152	153	139	E	173
+E 173	137	151								
CHEXA	174	2	140	126	124	138	139	125	E	174
+E 174	123	137								
CHEXA	175	·2	126	112	110	124	125	111	E	175
+E 175	109	123								
CHEXA	176	2	112	98	96	110	111	97	E	176
+E 176	95	109								
CHEXA	177	2	98	84	82	96	97	83	E	177
+E 177	81	95								
CHEXA	178	2	84	70	68	82	83	69	E	178
+E 178	67	81								
CHEXA	179	2	70	56	54	68	69	55	E	179
+E 179	53	67								
CHEXA	180	2	56	42	40	54	55	41	E	180
+E 180	39	53								
CHEXA	181	2	42	28	26	40	41	27	E	181
+E 181	25	39								
CHEXA	182	2	28	14	12	26	27	13	E	182
+E 182	11	25								
CHEXA	183	2	209	204	203	210	207	201	E	183
+E 183	200	206								
CHEXA	184	2	204	188	187	203	201	186	E	184
+E 184	185	200								
CHEXA	185	2	188	172	170	187	186	171	E	185
+E 185	169	185								
CHEXA	186	2	172	152	150	170	171	151	E	186
+E 186	149	169								

```
CHEXA      187      2     152     138     136     150     151    137 E    187
+E   187   135    149
CHEXA      188      2     138     124     122     136     137    123 E    188
+E   188   121    135
CHEXA      189      2     124     110     108     122     123    109 E    189
+E   189   107    121
CHEXA      190      2     110      96      94     108     109     95 E    190
+E   190    93    107
CHEXA      191      2      96      82      80      94      95     81 E    191
+E   191    79     93
CHEXA      192      2      82      68      66      80      81     67 E    192
+F   192    65     79
CHEXA      193      2      68      54      52      66      67     53 E    193
+E   193    51     65
CHEXA      194      2      54      40      38      52      53     39 E    194
+E   194    37     51
CHEXA      195      2      40      26      24      38      39     25 E    195
+E   195    23     37
CHEXA      196      2      26      12      10      24      25     11 E    196
+E   196     9     23
CHEXA      197      2     210     203     202     208     206    200 E    197
+E   197   199    205
CHEXA      198      2     203     187     184     202     200    185 E    198
+E   198   183    199
CHEXA      199      2     187     170     168     184     185    169 E    199
+E   199   167    183
CHEXA      200      2     170     150     148     168     169    149 E    200
+E   200   147    167
CHEXA      201      2     150     136     134     148     149    135 E    201
+E   201   133    147
CHEXA      202      2     136     122     120     134     135    121 E    202
+E   202   119    133
CHEXA      203      2     122     108     106     120     121    107 E    203
+E   203   105    119
CHEXA      204      2     108      94      92     106     107     93 E    204
+E   204    91    105
CHEXA      205      2      94      80      78      92      93     79 E    205
+E   205    77     91
CHEXA      206      2      80      66      64      78      79     65 E    206
+E   206    63     77
CHEXA      207      2      66      52      50      64      65     51 E    207
+E   207    49     63
CHEXA      208      2      52      38      36      50      51     37 E    208
+E   208    35     49
CHEXA      209      2      38      24      22      36      37     23 E    209
+E   209    21     35
CHEXA      210      2      24      10       8      22      23      9 E    210
+E   210     7     21
CHEXA      211      2     208     202     192     194     205    199 E    211
+E   211    19,    193
```

103

CHEXA	212	2	202	184	182	192	199	183 E	212
+E	212	181	191						
CHEXA	213	2	184	168	166	182	183	167 E	213
+E	213	165	181						
CHEXA	214	2	168	148	146	166	167	147 E	214
+E	214	145	165						
CHEXA	215	2	148	134	132	146	147	133 E	215
+E	215	131	145						
CHEXA	216	2	134	120	118	132	133	119 E	216
+E	216	117	131						
CHEXA	217	2	120	106	104	118	119	105 E	217
+E	217	103	117						
CHEXA	218	2	106	92	90	104	105	91 E	218
+E	218	89	103						
CHEXA	219	2	92	78	76	90	91	77 E	219
+E	219	75	89						
CHEXA	220	2	78	64	62	76	77	63 E	220
+E	220	61	75						
CHEXA	221	2	64	50	48	62	63	49 E	221
+E	221	47	61						
CHEXA	222	2	50	36	34	48	49	35 B	222
+E	222	33	47						
CHEXA	223	2	36	22	20	34	35	21 E	223
+E	223	19	33						
CHEXA	224	2	22	8	6	20	21	7 B	224
+E	224	5	19						
CHEXA	225	2	194	192	178	180	193	191 E	225
+E	225	177	179						
CHEXA	226	. 2	192	182	176	178	191	181 E	226
+E	226	175	177						
CHEXA	227	2	182	166	164	176	181	165 E	227
+E	227	163	175						
CHEXA	228	2	166	146	144	164	165	145 B	228
+B	228	143	163						
CHEXA	229	2	146	132	130	144	145	131 B	229
+E	229	129	143						
CHEXA	230	2	132	118	116	130	131	117 E	230
+E	230	115	129						
CHEXA	231	2	118	104	102	116	117	103 E	231
+E	231	101	115						
CHEXA	232	2	104	90	88	102	103	89 E	232
+E	232	87	101						
CHEXA	233	2	90	76	74	88	89	75 E	233
+E	233	73	87						
CHEXA	234	2	76	62	60	74	75	61 E	234
+E	234	59	73						
CHEXA	235	2	62	48	46	60	61	47 E	235
+E	235	45	59						
CHEXA	236	2	48	34	32	46	47	33 E	236
+E	236	31	45						
CHEXA	237	2	34	20	18	32	33	19 E	237
+E	237	17	31						

CHEXA	238	2	20	6	4	18	19	5 E 238
+E 238	3	17						
CHEXA	239	2	180	178	160	162	179	177 E 239
+E 239	159	161						
CHEXA	240	2	178	176	158	160	177	175 E 240
+E 240	157	159						
CHEXA	241	2	176	164	156	158	175	163 E 241
+E 241	155	157						
CHEXA	242	2	164	144	142	156	163	143 E 242
+E 242	141	155						
CHEXA	243	2	144	130	128	142	143	129 E 243
+E 243	127	141						
CHEXA	244	2	130	116	114	128	129	115 E 244
+E 244	113	127						
CHEXA	245	2	116	102	100	114	115	101 E 245
+E 245	99	113						
CHEXA	246	2	102	88	86	100	101	87 E 246
+E 246	85	99						
CHEXA	247	2	88	74	72	86	87	73 E 247
+E 247	71	85						
CHEXA	248	2	74	60	58	72	73	59 E 248
+E 248	57	71						
CHEXA	249	2	60	46	44	58	59	45 E 249
+E 249	43	57						
CHEXA	250	2	46	32	30	44	45	31 E 250
+E 250	29	43						
CHEXA	251	2	32	18	16	30	31	17 E 251
+E 251	15	29						
CHEXA	252	·2	18	4	2	16	17	3 E 252
+E 252	1	15						
PSHELL	1		1 0.50000		1 1.12200		1	
PSHELL	85		1 0.25000		1 1.12200		1	

```
psolid,2,2
matl,1,1.0e7,,0.33,2.58e-4
matl,2,,251.4,0.49,9.067e-5
eigr,1,mgiv,0.0,5000.0,,30,,,+eigr
+eigr,mass
suport,106,12345
spc1,1,6,1,thru,210
param,autospc,yes
param,asing,1
rload1,10,2001,,,3001
darea,2001,79,3,1.0
tabled1,3001,,,,,,,,+tal
+tal,0.0,1.0,5000.0,1.0,endt
freq1,10,5.0,1.0,1000
tabdmp1,101,,,,,,,,+dmp
+dmp,40.0,0.214,63.0,0.216,95.0,0.218,160.0,0.222,+dmp1
+dmp1,200.0,0.224,285.0,0.225,320.0,0.224,440.0,0.216,+dmp2
+dmp2,460.0,0.215,480.0,0.212,520.0,0.208,580.0,0.197,+dmp3
+dmp3,630.0,0.189,665.0,0.163,715.C,0.171,825.0,0.142,+dmp4
+dmp4,870.0,0.130,885.0,0.125,1000.0,0.085,endt
```

LIST OF REFERENCES

1. Johnson, C.D. and Kienholz, D.A., "Finite Element Prediction of Damping in Structures With Constrained Viscoelastic Layers," AIAA Journal, Vol. 20, No. 9, September 1982.

2. Maurer, G.J., Vibration Response of Constrained Viscoelastically Damped Plates: Analysis and Experiments, M.S. Thesis, U.S. Naval Postgraduate School, Monterey, California, December 1987.

3. Nashif, A.D., Jones, D.I.G., and Henderson, J.P., Vibration Damping, Wiley–Interscience Publications, John Wiley and Sons, 1985.

4. Jones, D.I.G., and Henderson, J.P., "Fundamentals of Damping Materials," Vibration Damping Short Course Notes, Section 2.3, University of Dayton, Dayton, Ohio, June 1987.

5. Rogers, L., "Single Constrained Layer Damping Treatment Analysis," Vibration Damping Short Course Notes, Section 6.3, University of Dayton, Dayton, Ohio, June 1987.

6. Henderson, J.P., and Jones, D.I.G., "Fundamentals of Layered Damping Treatments," Vibration Damping Short Course Notes, Section 6.1, University of Dayton, Dayton, Ohio, June 1987.

7. MacNeal–Schwendler Corporation, MSC/NASTRAN Users Manual, Vol. 1, MacNeal–Schwendler Corporation, November, 1985.

8. Johnson, C.D., and Kienholz, D.A., "Finite Element Design of Viscoelastically Damped Structures," CSA Engineering, Inc., Palo Alto, California, 1984.

9. Nashif, A.D., "Layered Damping Treatment Design, Multiple Layer," Vibration Damping Short Course Notes, Section 6.4, University of Dayton, Dayton, Ohio, June 1987.

10. Ross, D., Ungar, E.E., and Kerwin, E.M., "Damping of Plate Flexural Vibrations by Means of Viscoelastic Laminae," Structural Damping, ASME, 1959.

11. Drake, M.L., "Design Techniques – Fourth Order Beam Theory," Vibration Damping Short Course Notes, Section 7.1, University of Dayton, Dayton, Ohio, 1987.

12. University of Dayton Research Institute, "ISD–112 Material Data Sheet," Vibration Damping Short Course Notes, University of Dayton, Dayton, Ohio, June 1987.

13. Gere, J.M., and Timoshenko, S.P., Mechanics of Materials, 2nd Edition, PWS Publishers, Boston, Massachusetts, 1984.

14. Richardson, N., and Potter, R., "Identification of the Modal Properties of an Elastic Structure From Measured Transfer Function Data," presented at the 20th International Instrumentation Symposium, May 1984, Albuquerque, New Mexico, Instrument Society of America reprint, 1974.

15. PDA Engineering, PAT/MSC Interface Guide, Release 2.1, PDA Engineering, September 1988.

16. Johnson, C.D., and Kienholz, D.A., "Finite Element Prediction of Damping in Structures With Constrained Viscoelastic Layers," Report No. 82.053, Anamet Laboratories, May 1982.

17. MacNeal–Schwendler Corporation, MSC/NASTRAN Handbook for Dynamic Analysis, Section 3.2.3, MacNeal–Schwendler Corporation, 1983.

18. PDA Engineering, PATRAN PLUS Users Manual, Vol. 2, Ch. 21, PDA Engineering, 1987.

INITIAL DISTRIBUTION LIST

1. Defense Technical Information Center   2
   Cameron Station
   Alexandria, Virginia 22304–6145

2. Library, Code 0142   2
   Naval Postgraduate School
   Monterey, California 93943–5002

3. Dean of Science and Engineering, Code 06   2
   Naval Postgraduate School
   Monterey, California 93943–5004

4. Research Administrations Office, Code 012   1
   Naval Postgraduate School
   Monterey, California 93943–5004

5. Department Chairman, Code 69   1
   Department of Mechanical Engineering
   Naval Postgraduate School
   Monterey, California 93943–5004

6. Curricular Officer, Code 34   1
   Naval Engineering Curriculum
   Naval Postgraduate School
   Monterey, California 93943–4004

7. Professor Y.S. Shin, Code 69Sg   3
   Department of Mechanical Engineering
   Naval Postgraduate School
   Monterey, California 93943–5004

8. Dr. K.S. Kim, Code 69Ki   1
   Department of Mechanical Engineering
   Naval Postgraduate School
   Monterey, California 93943–5004

9. Dr. Arthur Kilcullen, Code 1962   1
   David W. Taylor Naval Ship R&D Center
   Bethesda, Maryland 20084

10.   Dr. Lawrence Maga, Code 196   2
        David W. Taylor Naval Ship R&D Center
        Bethesda, Maryland 20084

11.   Mr. Doug Noll, Code 1944   1
        David W. Taylor Naval Ship R&D Center
        Bethesda, Maryland 20084

12.   LT Michael J. Bateman, USN   1
        5306 SE 64th
        Portland, Oregon 97206